AN EXPERIMENTAL ANALYSIS OF STRAIN AND DEFLECTION IN GRIDWORK PANELS FOR FLOOR SYSTEMS FOR LIVESTOCK

By

GEORGE LEWIS PRATT

Bachelor of Science
North Dakota State University
Fargo, North Dakota
1950

Master of Science
Kansas State University
Manhattan, Kansas
1951

Submitted to the faculty of the Graduate College of
the Oklahoma State University
in partial fulfillment of the requirements
for the degree of
DOCTOR OF PHILOSOPHY
July, 1967

AN EXPERIMENTAL ANALYSIS OF STRAIN AND DEFLECTION

IN GRIDWORK PANELS FOR FLOOR SYSTEMS

FOR LIVESTOCK

Thesis Approved:

B. J. Moan

Thesis Adviser

E. L. Rhodes

R. L. Jones

D. M. Macalpine

N. M. Durham

Dean of the Graduate College

PREFACE

The research reported in this thesis was done as a part of the Oklahoma Agricultural Experiment Station Project Number 1208 titled Caged Cattle Feedlot Pen System. The project was financed through Experiment Station funds under the administration of Professor E. W. Schroeder, Head of the Agricultural Engineering Department.

I extend my sincere appreciation to Dr. Gordon L. Nelson who has served as my major advisor. I am grateful to him for his guidance in my graduate program, in the classroom, and in the design and conduct of my research project.

I thank Professor G. W. A. Mahoney of the Agricultural Engineering Department, and Professors David Macalpine and Robert L. Janes of the Civil Engineering Department for serving on the advisory committee.

Jack Fryrear and Don McCrackin provided generous assistance in preparing illustrative material. The personnel of the research laboratory assisted greatly in fabricating special test equipment. I thank these men for their cooperation.

The administration at North Dakota State University arranged for my leave of absence from that University for further graduate study. I extend my appreciation to W. J. Promersberger, Head of the Agricultural Engineering Department, Arlon G. Hazen, Dean of the College of Agriculture, and H. R. Albrecht, President of North Dakota State University for these arrangements.

To my wife, Patti, and my children, Nancy and Tom, I am especially grateful for their understanding and encouragement during the time this study was made.

TABLE OF CONTENTS

LIST OF TABLES

LIST OF FIGURES

Figure Page

CHAPTER I

INTRODUCTION

Background

Perforated floor systems are being used in livestock barns as devices for collecting the waste material from livestock. Movement of the livestock on the floor forces the waste material through the perforations into storage pits located below the floor. Livestock waste collected and stored in this way may be mixed to form a slurry that can be pumped. The slurries can be transported in tank wagons and spread in fields as fertilizer or they can be conveyed to disposal systems to be reduced by the action of microorganisms. These methods of livestock waste disposal are proving to be more efficient than conventional solid waste handling systems have been.

A series of long slender beams positioned parallel to each other are used to form the perforated floors that are in general use. These beams are installed with a narrow space between them through which the waste material may pass.

All classes of livestock are being adapted to these slatted floor systems. Floor designs for hogs are well perfected. The greater weight of cattle as compared to hogs has made it necessary to use beams of larger proportions for cattle than for hogs. Single beam slats having spans up to twelve feet in length are commonly used.

The Problem

A design consisting of a series of beams interconnected to form a gridwork as illustrated in Figure 1 will be evaluated. Such a system could distribute a load applied to any one slat over the four or five beams in the series and thus reduce the stresses in the loaded beam.

For single beam type slats each beam must be designed for the maximum load that may be applied at any one time. For gridwork designs, it should be safe to assume that if one slat is fully loaded by cattle, the two or three beams adjoining each side of the loaded beam could not be fully loaded. This loading assumption plus the stress distribution away from a loaded slat that can be expected in a gridwork should provide economy of design.

Objectives

The objectives of the study are to:

1. Obtain data suitable for developing prediction equations that describe the strains and the deformations in a gridwork slat system when loads are applied to any of the component slats. Strains and deformations will be related mathematically to the variables that influence the strain and deformation.

2. Compare the prediction equation with theoretical design procedures that have been developed.

3. Adapt the prediction equation to the design of prototype slats suitable for use in commercial cattle producing systems.

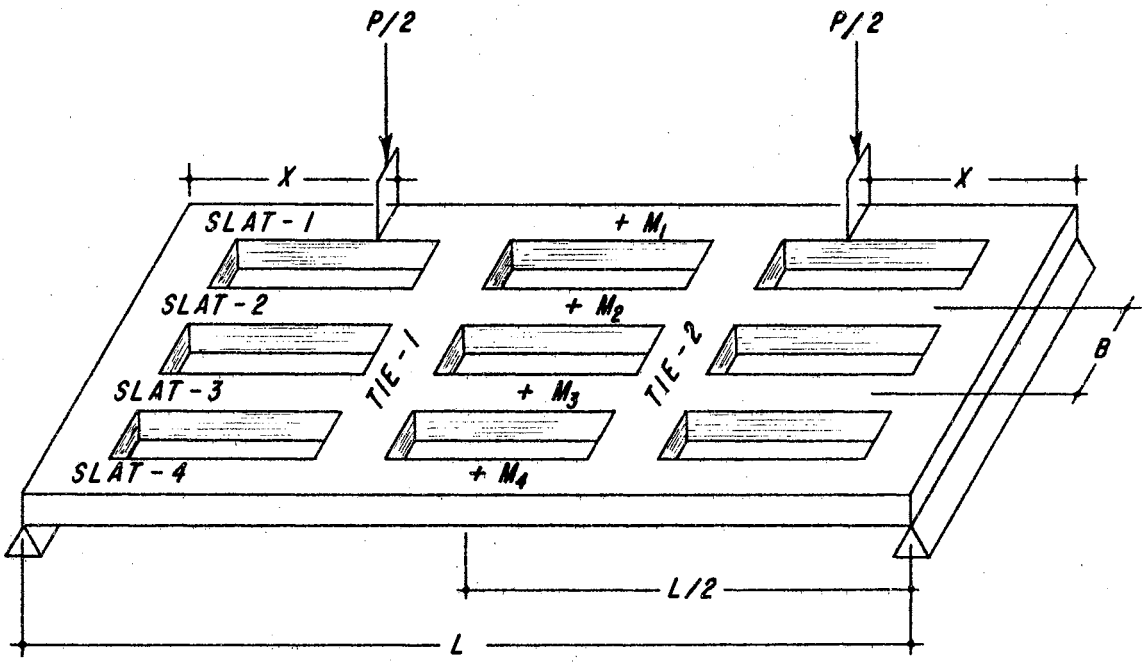

Figure 1. Configuration of Gridwork Suitable for Cattle Floor Systems

CHAPTER II

LITERATURE REVIEW

Load Assumptions for Slats for Cattle Floors

Hoibo (6) published a report in 1960 on the results of structural tests made in Norway on concrete floor slats for cattle. Burgener (2) adapted these test results to designs suitable for American needs. The floor slats designed for cattle in these papers are developed as simple beams. Hoibo presented an extensive analysis of the loading assumptions appropriate for the design of the slats. These assumptions suggest individual loads of one-fourth the animal weight. The distance between an animal's hoofs is assumed as one foot and the distance between adjacent animals as two feet. The maximum number of hoof loads possible with these spacings are placed on a slat. For moment calculations, two superimposed hoof loads at midspan are assumed. Figure 2 illustrates the application of these assumptions to a slat eight feet long.

Berhe (1) concluded from data on animal weight and configuration measurements that the ratio of the animal weight exerted through the front legs to that exerted through the hind legs is approximately one and one-fourth to one. These data may be adapted to the assumptions given by Hoibo.

Hoibo concluded that slats having a trapizoidal cross section provided for best disposal of droppings and that the slats need not

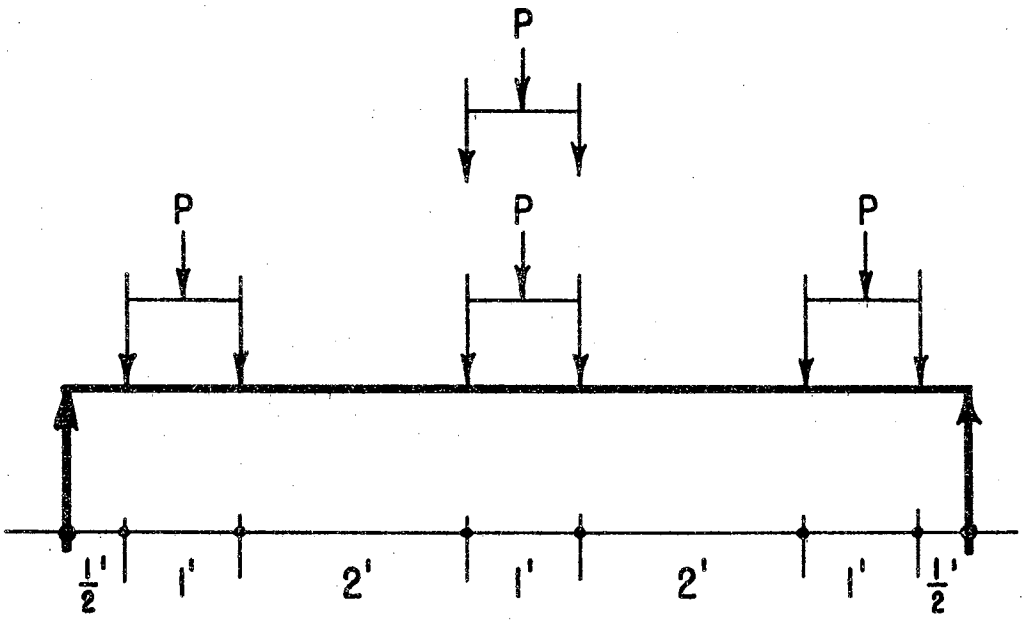

Figure 2. A Loading Assumption Used to Design a Single Slat that is Eight Feet Long

be reinforced for diagonal tension.

Using the results of Hoibo's work, the Portland Cement Association (18) has designed a set of reinforced concrete slats for cattle. Figure 3 illustrates the design for a single slat for cattle designed to span eight feet. Designs for prestressed concrete slats have not been published, but such slats are being produced commercially. All steel slats are also being fabricated.

Slope Deflection Analysis of Gridworks

The Portland Cement Association (18) suggests a design for precast slotted floor sections for hogs and sheep designed as gridworks. These are cast in individual sections from sixteen to twenty-four inches wide with openings cast into the sections. The publication points out that such sections are heavier to handle than individual slats, but that they do not need spacers to hold all slats in position. For hogs and sheep the slat cross section for the grids is suggested but no design procedures are provided. Designs of grids for cattle floors are not included in this publication.

Tolaba (21), and Tuma and Tolaba (22) have tabulated the equations needed to analyze for stresses and deformations in rectangular gridworks using slope deflection equations. In the analysis, a rectangular planar grid is assumed to be loaded as shown in Figure 4.

These analyses include the torsional stiffness of the slats. The slope deflection equations are written for the members that meet at a common junction as illustrated in Figure 5.

V represents shear, T represents torque, and M represents bending moment. Torque is a moment acting around the axis of a slat or tie.

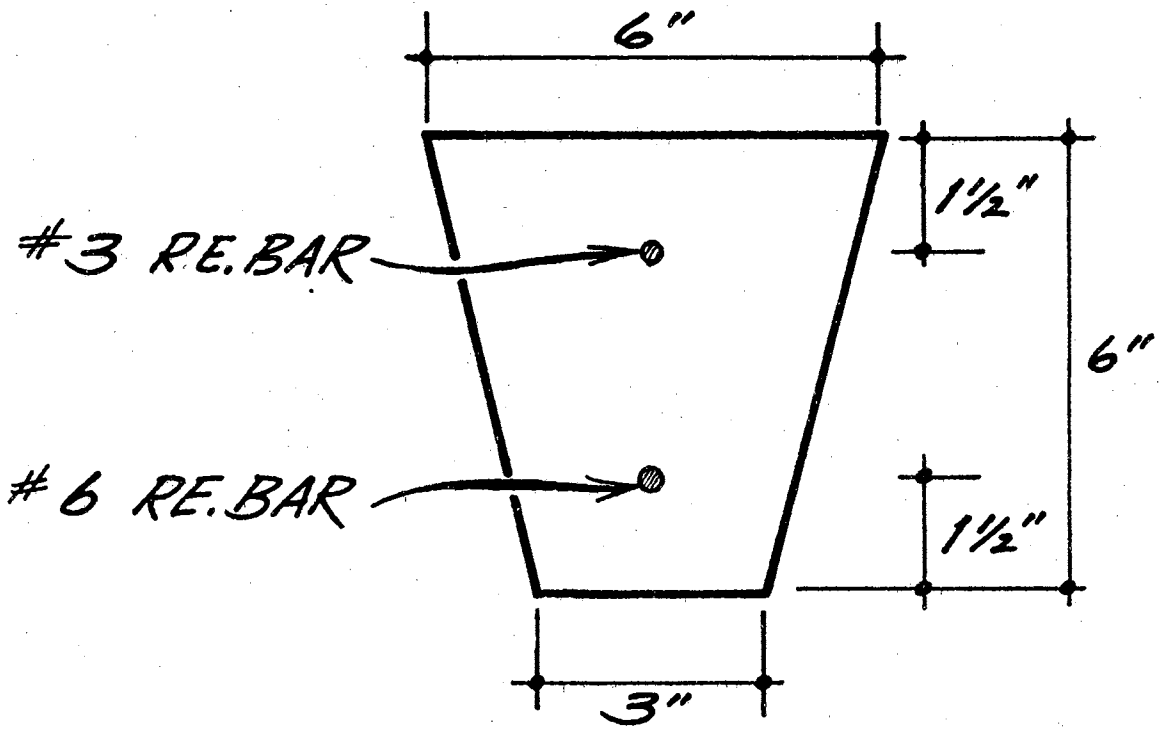

Figure 3. Cross Section of a Single Slat for Cattle Designed to Span Eight Feet

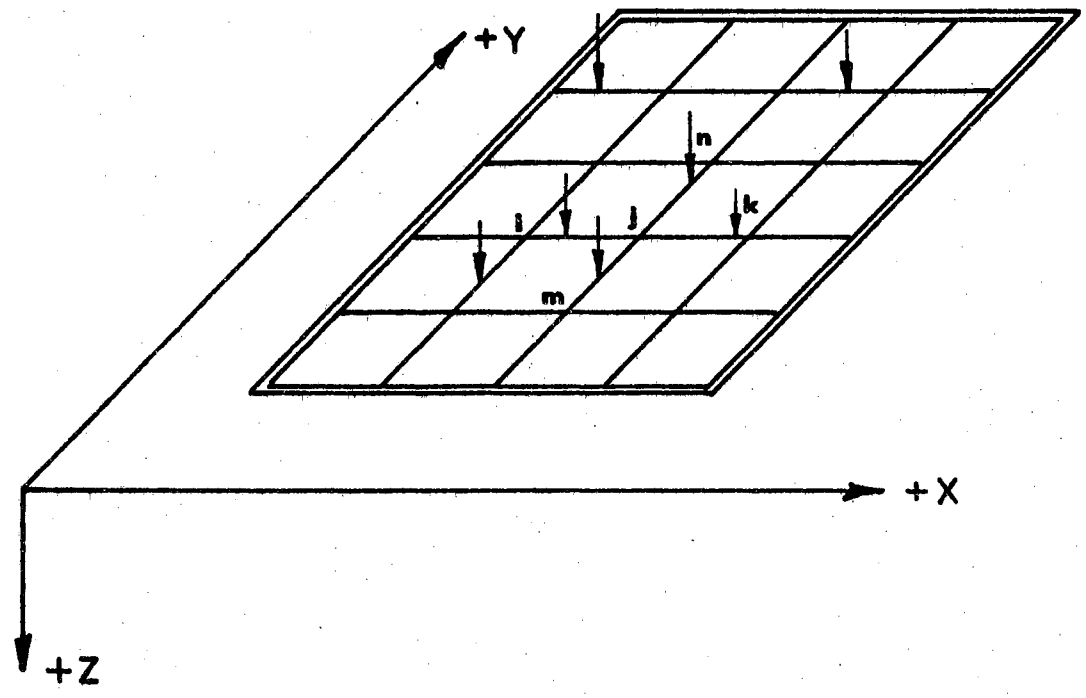

Figure 4. Rectangular Planar Grid Configuration Used for Slope Deflection Analysis

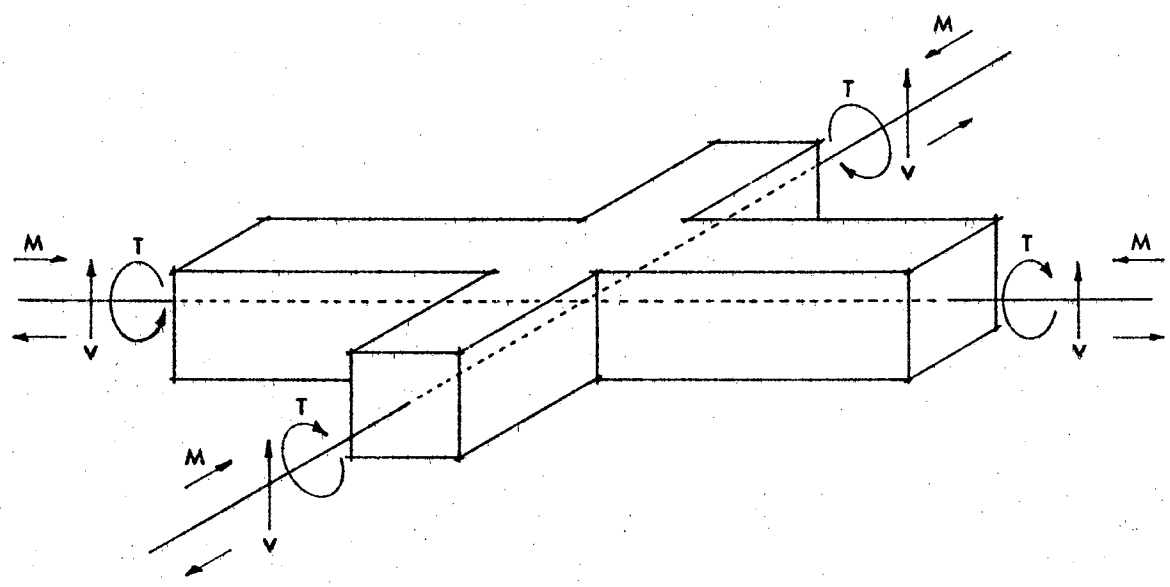

Figure 5. Free Body Diagram of a Slat-Tie Junction in a Gridwork

Bending moment changes the curvature of the longitudinal axis of a slat or tie.

Joint equilibrium equations are then written such that the sum of all end moments, end forces, and joint loads at a given joint with respect to a given axis is equal to zero. The equations are written as follows:

$$M_{ji} + M_{jk} + T_{jn} + T_{jm} = 0$$

$$M_{jm} + M_{jn} + T_{ji} + T_{jk} = 0$$

$$V_{ji} + V_{jn} + V_{jk} + V_{jm} - P_j = 0$$

Subscripts define the members under stress as identified in Figure 4.

Moment equations used are:

$$M_{ji} = K_{ji}\theta_j + CK_{ij}\theta_i + S_{ji}\,(\Delta_i - \Delta_j) + FM_{ji}$$

$$M_{jk} = K_{jk}\theta_j + CK_{kj}\theta_k + S_{jk}\,(\Delta_j - \Delta_i) + FM_{jk}$$

$$M_{jm} = K_{jm}\phi_j + CK_{mj}\phi_m + S_{jm}\,(\Delta_m - \Delta_j) + FM_{jm}$$

$$M_{jn} = K_{jn}\phi_j + CK_{nj}\phi_n + S_{jn}\,(\Delta_j - \Delta_n) + FM_{jn}$$

Torsion equations used neglecting externally applied torque are:

$$T_{jm} = K'_{jm}\theta_j + CK'_{mj}\theta_m$$

$$T_{jn} = K'_{jn}\theta_j + CK'_{nj}\theta_n$$

$$T_{ji} = K'_{ji}\phi_j + CK'_{ij}\phi_i$$

$$T_{jk} = K'_{jk}\phi_j + CK'_{kj}\phi_k$$

Shear equations used are:

$$V_{ji} = -S_{ji}\theta_j - S_{ij}\theta_i - R_{ji}\,(\Delta_i - \Delta_j) + FV_{ji}$$

$$V_{jk} = +S_{jk}\theta_j + S_{kj}\theta_k + R_{jk}\,(\Delta_j - \Delta_k) + FV_{jk}$$

$$V_{jm} = +S_{jm}\phi_j + S_{mj}\phi_m - R_{jm}\,(\Delta_m - \Delta_j) + FV_{jm}$$

$$V_{jn} = -S_{jn}\phi_j - S_{nj}\phi_n + R_{jn}\,(\Delta_j - \Delta_n) + FV_{jn}$$

The following notations are used:

θ - rotation around y axis

ϕ - rotation around x axis

Δ - vertical translation

FM - fixed end moments

FV - end shears

If each slat has a uniform cross section and if E is the modulus of elasticity, I is the moment of inertia, and L is the length of the slat or tie between gridwork junctions, the constants used in the moment and shear equations are as follows:

$$K_{ji} = \frac{4E_{ji}I_{ji}}{L_{ji}}$$

$$CK_{ij} = \frac{2E_{ij}I_{ij}}{L_{ij}}$$

$$S_{ji} = \frac{6E_{ji}I_{ji}}{(L_{ji})^2}$$

Similar terms are written for K, CK, and S terms having other subscripts.

If each slat has a uniform cross section, and if G is the shear modulus, J is the torsional moment of inertia, and L is the length of the member, the constant used in the torsion and shear equations are as follows:

$$K'_{ji} = \frac{G_{ji}J_{ji}}{L_{ji}}$$

$$CK'_{ij} = \frac{-G_{ij}J_{ij}}{L_{ij}}$$

$$R_{ji} = \frac{12E_{ji}I_{ji}}{L_{ji}}$$

Similar terms are written for K', CK', and R terms having other subscripts.

Fixed end moment expressions are written:

$$FM_{ji} = + \frac{Pu^2v}{L^2_{ji}}$$

$$FM_{jk} = - \frac{Puv^2}{L^2_{jk}}$$

$$FM_{jm} = + \frac{Pu^2v}{L^2_{jm}}$$

$$FM_{jn} = - \frac{Puv^2}{L^2_{jn}}$$

where v is the distance of the load from j and L - v = u.

Defining the location of P for end shears the same as was done for FM, the end shear expressions are written as follows:

$$FV_{ji} = - \frac{Pu^2 (L + 2v)}{(L_{ji})^3}$$

$$FV_{jk} = - \frac{Pv^2 (L + 2u)}{(L_{jk})^3}$$

$$FV_{jm} = - \frac{Pu^2 (L + 2v)}{(L_{jm})^3}$$

$$FV_{jn} = - \frac{Pv^2 (L + 2u)}{(L_{jn})^3}$$

When appropriate expressions for moment, torque, and shear are substituted into the joint equilibrium equations, they are then transformed into expressions in terms of rotations around the x axis, rotations around the y axis, and translation parallel to the z axis.

Analysis of a grid is accomplished by writing equations for each point at which members meet to form a junction in the gridwork. This results in a series of simultaneous equations. Appropriate end

conditions for θ, $\emptyset$, and Δ terms are assumed. Solution of the equations is usually best accomplished by writing the equation in a matrix form called a stiffness matrix, inverting this matrix, and multiplying the inverted matrix by the original stiffness matrix. This evaluates the unknown θ, $\emptyset$, and Δ terms. Electronic computer solutions are a practical way to evaluate these equations.

Similar analyses are presented by Martin and Hernandes (9) and Ferguson (3). In England, Lightfoot and Swako (8) published the matrix form of the generalized slope deflection equations for grid frameworks. Adapting this solution to the electronic computer is discussed. Presentations are similar to those of Tolaba (21), and Tuma and Tolaba (22).

Plate Theory

Theory using the differential equation that describes the deformation of thin plates can be extended to the analysis of gridworks. Timoshenko and Woinowsky - Krieger (20) record the modifications of the plate equation needed to adapt it to grid design. Figure 6 illustrates the definitions of the variables used in the equation.

$$M_{xy} = \frac{C_1}{b_1} \frac{\partial^2 W}{\partial_x \partial_y}$$

$$M_{yx} = \frac{C_2}{a_1} \frac{\partial^2 W}{\partial_x \partial_y}$$

where C_1 and C_2 are the torsional rigidities of the beams parallel to the x and y axis respectively and W is the deflection of the plate.

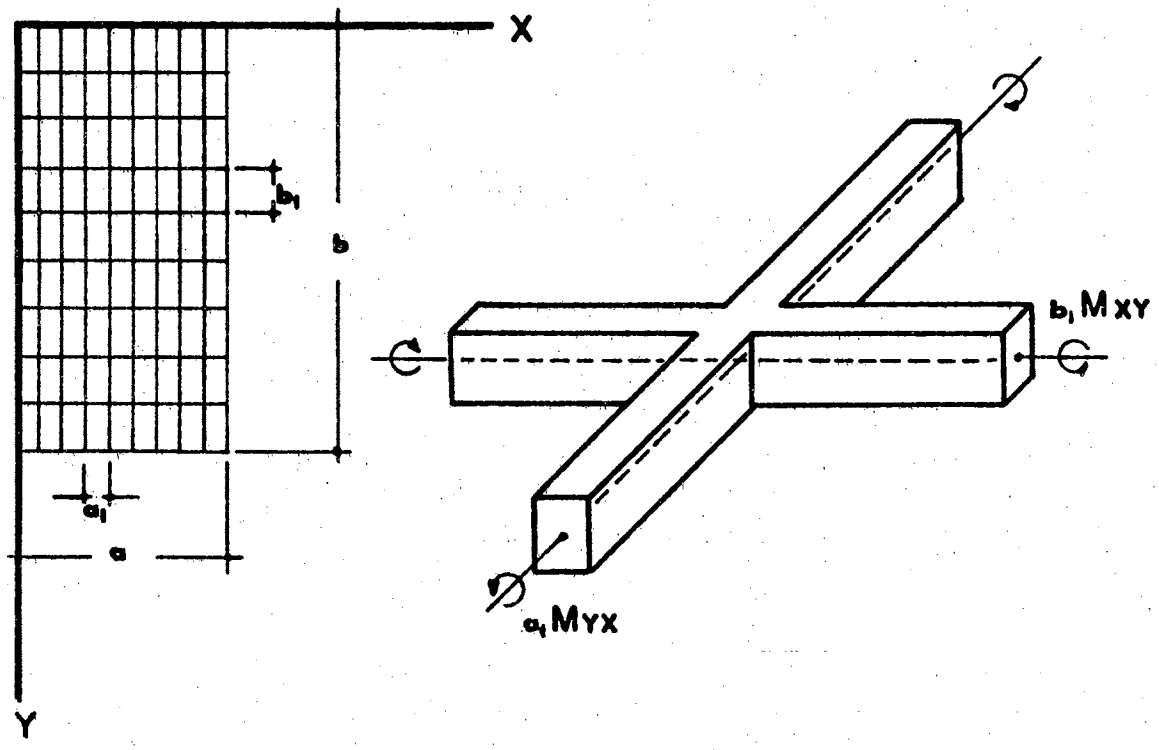

Figure 6. Variables Used in Gridwork Analysis Using Plate Theory

The differential equation adapting plate theory to gridwork analysis is:

$$\frac{B_1}{b_1}\frac{\partial^4 W}{\partial x^4} + \left(\frac{C_1}{b_1} + \frac{C_2}{a_1}\right)\frac{\partial^4 W}{\partial x^2 \partial y^2} + \frac{B_2}{a_1}\frac{\partial^4 W}{\partial y^4} = P$$

where B_1 and B_2 are the flexural rigidities of the beams parallel to the X and Y axis respectively and P is the load.

The solution for a uniform load over the grid surface can be found by assuming that the deflection, W, takes the form of a sine series.

Guyon-Massonnet Grid Analysis

Guyon (4) utilized the application of the plate theory to gridworks to analyze grids for cases where the torsional stiffness equals zero. In his analysis, he developed coefficients, K, suitable for distributing the deflection of the loaded slats to the other slats in the grid system.

Massonnet (10) extended the study to include cases that had torsional stiffnesses that are not equal to zero.

Morice and Little (12) plotted the distribution coefficients, K, from Guyon and Massonnet in a series of curves that can be used for the solution of the stresses and deformations of unsymmetrically loaded gridwork systems. His investigation was designed to check the validity of the plate theory for the design of bridge beams connected to form a grid.

Figure 7 illustrates the symbols used to define the dimensions of a gridwork under analysis. The effective width is 2b and is equal to S + p.

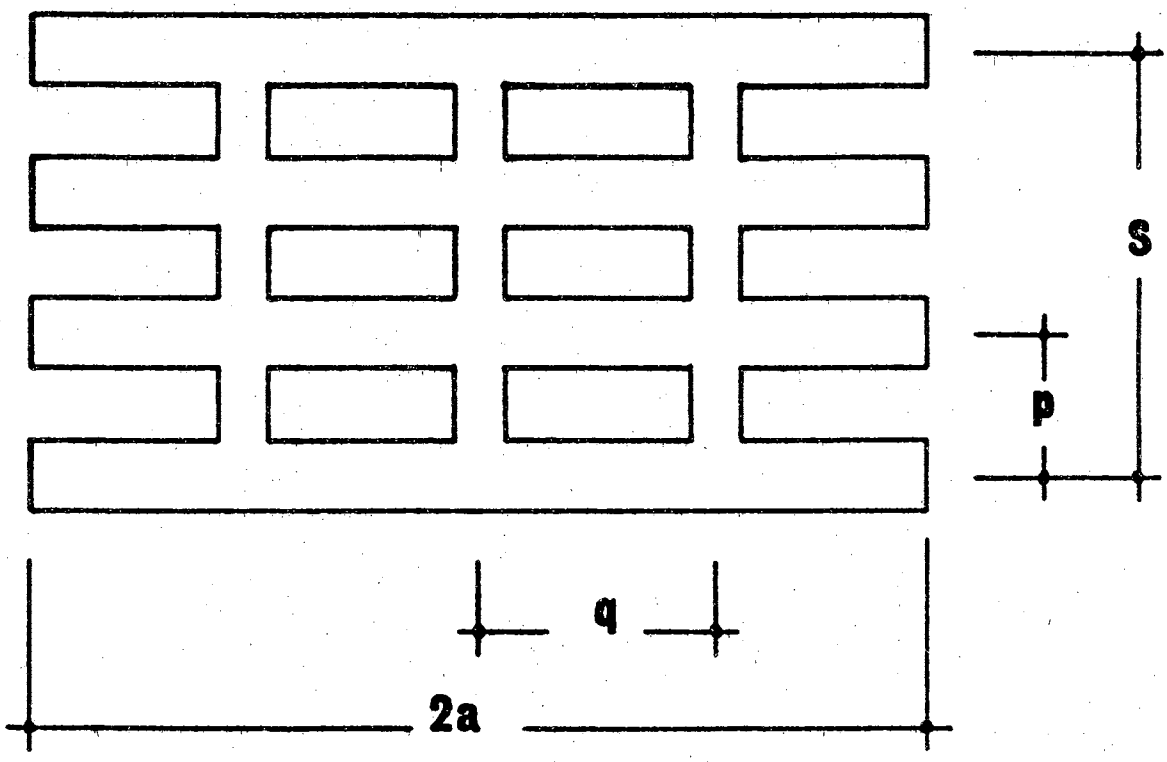

Figure 7. Variables Used in Guyon-Massonnet Analysis of Grids

Distribution coefficients, K, taken from the Guyon-Massonnet curves are plotted by Morice in terms of rigidity factors, θ, effective beam position, EBP, and torsion parameters, α.

The rigidity factor is defined as follows:

$$\theta = \frac{b}{2a} \sqrt[4]{\frac{i}{j}}$$

The effective beam position is defined as follows:

$$EBP = \left(\frac{n - 1}{n}\right) (\pm \text{ actual beam position})$$

The torsion parameter is defined as follows:

$$\alpha = \frac{G\ (i_o + j_o)}{2E\ \sqrt{ij}}$$

The variables in the expressions for θ, EBP, and α are defined as follows:

$i = \frac{I}{p}$

I = moment of inertia of main beam

$j = \frac{J}{q}$

J = moment of inertia of cross beam

n = the number of main beams

G = shear modulus

E = modulus of elasticity

$i_o = \frac{I_o}{p}$

I_o = torsional moment of inertia of the main beam

$j_o = \frac{J_o}{q}$

J_o = torsional moment of inertia of the cross beam

Morice presents two sets of curves. One is for cases where $\alpha = 0$. The other for cases where $\alpha = \infty$. In these curves θ is

plotted on the abscissa and K on the ordinate.

On each plot, separate curves are plotted for EPB values of -b, $-\frac{3b}{4}$, $-\frac{b}{2}$, $-\frac{b}{4}$, 0, $\frac{b}{4}$, $\frac{b}{2}$, $\frac{3b}{4}$, and b.

When $0 < \alpha < 1$, the distribution coefficient, K, is adjusted by the equation:

$$K_\alpha = K_o + (K_1 - K_o)\sqrt{\alpha}$$

K_α is the distribution coefficient for a torsion parameter equal to α, K_o is the distribution coefficient for the case where $\alpha = 0$. K_1 is the distribution coefficient for the case where $\alpha = \infty$.

To determine the deflections that occur in each main beam when the load is applied to one of the beams, the deflection, W, of the loaded beam is calculated as if it were a single beam. The mean deflections, MW, are calculated by the following equations:

$$MW = \frac{W}{n}$$

where n is the number of main beams. The design deflection, DW, is then:

$$DW = (K)(MW)$$

The distribution of the moments across the grid are determined in a similar manner. The bending moment, BM, of the loaded beam is calculated as if it were a single beam. The mean bending moment is computed by the following equation:

$$MBM = \frac{BM}{n}$$

The design bending moment, DBM, is then:

$$DBM = (K)(MBM)$$

Rowe (16) has included the Guyon-Massonnet analysis for gridwork systems for bridges in his book on concrete bridge design. Examples of designs for grids are included.

Dimensional Analysis and Similitude

Murphy (13) presents a procedure for the design of engineering research tests. His approach employs the principles of dimensional analysis and similitude to evaluate the response that can be expected from a prototype system based on experiments with models. Models are designed on the basis of similitude theory.

The first step in the design of a model study is to identify and list all variables that influence the performance of the system being modeled. These variables should include those that are to be predicted called the dependent variables and the independent variables that influence those being predicted. All variables influencing the system must be included if dependable predictions are to be made for the system. Redundancy in the list will cause unnecessary test work.

The variables are arranged into dimensionless groups. The Buckingham Pi Theorem discussed by Murphy (12) provides a means for making these arrangements. Dimensions are assigned to each variable to properly describe the variable. The variables are then grouped into dimensionless parameters called pi terms. The Buckingham Pi Theorem states that the number of independent pi terms that can be formed equals the number of variables involved in the system minus the rank of the dimensional matrix. The number of variables that must be considered in a sequence of tests are reduced by this technique. If the first pi term is considered as the parameter containing the dependent

variable, the general relationship between the variables influencing the system can be written:

$$\pi_1 = f(\pi_2, \pi_3, \pi_4, \ldots \pi_n)$$

Murphy (13) outlines procedures that are suitable for evaluating a function that describes the performance of a system by the use of models. The theory states that observations in an experiment should be arranged so that all independent pi terms except one involved in the function remain constant with that one varied to establish a relationship between it and the dependent pi term. The procedure is repeated for each independent pi term in the system. If π_1 is the dependent pi term, these relationships can be written in the following form if the bar over the pi symbol indicates that the term is held constant:

$$\pi_1 = \phi_1(\pi_2, \bar{\pi}_3, \bar{\pi}_4, \ldots \bar{\pi}_n)$$

$$\pi_1 = \phi_2(\bar{\pi}_2, \pi_3, \bar{\pi}_4, \ldots \bar{\pi}_n)$$

$$\pi_1 = \phi_3(\bar{\pi}_2 \ \bar{\pi}_3 \ \pi_4, \ldots \bar{\pi}_n)$$

$$\pi_1 = \phi_{n-1}(\bar{\pi}_2, \bar{\pi}_3, \bar{\pi}_4, \ldots \pi_n)$$

Models may be used to obtain the relationship between the parameters. Models may be of any size in relation to a prototype, but in engineering research greatest economy and convenience is usually obtained by using models smaller than the prototypes being evaluated. For structural testing, models need not be geometrically similar, but they may be.

A set of relationships established for a model will be valid for a prototype if the following conditions are met:

$$(\pi_1)_{model} = (\pi_1)_{prototype}$$
$$(\pi_2)_{model} = (\pi_2)_{prototype}$$
$$(\pi_3)_{model} = (\pi_3)_{prototype}$$
$$\vdots \qquad\qquad \vdots$$
$$(\pi_n)_{model} = (\pi_n)_{prototype}$$

If the range of values used for pi terms for models is the same as the range expected for prototypes, test results for models will be valid for predicting the performance of the prototype. Murphy (13) outlines a method that can be used to combine these relationships into one equation.

One possible form of a suitable prediction equation is:

$$\pi_1 = \emptyset(\pi_2^{m_2}, \pi_3^{m_3}, \pi_4^{m_4}, \ldots \pi_n^{m_n})$$

Experimental data can be used to define values of $\emptyset$, m_2, m_3, m_4, ... m_n for the range of values of the component pi terms being evaluated.

Structural Modeling with Plaster of Paris

Plaster of Paris possesses characteristics that make it suitable for many structural modeling applications. Many prototype materials are characterized by a stress strain relationship that is approximately linear in the elastic range. Preece and Sandover (14) and Mattock (11) suggest that materials used to model these prototype materials should also have a linear modulus of elasticity in the elastic range. Preece and Sandover (14) further point out that the material used for modeling should be easily worked and should be a stable material.

Figure 8 shows a typical stress-strain diagram for cured plaster of Paris and concrete in compression. These curves are given by Roark and Hartenberg (15). It will be noted that the modulus of the elasticity of the plaster of Paris appears to be nearly linear up to the rupture point. All test data from plaster of Paris models will be taken when the stress-strain relationship is in the elastic range. These results applied to a prototype will be suitable for evaluating the stress-strain relationships in its elastic range only. Beyond its elastic range, test results will not be valid. Poisson's ratio is reported by Roark and Hartenberg (15) to range from .06 to .10. Wianecki (22) presents a series of curves showing the stress-strain relationship for plaster of Paris in both compression and tension and his data indicates that the curves by Roark and Hartenberg are valid. Wainecki presents a series of curves on plaster of Paris manufactured with varying quantities of water. The influence of the variation in the water on the quality of the plaster of Paris is shown in these curves. His calculations for Poisson's ratio indicate that it ranges from 0.196 to 0.206 depending on the water used for mixing. Hetenyi (5) points out that a variety of plaster materials are available commercially that are suitable for model tests. These include molding plaster, plaster of Paris, or a high-grade pottery plaster. The chemical composition of these materials is about the same but the pottery plaster is preferable in many ways because it has a somewhat slower setting time and permits a longer time for working the material. It is pointed out again that the quantity of water used in mixing the plaster affects its quality. Proportions of 70 pounds of water to 100 pounds of plaster of Paris when properly mixed will give materials with a modulus of

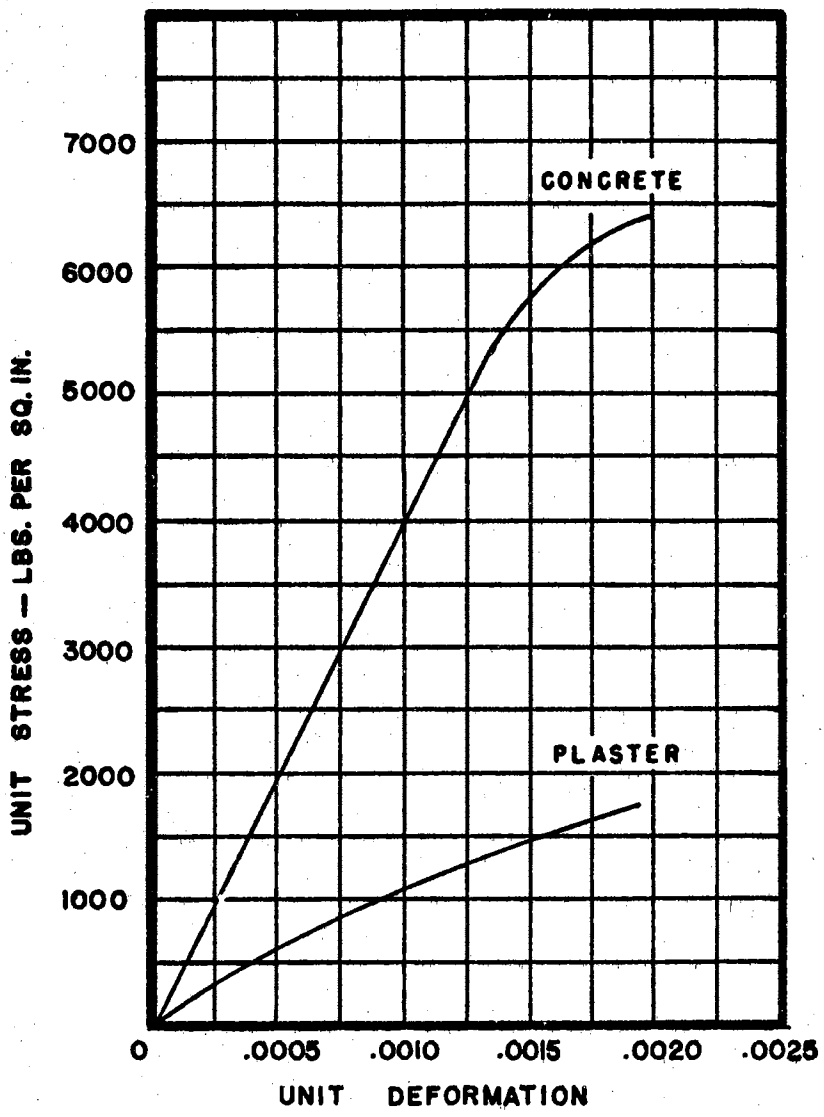

Figure 8. Typical Stress-Strain Diagram for Concrete and Plaster of Paris

elasticity of about one million PSI, a compressive stress of about 1,800 PSI, and tensile strength from 600-800 PSI.

Recommendations for mixing the plaster of Paris suggest that pure drinking water at room temperature should be used. The plaster should be slowly mixed into the water and the mixture should be permitted to blend for 10-12 minutes. After the curing period, the plaster of Paris should be slowly stirred to permit entrapped air bubbles to escape. This should continue for about five minutes.

Plaster of Paris undergoes a small volume expansion as it cures. The curing process also involves a reaction that warms the plaster and causes it to sweat. This sweating characteristic makes it easy to remove the curing plaster of Paris from oiled molds after it has hardened. For best strength characteristics, the specimens should be cured in a moist room for about two days and then dried for a minimum of three weeks at room temperature. Rapid curing at room temperature is not recommended.

CHAPTER III

THE DESIGN OF EXPERIMENTS

The design of a series of slats interconnected to form a gridwork in such a way that it would be suitable for cattle floors is an indeterminate structural problem. Designing such systems may be based on theoretical analyses. A model study was designed for the purpose of validating the techniques used in theoretical analyses. To facilitate the use of theoretical analyses, a gridwork system must be idealized. Slat and tie lengths are taken from the center of one junction to the center of an adjoining one. In grids where the length of the ties is short, slat width could have a significant effect. Validation of theoretical analyses by experimental techniques would indicate the reliability of idealizations such as these.

The study was limited to gridwork systems having four slats only. Four slat reinforced concrete grids adapt well to cattle barn designs.

Plaster models of gridwork systems were fabricated and tested under loads. The loading system suggested by Hoibo (6) was used as a basis for determining the loadings that might be anticipated on slat systems. With cattle loads it was considered that adjoining slats would not be loaded simultaneously. In a four-slat gridwork, it is conceivable that one outside slat only might be loaded and in this way would give maximum eccentricity to the loading on the gridwork.

Symmetrical loading across the gridwork might also occur. Load tests were therefore done by applying pairs of loads symmetrically placed on slats in the model gridwork system, as shown in Figure 1. One slat was loaded at a time. The effects of several pairs of loads could be obtained by using the principle of superposition if the system were stressed within its linear stress-strain range.

Factors needed for the design of the main slats in a gridwork system include the deflection of the slats and the strain developed on the surfaces of the slats. With bending occurring in the slats, maximum strain should occur on the top and bottom surfaces of each of the slats. Loads were applied to the slats in a symmetrical pattern. If the grid systems are assumed to deform as plates deform in the theory of plates, maximum translation and strain should occur at the center of the slats. All measurements of these characteristics were taken at slat centers.

End support systems for the gridworks were designed as simple supports. The cross sectional configuration of the slats and ties was assumed to be identical.

The principles of engineering similitudes along with dimensional analysis were utilized in the design of the series of tests. Prediction equations were developed. A prototype grid was tested and test results were compared with values computed from the prediction equations.

Pertinent Quantities and Dimensionless Parameters

The pertinent quantities that are considered to influence the deflection and strain encountered in a gridwork system are tabulated in Table I. Definitions of pertinent quantities are illustrated in Figure 1. This listing includes both strain and deflection as dependent variables. The same independent variables are considered as influencing the strain and deflection in a gridwork system.

Forming the pi terms is done by considering e and d as the terms that are used to develop the dependent dimensionless parameter. The remaining eleven are used to form independent pi terms for analyzing for both e and d. Two dimensions are required to describe all variables so the number of independent pi terms required to predict each dependent pi term is calculated as follows:

11 independent variables - 2 dimensions = 9 independent pi terms.

Including the two dependent pi terms, a total of 11 pi terms should be formed. One set of parameters that can be formed are shown in Table II.

Prediction equations that may be written are:

$$\pi_1 = f(\pi_3, \pi_4, \pi_5, \pi_6, \pi_7, \pi_8, \pi_9, \pi_{10}, \pi_{11})$$

or

$$e = f(EI/GJ,\ EI/PL^2,\ L/B,\ L/X,\ T,\ S,\ b/L,\ h/L,\ XX/L)$$

and

$$\pi_2 = f(\pi_3, \pi_4, \pi_5, \pi_6, \pi_7, \pi_8, \pi_9, \pi_{10}, \pi_{11})$$

or

$$L/d = f(EI/GJ,\ EI/PL^2,\ L/B,\ X/L,\ T,\ S,\ b/L,\ h/L,\ XX/L)$$

TABLE I

PERTINENT QUANTITIES

No.	Symbol	Description	Dimensional Symbol
1	e	Strain (microinches/inch)	LL^{-1}
2	d	Deflection (inches)	L
3	EI	Stiffness; slat and tie (pounds – inches^2)	FL^2
4	GJ	Torsional rigidity; slat and tie (pounds – inches^2)	FL^2
5	L	Grid length (inches)	L
6	P	Concentrated loads (total of pair of loads symmetrically placed on a slat) (pounds)	F
7	B	O. C. slat spacing (inches)	L
8	X	Distance end of grid to load (inches)	L
9	T	Number of ties	--
10	S	Number of slats	--
11	b	Slat and tie width (inches)	L
12	h	Slat and tie depth (inches)	L
13	XX	Distance reference end of grid to point where strain and deflection are measured (inches)	L

TABLE II

DIMENSIONLESS PARAMETERS

$\pi_1 = e$	$\pi_5 = L/B$	$\pi_8 = S$
$\pi_2 = L/d$	$\pi_6 = X/L$	$\pi_9 = b/L$
$\pi_3 = EI/GJ$	$\pi_7 = T$	$\pi_{10} = h/L$
$\pi_4 = EI/PL^2$		$\pi_{11} = XX/L$

Discussion of Pi Terms

$\pi_1 = e$ is the parameter describing the strain encountered at the center of each slat due to a pair of loads on any slat. Strain by itself is a dimensionless term usually measured as microinches of strain per inch of beam length. With proper assumptions as to the variation in strain from the top to the bottom of the slat, the bending moment can be evaluated.

$\pi_2 = L/d$ is the parameter describing the deflection at the center of the slats in a loaded grid. The ratio of grid length to deflection is an index of deflection.

$\pi_3 = EI/GJ$ is a term that includes the bending stiffness and torsional rigidity of the slats and cross ties. The testing program was limited to grid systems in which these values were equal for slats and cross ties. This limitation results in a design that is suitable for a cattle floor system. E represents the modulus of elasticity and G the shear modulus of the material used in a grid. I represents the moment of inertia and J the torsional moment of inertia of the slats and cross ties.

$\pi_4 = EI/PL^2$ is the pi term that includes the effect of variation in load. The load is a force which is expressed in pounds.

$\pi_5 = L/B$ is the term that includes the on center spacing of the slats. The dimension of B is length and any other length term could be used to form the dimensionless parameter.

$\pi_6 = X/L$ represents the location of the load. X is a length measured from the end of the grid. It could be paired with any other length term to form a dimensionless parameter.

$\pi_7 = T$ has been defined as the term indicating the number of cross ties in the grid system. A cross tie is considered as extending across the width of the grid. This parameter is dimensionless.

$\pi_8 = S$ is defined as the term indicating the number of slats in the grid system. A slat extends from one end of the grid to the other. This parameter is dimensionless. These studies were limited to grids having four slats only.

$\pi_9 = b/L$ is the term that includes the width of a slat or tie. This term probably has local effects at the joints. These effects are of secondary importance and are therefore neglected in this study.

$\pi_{10} = h/L$ is the term that includes the depth of a slat or tie. This term was neglected in this study for the same reasons given for neglecting π_9.

$\pi_{11} = XX/L$ represents the distance from a reference end of a grid to the point at which strain and deflection are measured. In this study, only maximum values were considered. Two loads were placed an equal distance from each end of a slat to provide maximum deformations at the center of slats. This assumption is derived from plate theory.

Location of deformation measurements was not varied, but was recorded at the center of slats only.

Schedule of Experiments

The independent parameters that were selected as those that influenced the dependent strain parameter also were selected as those that influenced the dependent deflection parameter. $\pi_9 = b/L$ and $\pi_{10} = h/L$ were neglected. $\pi_8 = S$ and $\pi_{11} = XX/L$ were held constant in all tests. Prediction equations that include the significant independent parameters are:

$$\pi_1 = f(\pi_3, \pi_4, \pi_5, \pi_6, \pi_7)$$

or

$$e = f(EI/GJ, EI/PL^2, L/B, X/L, T)$$

and

$$\pi_2 = f(\pi_3, \pi_4, \pi_5, \pi_6, \pi_7)$$

or

$$L/d = f(EI/GJ, EI/PL^2, L/B, X/L, T)$$

The schedule of experiments in Table III summarizes the schedule of treatments for both grid strain and deflection tests.

The effect of each independent pi term on the dependent pi term describing strain or deflection was evaluated by five series of tests. In experiment series A, for example, π_3 was varied while the other four independent parameters were held constant. The other four independent pi terms were each varied in turn in a similar manner in the remaining four series of tests. A bar over the symbol for pi written as $\bar{\pi}$ in Table III indicates that the pi term is held constant in the test sequence under consideration.

TABLE III

SCHEDULE OF TREATMENTS FOR GRID STRAIN AND DEFLECTION TESTS*

Test Series	$\pi_3 = \frac{EI}{GJ}$	$\pi_4 = \frac{EI}{PL^2}$	$\pi_5 = \frac{L}{B}$	$\pi_6 = \frac{X}{L}$	$\pi_7 = T$
A	$(\pi_3)_1$ $(\pi_3)_2$ $(\pi_3)_3$ $(\pi_3)_4$	$\bar{\pi}_4$	$\bar{\pi}_5$	$\bar{\pi}_6$	$\bar{\pi}_7$
B	$\bar{\pi}_3$	$(\pi_4)_1$ $(\pi_4)_2$ $(\pi_4)_3$ $(\pi_4)_4$	$\bar{\pi}_5$	$\bar{\pi}_6$	$\bar{\pi}_7$
C	$\bar{\pi}_3$	$\bar{\pi}_4$	$(\pi_5)_1$ $(\pi_5)_2$ $(\pi_5)_3$ $(\pi_5)_4$	$\bar{\pi}_6$	$\bar{\pi}_7$
D	$\bar{\pi}_3$	$\bar{\pi}_4$	$\bar{\pi}_5$	$(\pi_6)_1$ $(\pi_6)_2$ $(\pi_6)_3$ $(\pi_6)_4$	$\bar{\pi}_7$
E	$\bar{\pi}_3$	$\bar{\pi}_4$	$\bar{\pi}_5$	$\bar{\pi}_6$	$(\pi_7)_1$ $(\pi_7)_2$ $(\pi_7)_3$ $(\pi_7)_4$

*π_1 = e and π_2 = L/d are the measured variables.

Experimental Equipment

Slat Stiffness Determinations

To evaluate EI and GJ for the grid tests, single slat tests were conducted to determine E and G. E was determined by measuring the deflection on a single slat that was symmetrically loaded with a pair of point loads. G was determined by measuring the angular rotation of a single slat to which a torsional load was applied.

Figures 9 and 10 illustrate the test equipment used to determine E. The equipment included:

1. Model support stand designed to reduce the deformation in the stand as much as possible when the models were loaded.
2. Molding plaster single beam model.
3. Low friction bearings supporting the ends of the beams.
4. Loading yokes.
5. Loading bar for distributing load to two loading yokes.
6. Weights.
7. Ames dial indicators. Deflection readings to the nearest .001 inch.
8. Dial indicator support stand.

Figures 11-14 illustrate the test equipment used to determine G. The equipment includes:

1. Molding plaster single slat model.
2. Model support stand. One end of the model was clamped rigidly to the stand. The other end was clamped to a circular plate which was supported on a pair of low friction rollers. A loading arm of known length was attached to the circular plate. An arm was placed on each side of the plate to equalize the dead load of the bars. Loads applied at one end of the bar would then be the only load causing torsion.
3. Weights.
4. Mirrors glued to the models a measured distance apart.

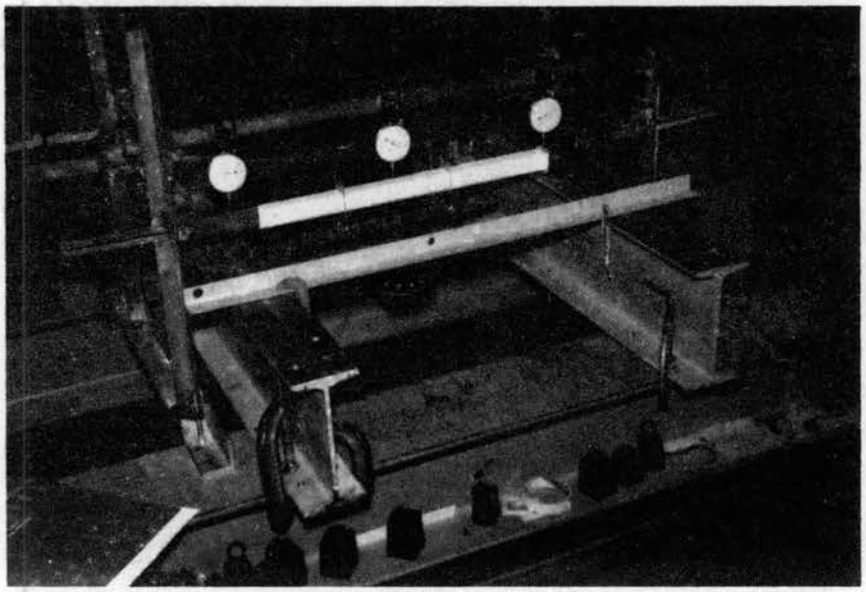

Figure 9. Test Equipment Used to Evaluate E for the Molding Plaster

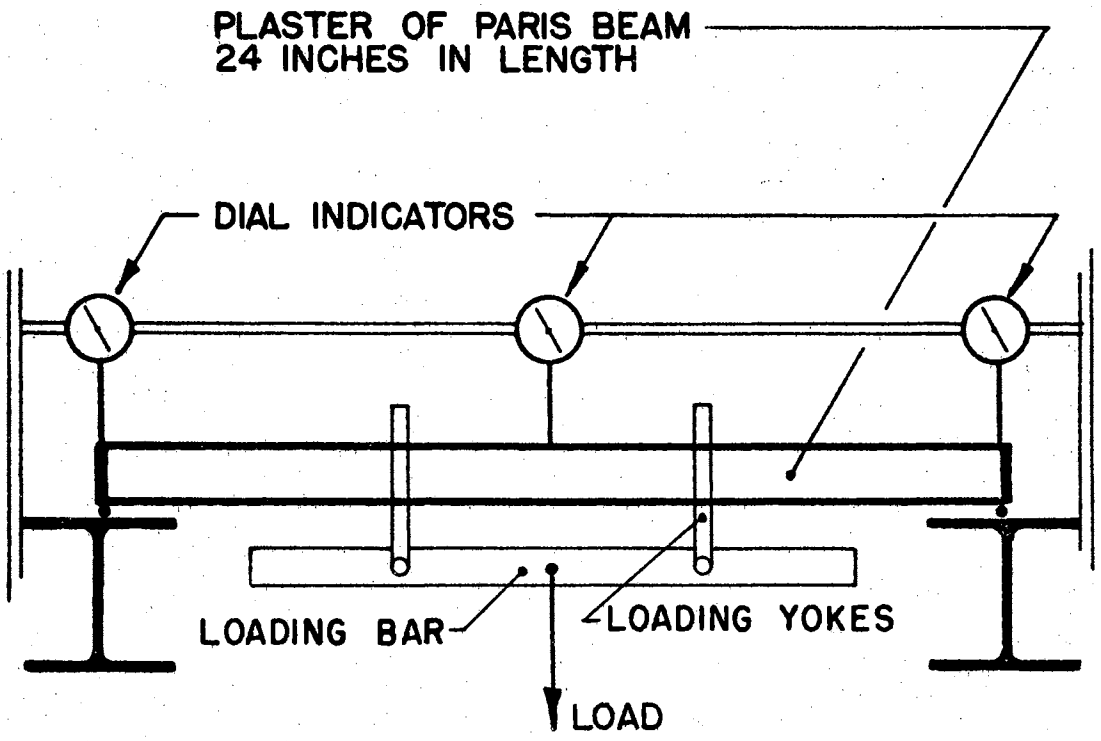

Figure 10. Diagram of Test Equipment Used to Evaluate E of Plaster

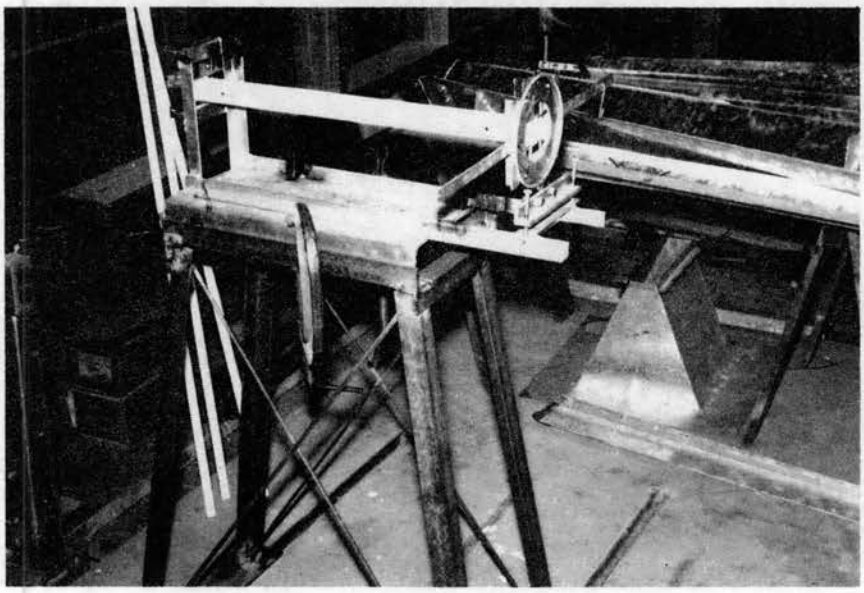

Figure 11. Torsion Machine Used to Evaluate G of the Molding Plaster

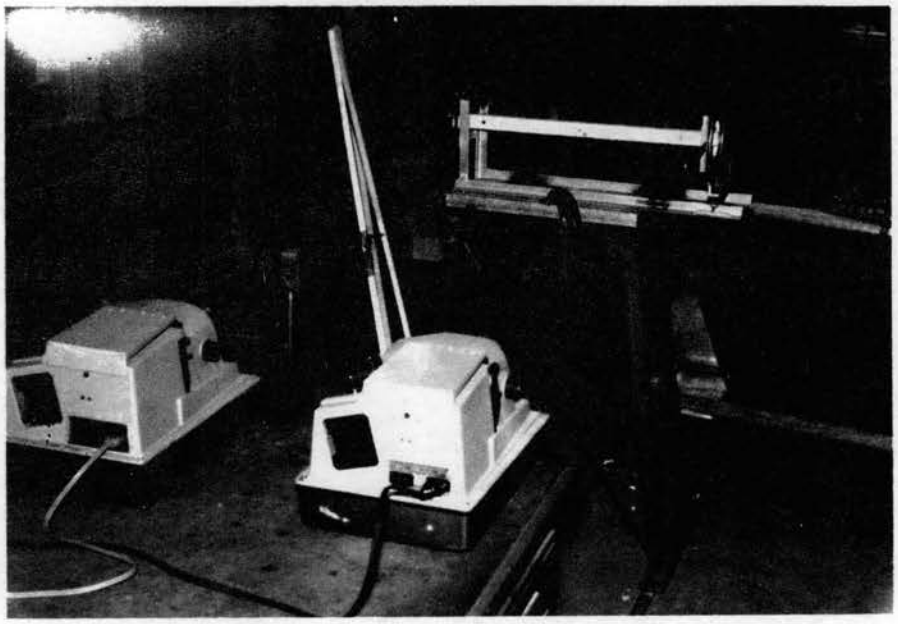

Figure 12. Projectors Directed at Mirrors on Test Slat for Evaluating the Twist in the Slat Under a Torsional Load

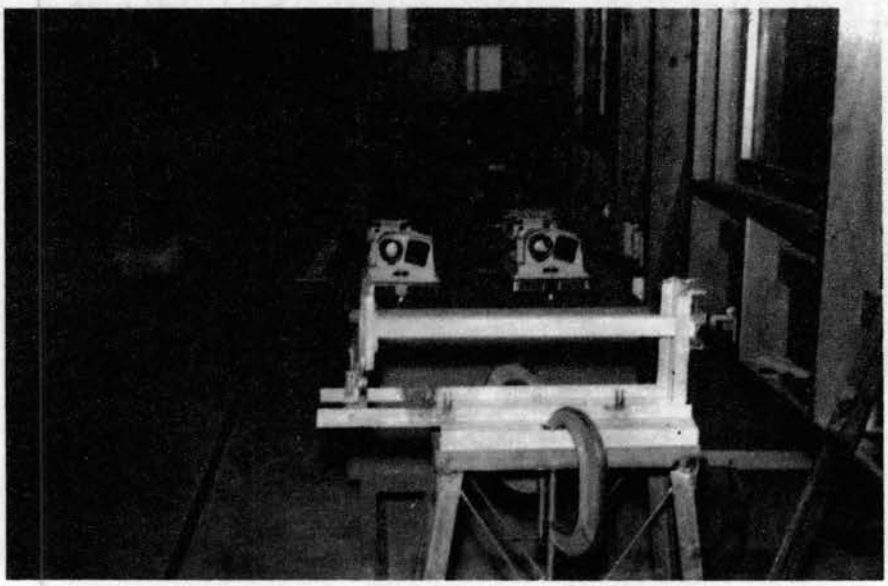

Figure 13. Relationship Between Projectors, Slat, and Measuring Scale Used for Evaluating the Twist in the Slat Under a Torsional Load

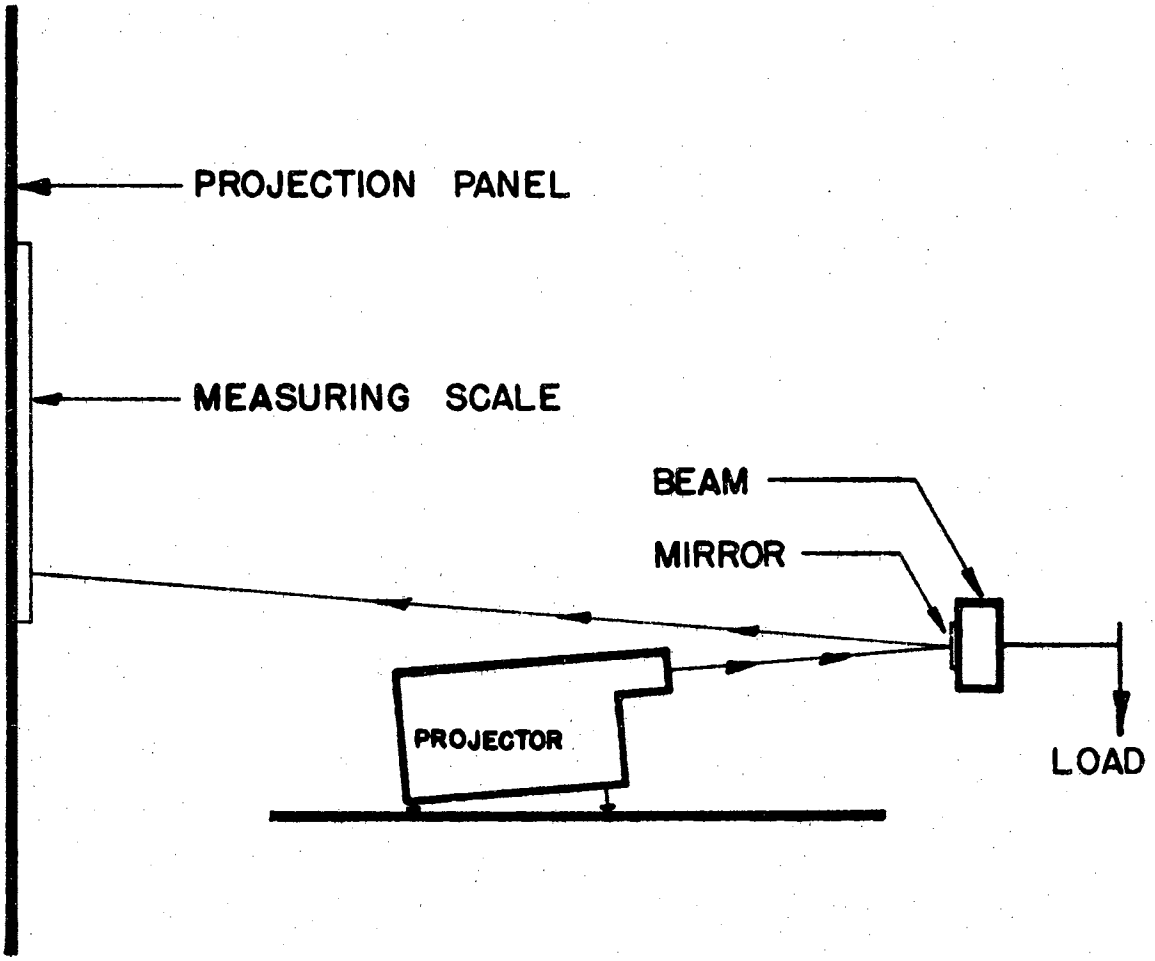

Figure 14. Diagram of Relationship Between Projectors, Slat and Measuring Scales Used for Evaluating Twist in the Slat Under a Torsional Load

5. Two 35 millimeter slide projectors.

6. Slides with mounted cross hairs. Human hairs were mounted in glass slides to provide the cross hairs.

7. Projecting boards with measuring scales. Cross hairs were projected from the projectors and were reflected from the mirrors to the projection board. Measurements provided data to determine beam twist.

Grid Tests

The same models were used for grid strain and grid deflection measurements. In one test sequence, these measurements were taken in separate tests. Based on the experience gained from these first tests, it was concluded that both sets of measurements could be taken concurrently. This was done on succeeding tests.

Figures 15 and 16 illustrate the test equipment used to determine the strain and deflection at the center of the slats in the grids. The support, loading, and strain gauge arrangement are similar to that of the single beam illustrated in Figures 9 and 10.

The equipment included:

1. Model support stand designed to reduce the deformation in the stand as much as possible when the models were loaded.

2. Molding plaster gridwork models.

3. Low friction bearings supporting the ends of the grids.

4. Loading yokes used to apply pairs of loads to each beam in turn in the grids.

5. Loading bar for distributing load to the two loading yokes.

6. Weights.

7. Ames dial indicators. Deflection reading to the nearest .001 inch.

8. Dial indicator support stand.

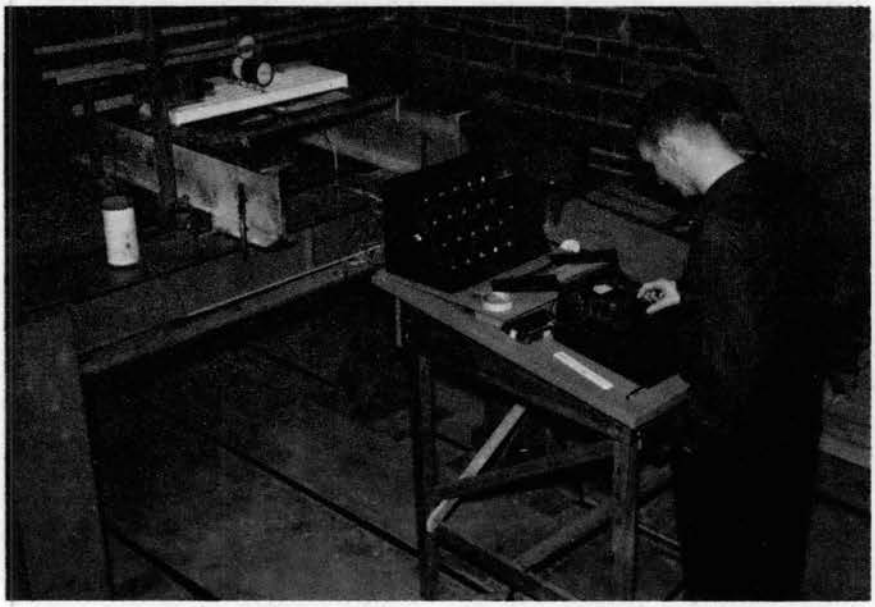

Figure 15. Apparatus Used to Test Plaster Grids Showing Dial Indicators and Strain Gauge Installation

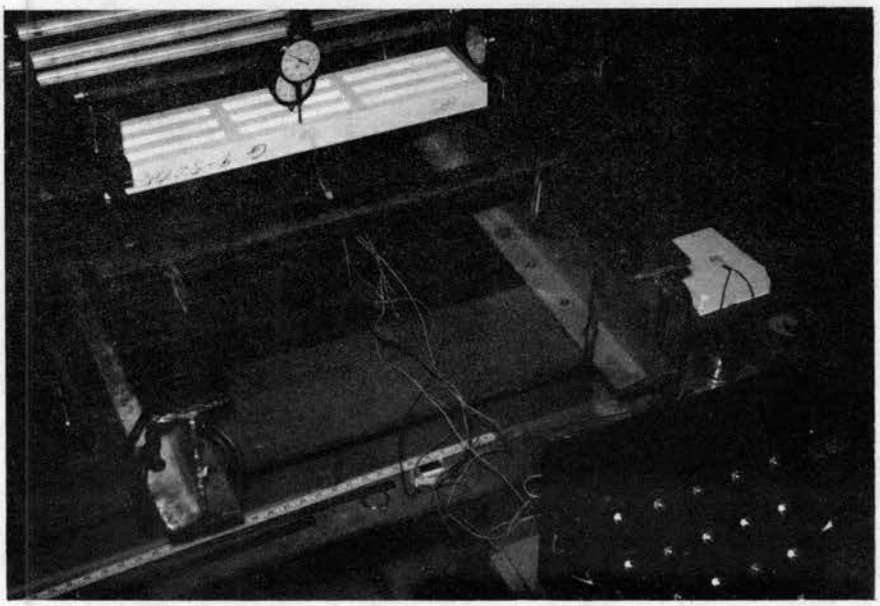

Figure 16. Plaster Grid Model in Position for Testing

9. SR-4 strain gauges, Baldwin-Lima-Hamilton. Type FAP-25-12 S-6 Constantan foil paper backed gauges. Gauge length: one-fourth inch.

10. Epoxy cement.

11. Baldwin-Lima-Hamilton strain gauge switch.

12. Baldwin-Lima-Hamilton single channel strain indicator.

CHAPTER IV

CHARACTERISTICS OF PROTOTYPE GRIDS SUITABLE FOR CATTLE FLOOR SYSTEMS

The range of values selected for the independent pi terms for the model tests was based on the characteristics of prototype gridworks suitable for livestock floor systems. Table IV lists the maximum and minimum values assigned to the independent pi terms.

TABLE IV

LIMITS OF VALUES ASSIGNED TO INDEPENDENT DIMENSIONLESS PI TERMS FOR MODEL TESTS AS DETERMINED FROM THE CHARACTERISTICS OF SUITABLE PROTOTYPE GRIDS

Pi Terms	Dimensionless Pi Term Values for Prototypes	
	Minimum	Maximum
$\pi_3 = EI/GJ$	0.80	4.63
$\pi_4 = EI/PL^2$	4.0	44.0
$\pi_5 = L/B$	9.0	24.0
$\pi_6 = X/L$	0.17	0.46
$\pi_7 = T$	1.0	4.0

π_3 is defined as EI/GJ. Placing limits on this pi term required that strength characteristics of the materials used for the prototype concrete grids be considered as well as the cross sectional shape of

the slats. It is common practice in reinforced concrete design of indeterminate structures to assume values of EI and GJ based on unreinforced concrete sections. This procedure was adopted for estimating the ratio EI/GJ for concrete prototypes. Roark and Hartenberg (15) have reported that Poisson's ratio, μ, for concrete may be taken as approximately 0.2. Using the relationship:

$$G = \frac{E}{2(1 + \mu)}$$

we find that:

$$G = \frac{E}{2(1 + 0.2)}$$

$$G = \frac{E}{2(1.2)}$$

$$G = \frac{E}{2.4}$$

$$G = 0.4167E$$

Morice and Little (12) also suggest that for concrete design, the approximation $G = 0.4E$ may be assumed.

Two extremes considered practical as cross section dimensions for concrete slats include one having a depth of two inches and a width of six inches and a second having a depth of six inches and a width of three inches.

Rectangular cross sections are not normally used for concrete slats, but were considered satisfactory for determining the approximate limits for the ratio, EI/GJ. The equation $I = 1/12\ bh^3$ provides an estimate of the moment of inertia of a rectangular cross section of homogeneous material if b is the width and h is the depth of the section. This is an expression for the moment of inertia about an x axis located at the center of the section.

Seely (17) and Timoshenko and Young (20) summarize the work of de St. Venant published in 1855 in Mém des Savanis éstrangers, y. 14. They report that a satisfactory expression for the torsional moment of inertia of a rectangular cross section of homogeneous material may be written:

$$J = 1/16(16/3 - 3.36\ b/h\ (1 - 1/12\ (b/h)^4))hb^3$$

where h equals the long dimension and b equals the short dimension. J has been interpreted to be equal to $\beta(hb^3)$ in the equation $\theta = T/\beta hb^3G$ as given by Timoshenko and Young (20). It is the expression used in the equation for θ as it is adapted to rectangular cross sections only. The stress distribution across the face of a bar having a rectangular cross section is difficult to describe mathematically. The value given for (βhb^3) by the equation developed by St. Venant gives a good approximation of the distribution. The equation was developed from experimental data and assumes an approximate stress distribution across the face of the cross section. Other equations have been developed for estimating $J = (\beta hb^3)$, but the one by St. Venant is used here. In this report J is defined as being equal to βhb^3.

Table V lists the computed moments of inertia, I, and torsional moments of inertia, J, for the two extreme cross sections being considered. It also includes the value of the relationships of EI/GJ assuming it can be approximated as I/0.4J.

TABLE V

PROTOTYPE GRID SLAT CHARACTERISTICS USED TO DETERMINE TEST LIMITS FOR EI/GJ

Slat Width (in.)	Slat Depth (in.)	I ($in.^4$)	J ($in.^4$)	$\frac{EI}{GJ} = \frac{I}{.4J}$
6	2	4	12.6	0.795
3	7	85.7	46.2	4.630

The limits of $\pi_4 = EI/PL^2$ were influenced by the range of values used for bending stiffness and the loads that could be applied. Table VI lists the values used to establish the upper and lower limits of the pi term EI/PL^2.

TABLE VI

VALUES USED TO DETERMINE TEST LIMITS FOR EI/PL^2

E (psi)	I ($in.^4$)	P (lbs.)	L (in.)	EI/PL^2
3×10^6	4	500	72	4.63
3×10^6	85.7	500	120	35.70

E for concrete was taken as 3×10^6 psi to establish these limits.

P was taken as 500 pounds since Burgener (2) suggested that a suitable loading assumption for simple reinforced concrete beam design would be a pair of loads of 250 pounds each. Each of these 250 pound loads would represent a fourth of the weight of one animal.

For the lower limit of the pi term EI/PL^2 the moment of inertia value of four was taken from Table V. Under equal loads smaller bending moments will exist in short beams than in long beams. For this reason, the 72 inch beam length was associated with the moment of inertia value of four. The upper limit related the longer beam length of 120 inches with the moment of inertia value of 85.7. Values for the ratios were computed as follows:

$$\frac{EI}{PL^2} = \frac{3 \times 10^6 \times 4}{500 \times (72)^2} = 4.63$$

$$\frac{EI}{PL^2} = \frac{3 \times 10^6 \times 85.7}{500 \times (120)^2} = 35.70$$

The lower limit for the model tests was rounded off to four. The second value was selected at 12. An increment of 16 was used for selected third and fourth values which brought the upper value to 44.

The limits of $\pi_5 = L/B$ were established at nine and 24. Minimum length was estimated at 72 inches and maximum slat spacing at eight inches. This suggested the minimum value of nine for L/B. Minimum slat spacing for a maximum length of 144 inches was estimated at six inches. This suggested the maximum value of 24.

$\pi_6 = X/L$ describes the position of the loads on the slats as related to overall grid length. The limits were determined by establishing X as close to the center of the grid and as near to the end of the grid as possible. Cross tie location restricted these positions so the limits were set at 0.17 and 0.46.

π_7 describes the number of cross ties per grid excluding the ties fabricated into each end of the grid. It is a dimensionless pi term. Prototypes having a maximum of four ties were considered suitable for

livestock floor systems. Values assigned to the pi term, T, were 1, 2, 3, and 4 cross ties in addition to the two-end cross ties.

CHAPTER V

STRENGTH CHARACTERISTICS OF PLASTER OF PARIS

The workability of different grades of plaster was evaluated by casting grid specimens for preliminary tests. Plaster of Paris and a molding plaster called Barga Lucca were compared. Barga Lucca is manufactured by National Gypsum Company of Dallas, Texas. Plaster of Paris was found to have an extremely short setting time. When large quantities were mixed, the setting time was shorter than when smaller quantities were mixed. This was a serious limitation since it was desirable to cast several grids from one batch of plaster. This reduced the number of tests needed to evaluate E and G since one series of these tests would provide the needed data for the several grids made from each batch. The lack of workability of plaster of Paris made it necessary to eliminate it as a modeling material. Barga Lucca was selected in place of the plaster of Paris because tests indicated that it had a desirable setting time. Adequate time was available to thoroughly mix the plaster and work it to permit air bubbles to escape before the castings were poured. Its chemical composition is similar to plaster of Paris.

Strain Measurement at Top and Bottom of Beam

A series of tests were carried out to verify that the Barga Lucca plaster models would exhibit a relationship in which the compressive strain at the top of a beam would equal the tension strain at the

bottom under concentrated loads. This would indicate that the modulus of elasticity would be the same for tensile and compressive stresses in the material. To accomplish this, a single beam was cast of Barga Lucca plaster. Its dimensions were two inches wide, two inches deep, and 24 inches long. An SR-4 strain gauge having a length of one-fourth inch was mounted at the center of the top side of the beam to measure strain along the length of the beam. A second strain gauge was mounted in a similar manner on the lower side of the beam. The beam was loaded as shown in Figure 17.

Loads were applied in increments and the strains at the top and bottom of the center of the beam were recorded for each increment. Table VII lists the stress-strain data recorded for the test series. The average increase in strain on the top under a five pound load increment for the three tests was 40 microinches per inch. The average strain increase on the bottom under the five pound increment for the three tests was 39.7 microinches per inch. It was concluded that compressive strain at the top of the beam compares very closely with the tension strain on the bottom. Based on these results, strain gauges were used on one surface only in subsequent tests.

Ultimate Strength Tests

Three tests were carried out to provide information for estimating the ultimate strength of Barga Lucca plaster when used for modeling. Loads were applied to beams having lengths of 24 inches in the manner illustrated in Figure 18.

The shear and moment diagrams in Figure 18 show that the value of the bending moment is equal to nine times one of the loads. Using

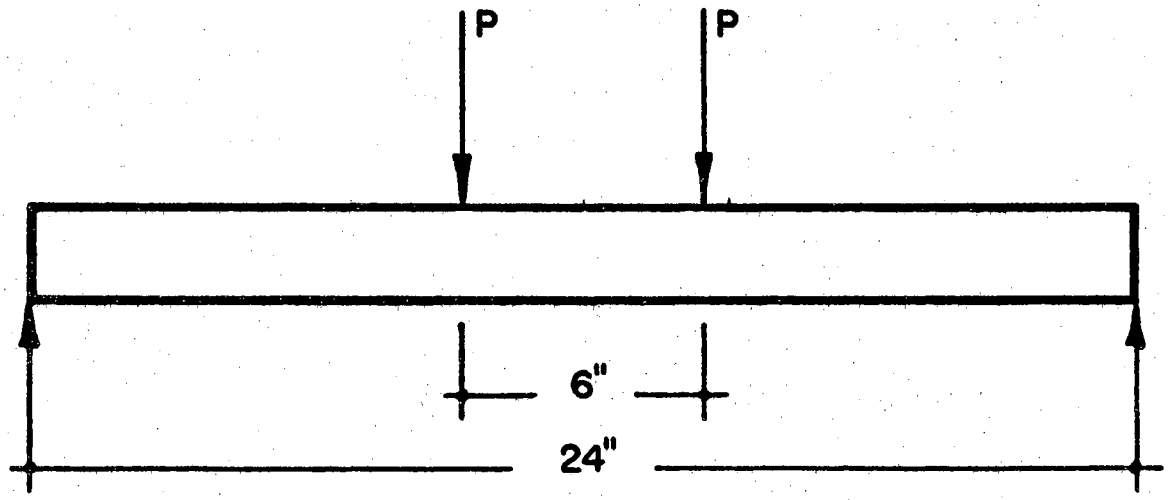

Figure 17. Loading Arrangement of Test Beam Used to Verify that Strain Gauges on the Top and Bottom of Plaster Beams Yield Readings that are Equal but Opposite in Sign

TABLE VII

RELATIONSHIP BETWEEN COMPRESSIVE STRAINS AT THE TOP AND TENSION STRAINS AT THE BOTTOM OF BEAMS MADE OF MODELING PLASTER

Load (Pounds)	Test 1		Test 2		Test 3	
	Strain on Top (microinches/inch)	Strain on Bottom (microinches/inch)	Strain on Top (microinches/inch)	Strain on Bottom (microinches/inch)	Strain on Top (microinches/inch)	Strain on Bottom (microinches/inch)
0	0	0	0	0	0	0
5	35	35	35	40	35	40
10	75	70	70	75	70	75
15	110	110	110	115	110	110
20	155	150	150	150	150	150
25	195	190	190	190	190	190
30	240	230	230	230	230	230
35	285	280	280	275	275	280

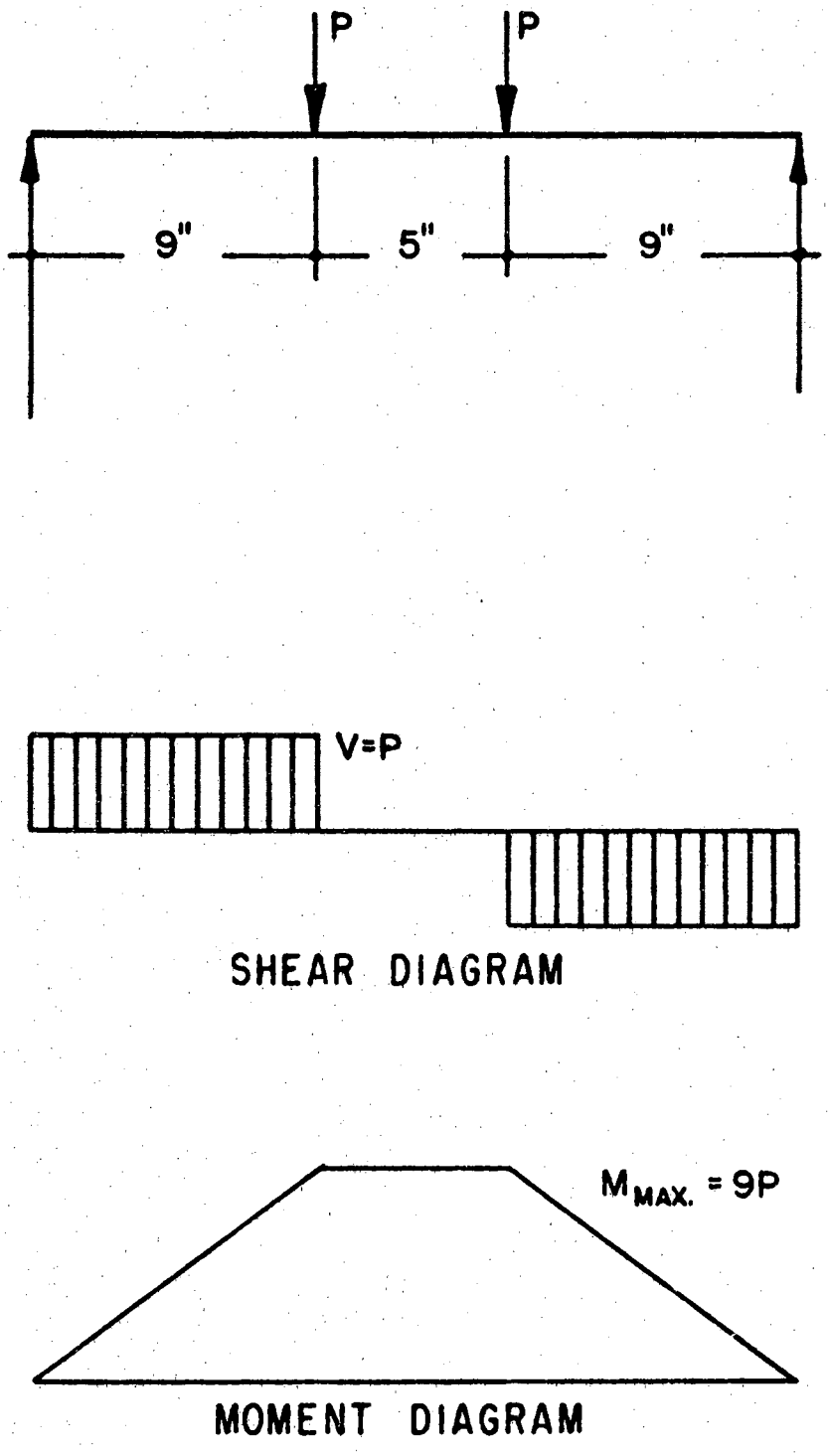

Figure 18. Beam Loadings Used to Determine Ultimate Stress of Plaster

beams having rectangular cross sections, the flexure formula is as follows:

$$S = MC/I$$

$$M/S = 1/6\ bh^2$$

$$S = 6M/bh^2$$

$$M = 9P$$

$$S = 54P/bh^2$$

The three plaster beams that were tested were loaded until failure occurred. The failure load was used to calculate the ultimate stress in bending. Table VIII is a record of the test results.

TABLE VIII

CHARACTERISTICS OF BEAMS IN ULTIMATE STRENGTH TESTS

Test No.	b (in.)	h (in.)	h^2 (sq. in.)	bh^2 (cu. in.)	P (pounds)	S (psi)
1	1-1/4	2	4	5	32	345.6
2	1-1/4	2	4	5	33	356.4
3	1-1/2	2	4	6	42	378.0

An ultimate stress of approximately 350 psi was used along with a suitable safety factor to estimate the safe loads used for testing the plaster grid models. The modulus of elasticity was determined experimentally for each plaster batch. This value along with the working stress was used to calculate a safe strain for each grid. Grids were loaded up to a point where strain gauge readings in the tests approached the safe calculated strain.

Experimental Modulus of Elasticity Determinations

The modulus of elasticity of each batch of plaster used to make model grids was determined experimentally. Simple beams were fabricated from each plaster batch. Deformation tests were made on these beams and the test results were used to compute the modulus of elasticity.

All test beams were made 24 inches long. Some beams were supported on rollers in such a way that the center of the support coincided with the end of the beam. The effective length of these beams was taken as 24 inches. These supports could not be glued securely to the plaster so the support was placed one-eighth inch from the end of the beam. This left an effective length of 23.75 inches.

Figure 19 illustrates the load positions used for testing.

The expression for deflection at the center of the beam under the loading shown is written:

$$d = \frac{Pa}{24EI} (3L^2 - 4a^2)$$

$$E = \frac{a}{24I} \times \frac{P}{d} \quad (3L^2 - 4a^2)$$

Deflection measurements were taken at each end and the center of the beam. End deflections were averaged and the average was subtracted from the center deflection reading to give the actual deflection.

Loads were applied in the tests in one pound increments from one pound up to eight pounds. Deflection readings were recorded for each load increment. A linear regression analysis was made for each beam with load plotted on the y axis and deflection plotted on the x axis. Regression line slope from the linear regression represented the ratio, P/d. This ratio was substituted into the equation for the modulus of elasticity calculations.

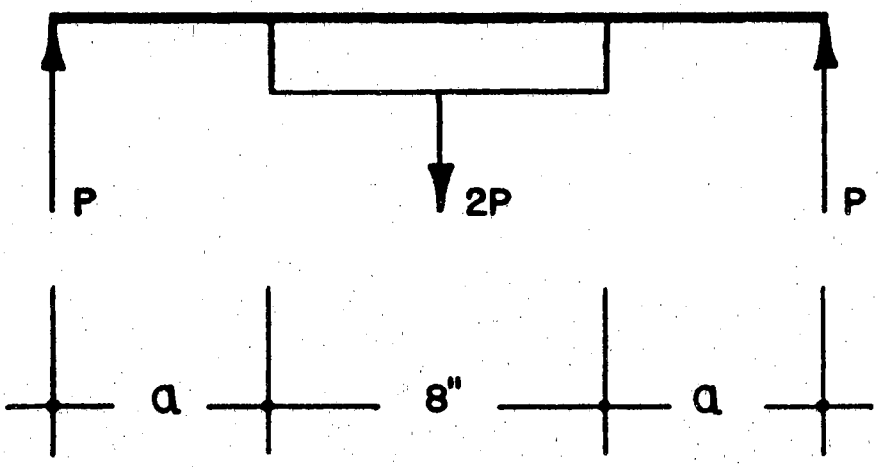

Figure 19. Load Arrangement Used to Test Single Beams to Determine Modulus of Elasticity of Plaster Modeling Material

Four beam tests were made to serve as replications for each batch of molding plaster. In most cases, two beams were used for testing. Replications were obtained by testing in one position and then inverting the beam for a second set of test data. Different plaster batches are identified by the prefix letters in the test beam numbers in Tables IX and X. Seven batches of plaster were used for the models. An eighth batch is identified as batch T and was used for a prototype grid for validating the test results.

Table IX records the dimensions of each beam tested and the calculated moment of inertia. Table X records the results of the linear regression analysis for each test beam. The linear regression equation is $P = A + B(d)$, where A is the Y intercept and B is the slope of the line. All linear correlation coefficients are larger in magnitude than 0.99 which indicates that the relationship between load and deflection closely fits a straight line.

An analysis of variance designed to test for differences between the values for the moduli of elasticity between beams in a batch and between batches is recorded in Table XI. Calculated F for the replications was 2.86. Tabulated F at the 95 per cent level was 3.07 which indicates that there probably was no difference between the values between replications. Calculated F for differences between batches was 4.44. Tabulated F at the 95 per cent level was 2.49 which indicates that differences probably did exist between the values for different batches of plaster.

Since differences existed between the eight batches of plaster, it was necessary to determine a value for the modulus of elasticity

TABLE IX

CHARACTERISTICS OF BEAMS USED IN MODULUS OF ELASTICITY DETERMINATIONS

Test Beam Number	Beam Width (in.)	Beam Depth (in.)	Beam Span (in.)	Moment of Inertia ($in.^4$)
T11	1.27	1.75	23.75	0.57
T12	1.27	1.75	23.75	0.57
T21	1.22	1.27	23.75	0.21
T22	1.22	1.27	23.75	0.21
G11	1.32	1.73	23.75	0.57
G12	1.32	1.73	23.75	0.57
G21	1.33	1.49	23.75	0.37
G22	1.33	1.49	23.75	0.37
N11	1.24	1.29	23.75	0.22
N12	1.24	1.29	23.75	0.22
N31	1.27	1.23	23.75	0.20
N32	1.27	1.23	23.75	0.20
P11	1.24	1.23	23.75	0.19
P12	1.24	1.23	23.75	0.19
P21	1.24	1.24	23.75	0.19
P22	1.24	1.24	23.75	0.19
F41	1.20	1.21	23.75	0.18
F42	1.20	1.21	24.00	0.18
F31	1.24	1.24	24.00	0.20
F51	1.25	1.24	24.00	0.20
M31	1.28	1.22	24.00	0.19
M11	1.22	1.28	23.75	0.22
M21	1.22	1.29	23.75	0.22
M22	1.22	1.29	23.75	0.22
D31	1.24	1.46	23.75	0.32
D32	1.24	1.46	24.00	0.32
D11	1.05	1.23	24.00	0.16
D12	1.05	1.23	23.75	0.16
B21	1.23	1.23	23.75	0.19
B31	1.19	1.23	23.75	0.18
B11	1.18	1.22	23.75	0.18
B12	1.18	1.22	23.75	0.18

TABLE X

LINEAR REGRESSION ANALYSES OF LOAD VERSUS DEFLECTION FOR MODULUS OF ELASTICITY DETERMINATIONS

Test Beam Number	Regression Line Slope	Regression Line Intercept	Linear Correlation Coefficient	Modulus of Elasticity (psi)
T11	783.91	.25	.998	656,000
T12	842.56	.23	.997	705,000
T21	333.89	-.04	.997	761,000
T22	277.89	.21	.994	633,000
G11	707.57	-.07	.994	586,000
G12	836.96	.10	.998	693,000
G21	516.32	-.16	.998	660,000
G22	545.66	.05	.998	698,000
N11	315.27	.15	.998	680,000
N12	332.82	.16	.999	718,000
N31	323.73	.05	.999	785,000
N32	328.14	.09	.999	795,000
P11	312.89	.01	.999	766,000
P12	314.72	-.03	.999	771,000
P21	298.82	.00	.999	727,000
P22	306.83	.04	.999	746,000
F41	271.67	-.02	.999	725,000
F42	280.09	.03	.999	774,000
F31	314.86	.00	.999	787,000
F51	320.47	.02	.999	800,000
M31	312.09	-.04	.999	787,000
M11	343.00	.05	.999	755,000
M21	349.96	-.20	.999	764,000
M22	333.44	.07	.999	728,000
D31	387.45	.03	.999	569,000
D32	424.56	-.04	.999	645,000
D11	233.59	.01	.999	704,000
D12	252.88	.06	.999	736,000
B21	276.92	-.03	.999	686,000
B31	244.03	.14	.998	634,000
B11	278.97	-.01	.999	738,000
B12	266.51	.01	.999	705,000

for each plaster batch to use to evaluate the pi terms in the grid model tests.

TABLE XI

ANALYSIS OF VARIANCE OF MODULI OF ELASTICITY FOR FOUR REPLICATIONS OF EIGHT BATCHES OF MOLDING PLASTER

Source	Degrees of Freedom	Sum of Squares	Mean Squares	F
Replications	3	15,904,000,000	5,301,333,300	2.86
Treatments	7	57,552,000,000	8,221,714,200	4.44
Error	21	38,805,000,000	1,847,857,100	
Total	31			

No differences were found by the analysis of variance between replications within batches. A value of modulus of elasticity representative of each plaster batch was selected using the data from the four replications for each batch.

One method of selecting the value of modulus of elasticity for each batch would be to take an arithmetic average of the four replicated values.

A second method could be used if the configuration of each test beam were the same. In this method, all test data for each plaster batch could be subjected to a single linear regression analysis in which load would be plotted on the y axis and deflection on the x axis. Substituting the slope of the line determined in this analysis in the deflection equation for the beam shown in Figure 19 would provide an estimate of the value of the modulus of elasticity. A modification of

the second method was selected for these tests since the characteristics of each test beam were different. L was either 23.75 inches or 24 inches. The moments of inertia varied.

The modification used in the analysis was to adjust beam characteristics to standard conditions. Standard beam characteristics were selected at I equal to 0.25 inches^4 and L equal to 24 inches.

Deflections were computed for each of the four E values using P values ranging from one to eight pounds in increments of one pound. A linear regression analysis was developed using the P and deflection relationships for all four replications at one time. The slope of the line from this regression was used to compute an E value for the composite of the plaster batch. This procedure was repeated for each of the eight batches of plaster. Table XII records these values.

TABLE XII

LINEAR REGRESSION ANALYSIS OF LOAD VERSUS DEFLECTION FOR MODULUS OF ELASTICITY FOR REPLICATIONS COMBINED FOR EACH BATCH OF PLASTER

Test Batch Number	Regression Line Slope	Regression Line Intercept	Linear Correlation Coefficient	Modulus of Elasticity (psi)
T	341.25	.05	.988	669,764
G	326.05	.06	.988	639,919
N	370.27	.05	.990	726,612
P	382.17	.01	.999	750,072
F	389.95	.02	.997	765,333
M	384.62	.01	.998	754,879
D	319.04	.11	.976	626,174
B	345.64	.03	.993	678,372

Experimental Shear Modulus Determinations

The shear modulus for each batch of plaster used for models was determined experimentally. Single beams were deformed in a torsion test machine. Data on loads applied and angle of twist were used to evaluate the shear modulus of the molding plaster.

One end of each test beam was clamped into the stationary base of the torsion test device developed for these experiments. The other end was clamped to the part of the device that included the lever arm for applying the torque. Two mirrors were glued on one side of the beam along its longitudinal center line. They were spaced 18 inches on center and each was the same distance from the ends. Light projected crossed hair lines from each of the two slide projectors and each set was focused on the appropriate one of the two mirrors glued to the test beam. The projectors were then refocused so that the cross hairs were reflected from the mirrors to a panel behind the projectors. The cross hairs were brought into focus on measuring scales on the panels.

Torques applied to one end of the test beam caused a twisting of the beam. One mirror rotated more than the other. The difference between the two rotations was taken as the total rotation of the 18 inch length of beam between the two mirrors.

Figure 20 illustrates the characteristics of the change in the angle of a beam of light reflected by a mirror as the mirror is rotated.

$$r = i$$

$$r' = i'$$

$$i' = i + \beta = r'$$

$$ROR' = r' - (r - \beta) = i' - (i - \beta) = (i + \beta) - (i - \beta) = 2\beta$$

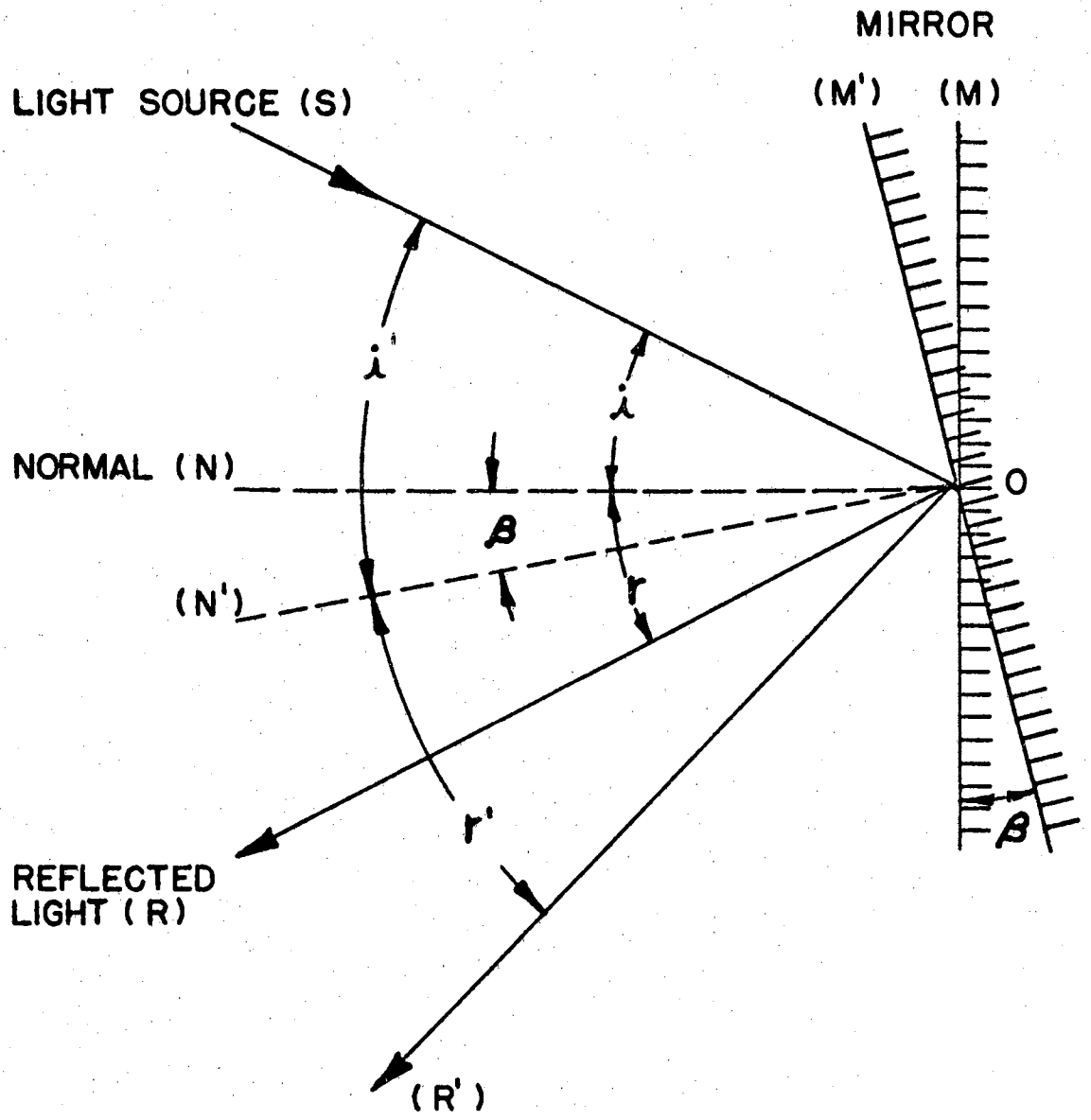

Figure 20. Characteristics of the Change in the Angle of a Beam of Light Reflected by a Mirror as the Mirror is Rotated

This indicated that the angle measured by the reflected light will equal two times the angle of rotation of the beam.

Angles were computed by measuring the movement of the reflected cross hairs on the measuring scales on the panel behind the projectors. The distance from the reflecting mirror to the measuring scale was measured. From these two dimensions, the angle was computed. Rotation of the mirrors on the beam was computed by dividing the reflected angle by two. The difference between the rotations at the two mirrors was taken as the twist in the 18 inch section of beam between the mirrors.

Torsional moment of inertia was computed using the formula:

$$J = 1/16(\frac{16}{3} - 3.36\,\frac{b}{h}\,(1 - \frac{b^4}{12h^4}))hb^3$$

where b is the short dimension and h is the long dimension of the beam cross section.

The expression for computing rotation for a bar is written:

$$\theta = \frac{TL}{GJ}$$

where T is the torque. Applied torque, beam length, torsional moment of inertia, and θ were determined for each test. The shear modulus (G) was computed using the expression $G = T/\theta\ (L/J)$.

Table XIII records the cross sectional dimension of each beam, the distance from the mirrors to the measuring scale, and the computed torsional moment of inertia.

Torques were applied in the tests in five inch pound increments from five inch pounds up to fifty inch pounds. The angle of twist was recorded for each load increment. For the small angles measured in the tests, the angle in radians was considered as equal to the tangent

TABLE XIII

CHARACTERISTICS OF BEAMS USED IN SHEAR MODULUS DETERMINATIONS

Test Beam Number	Beam Width (in.)	Beam Depth (in.)	Radius (in.)	Torsional Moment of Inertia ($in.^4$)
T11	1.22	1.27	239	0.335
T12	1.22	1.27	239	0.335
T21	1.27	1.75	239	0.664
T22	1.27	1.75	239	0.664
G11	1.33	1.49	239	0.552
G12	1.33	1.49	239	0.552
G21	1.32	1.73	239	0.712
G22	1.32	1.73	239	0.712
N11	1.24	1.29	239	0.357
N12	1.24	1.29	239	0.357
N21	1.24	1.25	239	0.339
N22	1.24	1.25	239	0.339
P11	1.23	1.24	239	0.328
P12	1.23	1.24	239	0.328
P31	1.24	1.25	239	0.337
P32	1.24	1.25	239	0.337
F41	1.20	1.21	239	0.298
F42	1.20	1.21	239	0.298
F31	1.22	1.23	239	0.314
F51	1.24	1.25	239	0.335
B11	1.18	1.22	239	0.292
B12	1.18	1.22	239	0.292
B21	1.23	1.23	239	0.323
B31	1.19	1.23	239	0.297
D31	1.24	1.46	239	0.451
D32	1.24	1.46	239	0.451
D11	1.05	1.23	239	0.229
D12	1.05	1.23	239	0.229
M31	1.22	1.28	239	0.344
M11	1.22	1.28	239	0.344
M21	1.22	1.29	239	0.345
M22	1.22	1.29	239	0.345

of the angles. The measured movement of the reflected beam was divided by the distance from the measuring scale to the mirror. This angle was divided by two to give the angle of rotation of the beam. For each load increment, these determinations were made for each mirror and the two values subtracted to give the rotation of the 18 inch section of beam.

A linear regression analysis was made for each set of beam data with torque plotted on the y axis and beam rotation on the x axis. Regression line slope from the linear regression represented the ratio T/θ. This ratio was substituted into the equation for the shear modulus calculations.

Table XIV records the results of the linear regression analyses along with the shear modulus for each beam. The linear regression equation is $T = A + B(\theta)$ where A is the Y intercept and B is the slope of the line. All correlation coefficients are larger in magnitude than 0.99 and most are larger than 0.999 which indicates that the relationship between torque and rotation closely fits a straight line.

As with the modulus of elasticity tests, four beam tests were made to serve as replications for each batch of molding plaster. The batches are identified by the prefix letters in the test beam numbers in Tables XIII and XIV. In most cases, the same beams were used for the tests to determine shear modulus as were used in the modulus of elasticity tests. Plaster batch T used for the prototype was again included.

The analysis of variance designed to test for differences between the values for shear moduli between beams in a batch and between batches is recorded in Table XV. Calculated F for the replications was 2.61.

TABLE XIV

LINEAR REGRESSION ANALYSES OF TORQUE (IN POUNDS) VERSUS ROTATION (RADIANS) FOR SHEAR MODULUS DETERMINATIONS

Test Beam Number	Regression Line Slope	Regression Line Intercept	Linear Correlation Coefficient	Shear Modulus (psi)
T11	5,931	-.03	.999	318,000
T12	5,896	.28	.999	317,000
T21	12,395	1.24	.999	336,000
T22	13,443	-1.50	.993	364,000
G11	9,457	-.45	.999	309,000
G12	9,485	.96	.999	310,000
G21	11,422	.62	.999	289,000
G22	11,772	1.18	.999	298,000
N11	7,006	.93	.999	353,000
N12	7,006	.52	.999	356,000
N21	6,669	.59	.999	354,000
N22	6,786	-.36	.999	360,000
P11	5,977	-.01	.999	328,000
P12	6,188	.26	.999	350,000
P31	6,538	-.26	.999	349,000
P32	6,575	-.44	.999	351,000
F41	5,268	.84	.999	319,000
F42	5,281	.29	.999	319,000
F31	6,280	.07	.999	360,000
F51	6,112	.32	.999	328,000
B11	4,825	.04	.999	298,000
B12	4,863	.47	.999	300,000
B21	5,290	-.03	.999	295,000
B31	4,858	.07	.999	295,000
D31	7,250	-.56	.999	289,000
D32	7,219	.41	.999	288,000
D11	3,955	-.12	.999	311,000
D12	3,944	-.06	.999	310,000
M31	6,160	.44	.999	323,000
M11	6,239	.33	.999	326,000
M21	6,421	-.21	.999	335,000
M22	6,499	.99	.999	339,000

Tabulated F at the 95 per cent level was 3.07 which indicates that there probably was no difference between the values between replications. Calculated F for differences between batches was 14.17. Tabulated F at the 95 per cent level was 2.49 which indicates that differences probably did exist between values for shear modulus for different batches of plaster. This is similar to the results from modulus of elasticity tests.

TABLE XV

ANALYSIS OF VARIANCE OF SHEAR MODULI FOR FOUR REPLICATIONS OF EIGHT BATCHES OF MOLDING PLASTER

Source	Degrees of Freedom	Sum of Squares	Mean of Squares	F
Replications	3	1,074,300,000	358,100,000	2.61
Treatments	7	13,602,200,000	1,943,171,400	14.17
Error	21	2,878,400,000	137,066,660	
Total	31	17,554,900,000		

Since differences existed between the eight batches of plaster, it was necessary to determine a value for the shear modulus for each plaster batch to use to evaluate the pi terms in the grid model tests.

As with the modulus of elasticity determinations, no differences were found by the analysis of variance between replications within batches. A value of shear modulus representative of each plaster batch was selected using the data from the four replications for each batch.

One method of selecting the value of shear modulus for each batch would be to take an arithmetic average of the four replicated values.

A second method outlined under determinations of modulus of elasticity could be used if the configuration of each test beam were the same. In this method, all test data for each plaster batch could be subjected to a single linear regression analysis in which torque would be plotted on the y axis and angle of twist on the x axis. Substituting the slope of the line determined in this analysis in the equation, $G = T/\theta \times L/J$ would provide an estimate of the value of shear modulus.

A modification of the second method was selected for these tests since the characteristics of each test beam were different. The modification used in the analysis was to adjust beam characteristics to standard conditions. Standard beam characteristics were selected at J equal to 0.35 inches^4 and L equal to 18 inches.

Torques were computed for each of the four G values using T values ranging from five to 50 inch pounds in increments of five inch pounds. A linear regression analysis was developed using the torque and angle of twist relationships computed for all four replications at one time. The slope of the line from this regression was used to compute a G value for the composite of the plaster batches by using the equation $G = T/\theta \times L/J$. This procedure was repeated for each of the eight batches of plaster. Table XVI records these values.

TABLE XVI

LINEAR REGRESSION ANALYSIS OF TORQUE (INCHES-POUNDS) VERSUS ROTATION (RADIANS) FOR SHEAR MODULUS FOR REPLICATIONS COMBINED FOR EACH BATCH

Test Batch Number	Regression Line Slope	Regression Line Intercept	Linear Correlation Coefficient	Shear Modulus (psi)
T	6,379	.39	.993	328,074
G	5,827	.11	.998	299,681
N	6,916	.01	.999	355,705
P	6,627	.09	.998	340,824
F	6,361	.30	.995	327,177
M	6,417	.05	.999	330,039
D	5,779	.17	.997	297,235
B	5,772	.01	.999	296,870

CHAPTER VI

DESIGN OF GRID MODELS

Molding plaster grid models were designed to have pi term values fall in the ranges established for prototype grids. Table XVII lists the values for the models. These values compare very closely with the values established for prototypes that are listed in Table IV. Table XVIII lists the characteristics of the models used to provide the pi term values listed in Table XVII. A total of four variations in each pi term was designed into the model study.

The modulus of elasticity of plaster of Paris was assumed to be 1×10^6 pounds per square inch as reported by Hetényi (5). Roark and Hartenberg (15) reported a Poisson's ratio of 0.1 for plaster of Paris. Using this data, an assumed shear modulus, G, was computed.

$$G = \frac{E}{2(1 + \mu)} = \frac{1 \times 10^6}{2(1 + 0.1)} = 454{,}545$$

G was rounded to 4.5×10^5 for the purpose of designing the models.

Moment of inertia, I, was assumed to be described by the formula $I = 1/12\ bh^3$ where b is the base width and h is the height of the beam cross section.

Torsional moment of inertia, J, was assumed to be described by the formula $J = 1/16(16/3 - 3.36\ b/h\ (1 - b^4/12h^4))hb^3$ where b is the short dimension and h is the long dimension of the beam cross section.

Values for the pi term, EI/GJ, were established for the prototype to range from 0.80 to 4.63. Values in the models ranged from 0.72 to

TABLE XVII

PI TERM VALUES REQUIRED IN PLASTER OF PARIS GRID MODELS FOR PREDICTING STRAIN AND DEFLECTION PI TERMS

Test Series	$\pi_3 = \frac{EI}{GJ}$	$\pi_4 = \frac{EI}{PL^2}$	$\pi_5 = \frac{L}{B}$	$\pi_6 = \frac{X}{L}$	$\pi_7 = T$
A	$(\pi_3)_1 = 0.72$ $(\pi_3)_2 = 1.32$ $(\pi_3)_3 = 2.13$ $(\pi_3)_4 = 4.12$	$\bar{\pi}_4 = 12$	$\bar{\pi}_5 = 16$	$\bar{\pi}_6 = 0.46$	$\bar{\pi}_7 = 2$
B	$\bar{\pi}_3 = 1.32$	$(\pi_4)_1 = 4$ $(\pi_4)_2 = 12$ $(\pi_4)_3 = 28$ $(\pi_4)_4 = 44$	$\bar{\pi}_5 = 16$	$\bar{\pi}_6 = 0.46$	$\bar{\pi}_7 = 2$
C	$\bar{\pi}_3 = 1.32$	$\bar{\pi}_4 = 12$	$(\pi_5)_1 = 24$ $(\pi_5)_2 = 16$ $(\pi_5)_3 = 12$ $(\pi_5)_4 = 9$	$\bar{\pi}_6 = 0.46$	$\bar{\pi}_7 = 2$
D	$\bar{\pi}_3 = 1.32$	$\bar{\pi}_4 = 12$	$\bar{\pi}_5 = 16$	$(\pi_6)_1 = 0.46$ $(\pi_6)_2 = 0.38$ $(\pi_6)_3 = 0.29$ $(\pi_6)_4 = 0.17$	$\bar{\pi}_7 = 2$
E	$\bar{\pi}_3 = 1.32$	$\bar{\pi}_4 = 12$	$\bar{\pi}_5 = 16$	$\bar{\pi}_6 = 0.46$	$(\pi_7)_1 = 1$ $(\pi_7)_2 = 2$ $(\pi_7)_3 = 3$ $(\pi_7)_4 = 4$

TABLE XVIII

CHARACTERISTICS OF PLASTER GRID MODELS REQUIRED FOR PI TERMS LISTED IN TABLE XVII

Grid Number	E (psi)	G (psi)	Slat Width b (in.)	Slat Depth h (in.)	I_4 ($in.^4$)	J ($in.^4$)	Load (lbs.)	Grid Length L (in.)	Slat Spacing B (in.)	Load Location X (in.)	Number of Ties T
A1	1×10^6	4.5×10^5	1.50	0.50	0.02	0.05	1.7	28	1.75	12.83	2
A2	1×10^6	4.5×10^5	1.25	1.25	0.20	0.34	29.5	24	1.50	11.00	2
A3	1×10^6	4.5×10^5	1.00	1.50	0.28	0.29	40.8	24	1.50	11.00	2
A4	1×10^6	4.5×10^5	0.75	1.75	0.33	0.18	48.3	24	1.50	11.00	2
B1	1×10^6	4.5×10^5	1.25	1.25	0.20	0.34	88.5	24	1.50	11.00	2
B2	1×10^6	4.5×10^5	1.25	1.25	0.20	0.34	29.5	24	1.50	11.00	2
B3	1×10^6	4.5×10^5	1.25	1.25	0.20	0.34	12.6	24	1.50	11.00	2
B4	1×10^6	4.5×10^5	1.25	1.25	0.20	0.34	8.0	24	1.50	11.00	2
C1	1×10^6	4.5×10^5	1.25	1.25	0.20	0.34	13.1	36	1.50	16.50	2
C2	1×10^6	4.5×10^5	1.25	1.25	0.20	0.34	29.5	24	1.50	11.00	2
C3	1×10^6	4.5×10^5	1.25	1.25	0.20	0.34	52.5	18	1.50	8.25	2
C4	1×10^6	4.5×10^5	1.25	1.25	0.20	0.34	52.5	18	2.00	8.25	2
D1	1×10^6	4.5×10^5	1.25	1.25	0.20	0.34	29.5	24	1.50	11.00	2
D2	1×10^6	4.5×10^5	1.25	1.25	0.20	0.34	29.5	24	1.50	9.00	2
D3	1×10^6	4.5×10^5	1.25	1.25	0.20	0.34	29.5	24	1.50	7.00	2
D4	1×10^6	4.5×10^5	1.25	1.25	0.20	0.34	29.5	24	1.50	4.00	2
E1	1×10^6	4.5×10^5	1.25	1.25	0.20	0.34	29.5	24	1.50	11.00	1
E2	1×10^6	4.5×10^5	1.25	1.25	0.20	0.34	29.5	24	1.50	11.00	2
E3	1×10^6	4.5×10^5	1.25	1.25	0.20	0.34	29.5	24	1.50	11.00	3
E4	1×10^6	4.5×10^5	1.25	1.25	0.20	0.34	29.5	24	1.50	11.00	4

4.12. This pi term was varied for each of the four models by using different cross section configurations for slats in each of the four models. Other pi terms were held constant.

The range of values for the pi term, EI/PL^2, was the same for the prototype and the models. Other pi terms were held constant. The grid model used for test A, $(\pi_3)_2$, was used in test series B to vary $(\pi_4)_1$, $(\pi_4)_2$, $(\pi_4)_3$, and $(\pi_4)_4$. Variation was achieved by varying P.

The range of values for the pi term, L/B, was the same for the prototype and models. To hold other pi terms constant and yet vary L/B, the grid lengths were adjusted. P was adjusted in the term EI/PL^2 and X was adjusted in the term X/L to hold these two pi terms constant while varying L/B.

The range of values for the pi term, X/L, was the same for the prototype and models. Here again the model used in test A, $(\pi_3)_2$, was used in test series D to vary $(\pi_6)_1$, $(\pi_6)_2$, $(\pi_6)_3$, and $(\pi_6)_4$. This was similar to the procedure used in test series B. This held the other pi terms constant. X/L was varied by placing loads at different positions on the slats.

The range of values for the pi term, T, was the same for the prototype and models. Model grids were made having 1, 2, 3, and 4 cross ties. Other pi terms were held constant.

All strain and deflection measurements were taken at the center of each slat in the grid. The SR-4 paper backed foil gauges were attached to each slat in this position. They were attached to only one surface of each slat since preliminary tests indicated that strains were approximately equal in magnitude and opposite in sign on the top and bottom surfaces of plaster beams.

All grids but two had no cross ties at the center point of the grid. In those grids having cross ties at the center, it was assumed that bending was not influenced at that point by the junction of the cross ties.

In the two grids having cross ties at the center, four strain gauges were placed on each slat at points away from the cross tie junctions. The four strains on each slat were used in a regression analysis. The regression equation was used to extrapolate the strain to the center of the grid.

Figure 21 illustrates the characteristics of the grid models. Grid width equals 3B + b. Three grids were modified to provide one with one cross tie, a second with three cross ties, and a third with four cross ties.

Testing Series for Strain

Table XIX lists the characteristics of the model grids used in the tests for strain. A difference exists between the assumed values for E and G as listed in Table XVIII and those actually obtained with the molding plaster. Plaster batch identification letters correspond to those in Tables XII and XVI. The configurations of the models actually used compared well with those established in Table XVIII. The values of the pi terms that resulted from the characteristics listed in Table XIX conform to those in Table XVII with two exceptions.

One exception was in the values of EI/GJ. In the strain tests, they were set at 0.74, 1.22, 2.06, and 3.87. The difference between these values and those listed in Table XVII is due to the difference between the assumed and actual values of E and G.

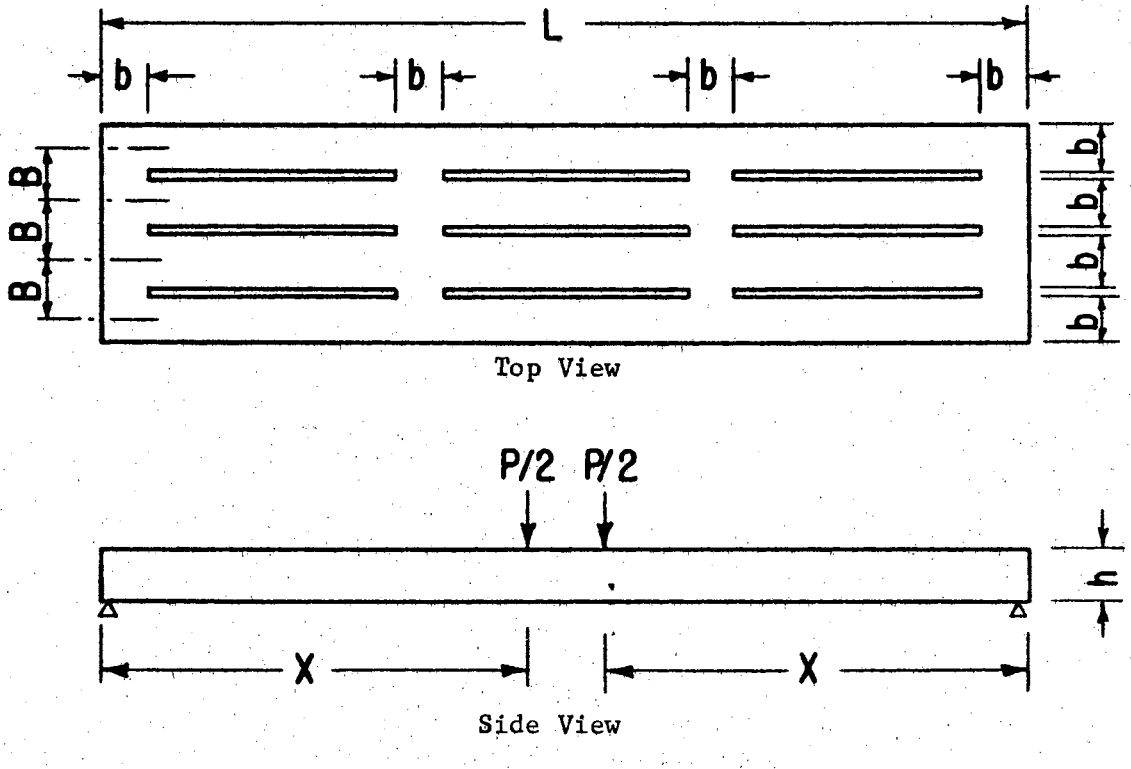

Figure 21. Diagram of Grid Model

TABLE XIX

CHARACTERISTICS OF PLASTER GRID MODELS USED FOR STRAIN EXPERIMENTS

Grid Number	Plaster Batch	E (psi)	G (psi)	Slat Width b (in.)	Slat Depth h (in.)	I ($in.^4$)	J ($in.^4$)	Load (lbs.)	Grid Length L (in.)	Slat Spacing B (in.)	Load Location X (in.)	Number of Ties T
A1	F	765,333	327,177	1.51	0.51	0.02	0.05	1.3	28	1.75	12.83	2
A2	D	626,174	297,235	1.25	1.22	0.19	0.33	17.1	24	1.50	11.00	2
A3	G	639,919	299,681	1.00	1.51	0.29	0.30	26.6	24	1.50	11.00	2
A4	G	639,919	299,681	0.75	1.72	0.32	0.18	29.5	24	1.50	11.00	2
B1	D	626,174	297,235	1.25	1.22	0.19	0.33	51.4	24	1.50	11.00	2
B2	D	626,174	297,235	1.25	1.22	0.19	0.33	17.1	24	1.50	11.00	2
B3	D	626,174	297,235	1.25	1.22	0.19	0.33	4.7	24	1.50	11.00	2
B4	D	626,174	297,235	1.25	1.22	0.19	0.33	2.1	24	1.50	11.00	2
C1	N	726,712	355,705	1.25	1.24	0.20	0.34	9.3	36	1.50	16.50	2
C2	D	626,174	297,235	1.25	1.22	0.19	0.33	17.1	24	1.50	11.00	2
C3	F	765,333	327,177	1.25	1.23	0.19	0.33	38.2	18	1.50	8.25	2
C4	B	678,372	296,870	1.25	1.24	0.20	0.34	34.2	18	2.00	8.25	2
D1	D	626,174	297,235	1.25	1.22	0.19	0.33	17.1	24	1.50	11.00	2
D2	D	626,174	297,235	1.25	1.22	0.19	0.33	17.1	24	1.50	9.00	2
D3	D	626,174	297,235	1.25	1.22	0.19	0.33	17.1	24	1.50	7.00	2
D4	D	626,174	297,235	1.25	1.22	0.19	0.33	17.1	24	1.50	4.00	2
E1	N	726,712	355,705	1.25	1.23	0.19	0.33	20.4	24	1.50	11.00	1
E2	D	626,174	297,235	1.25	1.22	0.19	0.33	17.1	24	1.50	11.00	2
E3	N	726,712	355,705	1.25	1.23	0.19	0.33	20.4	24	1.50	11.00	3
E4	P	750,072	340,824	1.25	1.24	0.20	0.34	21.5	24	1.50	11.00	4

A second exception was in the values of EI/PL^2. In the strain tests, they were set at 4, 12, 44, and 100. The upper value in Table XVII is 44. For the strain tests, this upper value was extended to 100 because it was convenient to do and it extended the range of validity for the resulting prediction equation. This was done by adjusting P in the pi term EI/PL^2.

Testing Series for Deflection

Table XX lists the characteristics of the model grids used in the tests for deflection. As with the grids used for strain tests, the assumed values for E and G as listed in Table XVIII are different from those actually obtained with the molding plaster. Plaster batch identification letters correspond to those in Tables XII and XVI. The configuration of the models actually used compared well with those established in Table XVIII. The pi terms that resulted from the characteristics listed in Table XX conform to those in Table XVII with one exception.

The exception is in the value of EI/GJ. In the deflection tests, these values were set at 0.74, 1.34, 2.06, and 3.87. In the other test series, this pi term was held constant at 1.34. The difference between these values and those listed in Table XVII is due to the differences between the assumed and actual values of E and G.

Grid for Validating Prediction Equations

A large plaster grid was tested and test data were compared to values computed from prediction equations. The comparison was made to validate the prediction equations.

TABLE XX

CHARACTERISTICS OF PLASTER GRID MODELS USED FOR DEFLECTION EXPERIMENTS

Grid Number	Plaster Batch	E (psi)	G (psi)	Slat Width b (in.)	Slat Depth h (in.)	I ($in.^4$)	J ($in.^4$)	Load (lbs.)	Grid Length L (in.)	Slat Spacing B (in.)	Load Location X (in.)	Number of Ties T
A1	F	765,333	327,177	1.50	0.51	0.17	0.05	1.3	28	1.75	12.83	2
A2	M	754,879	330,039	1.25	1.24	0.20	0.34	21.7	24	1.50	11.00	2
A3	G	639,919	299,681	1.00	1.51	0.29	0.30	26.6	24	1.50	11.00	2
A4	G	639,919	299,681	0.75	1.72	0.32	0.18	29.5	24	1.50	11.00	2
B1	M	754,879	330,039	1.25	1.24	0.20	0.34	65.1	24	1.50	11.00	2
B2	M	754,879	330,039	1.25	1.24	0.20	0.34	21.7	24	1.50	11.00	2
B3	M	754,879	330,039	1.25	1.24	0.20	0.34	9.3	24	1.50	11.00	2
B4	M	754,879	330,039	1.25	1.24	0.20	0.34	5.9	24	1.50	11.00	2
C1	N	726,712	355,705	1.25	1.24	0.20	0.34	9.3	36	1.50	16.50	2
C2	M	754,879	330,039	1.25	1.24	0.20	0.34	21.7	24	1.50	11.00	2
C3	F	765,333	327,177	1.25	1.23	0.19	0.33	38.2	18	1.50	8.25	2
C4	B	678,372	296,870	1.25	1.24	0.20	0.34	34.2	18	2.00	8.25	2
D1	M	754,879	330,039	1.25	1.24	0.20	0.34	21.7	24	1.50	11.00	2
D2	M	754,879	330,039	1.25	1.24	0.20	0.34	21.7	24	1.50	9.00	2
D3	M	754,879	330,039	1.25	1.24	0.20	0.34	21.7	24	1.50	7.00	2
D4	M	754,879	330,039	1.25	1.24	0.20	0.34	21.7	24	1.50	4.00	2
E1	N	726,712	355,705	1.25	1.23	0.19	0.33	20.4	24	1.50	11.00	1
E2	M	754,879	330,039	1.25	1.24	0.20	0.34	21.7	24	1.50	11.00	2
E3	N	726,712	355,705	1.25	1.23	0.19	0.33	20.4	24	1.50	11.00	3
E4	P	750,072	340,824	1.25	1.24	0.20	0.34	21.5	24	1.50	11.00	4

Molding plaster was the material used to fabricate the prototype because of its linear stress-strain relationship. The plaster batch used to fabricate the grid was identified as T. Table XX lists the modulus of elasticity as 669,764 and Table XVI lists the shear modulus as 328,074 for this plaster.

The length of the grid was 47 inches and its depth was 2.2 inches. The slat width was 2.2 inches. On center spacing of slats in the grid was three inches. The grid had four main slats and two cross ties in addition to those at each end.

The pi term EI/GJ was 1.21 and L/B equaled 15.7.

CHAPTER VII

ANALYSIS OF DATA FOR GRID STRAIN TESTS

Strain measurements using the five test series in Table XVII are tabulated in Appendix A. Appendix A, Table I lists strain measurements taken for test series A, Table XVII in which the independent pi term EI/GJ was varied while other independent pi terms were held constant. Appendix A, Table II lists strain measurements taken for test series B, Table XVII in which the independent pi term EI/PL^2 was varied while other independent pi terms were held constant. Appendix A, Table III lists strain measurements taken for test series C, Table XVII in which the independent pi term L/B was varied while other independent pi terms were held constant. Appendix A, Table IV lists strain measurements taken for test series D, Table XVII in which the independent pi term X/L was varied while other independent pi terms were held constant. Appendix A, Table V lists strain measurements taken for test series E, Table XVII in which the independent pi term T was varied while other independent pi terms were held constant.

Five curves were plotted using data taken from Appendix A, Tables I-V. The data plotted represent the strain measurements taken on slat one when slat one was loaded. In each of these figures, the function used to describe the relationships between strain and each of the five independent pi terms are also plotted. The relationships

of strain to the independent pi terms was similar for the other seven conditions of loading for each case so only one illustration is shown.

Strain Versus EI/GJ

The effects of EI/GJ on strain will be influenced by variations of EI and GJ separately. One of these variables cannot be changed without changing the other. The value of EI/GJ will be small if EI is small and GJ is large. A small EI will permit the loaded slat to bend to a great extent. The effect in the cross ties will be to distribute less of the bending to the unloaded slats. Large values of GJ will tend to nullify the effects of small values of EI to some extent.

The values of EI/GJ will be large if EI is large and GJ is small. A large EI will permit the loaded slat to bend very little. The effect in the cross ties will be to distribute much of the bending to the unloaded slats. The small torsional stiffness in the slats and ties will not modify the effects of a large EI to a very great extent. Strain probably could be expected to decrease as EI becomes large and GJ becomes small.

This effect may not be apparent in the testing sequence since the variable EI is also included in the pi term EI/PL^2. To vary EI/GJ, EI must be varied. To hold EI/PL^2 constant, P must be varied as EI is varied. For small values of EI/GJ, EI will be small; P will be small; and the strain can be expected to be small. If the values of EI/GJ are increased, EI, P, and strain can be expected to increase.

Experimental data showing the relationship between strain on slat one and EI/GJ with the load on slat one are plotted on Figure 22.

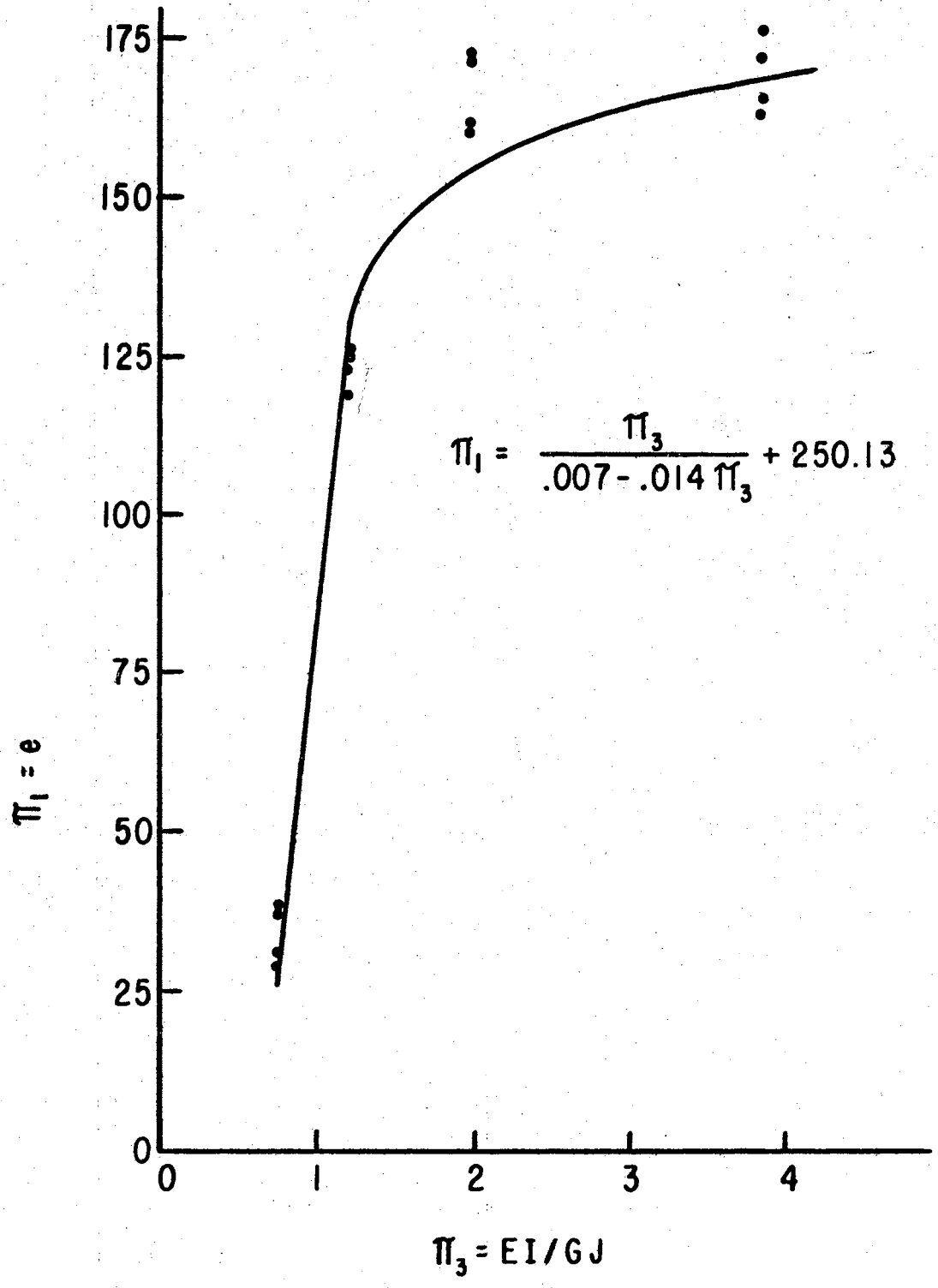

Figure 22. Relationship Between Strain on Slat One and the Pi Term, EI/GJ, With Other Pi Terms Held Constant; Load on Slat One; Extrapolating Values of Strain for Values of EI/GJ less than 0.74 is not Valid.

The plot illustrates that a linear relationship apparently does not describe the function. The data did not fall on a straight line in log-log plots or semi-log plots. The data were fitted to an equation suggested by Johnson (7). The form of the equation is:

$$y = \frac{x}{a + bx} + C$$

The data at the point where y was a minimum were selected as a base value for evaluating the equation. This point was identified as x_1 and y_1. The equation at this point is written:

$$y_1 = \frac{x_1}{a + bx_1} + C$$

If the equation for y_1 is subtracted from the general equation, an equation can be developed that can be fitted to a curve by linear regression. The development of this equation is as follows:

$$y - y_1 = \frac{x}{a + bx} - \frac{x_1}{a + bx_1}$$

$$y - y_1 = \frac{a(x - x_1)}{(a + bx)\ (a + bx_1)}$$

$$\frac{x - x_1}{y - y_1} = \frac{(a + bx)\ (a + bx_1)}{a}$$

$$\frac{x - x_1}{y - y_1} = \frac{a^2 + abx_1 + abx + b^2xx_1}{a}$$

$$\frac{x - x_1}{y - y_1} = (a + bx_1) + \frac{b}{a}\ (a + bx_1)\ x$$

If $a' = a + bx_1$ and $b' = \frac{b}{a}\ (a + bx_1)$

then $\frac{x - x_1}{y - y_1} = a' + b'x$.

This is a linear equation having four constants, x_1, y_1, a', and b'. a' and b' can be evaluated by a linear regression of $\frac{x - x_1}{y - y_1}$ versus x.

a and b can be determined after a' and b' are known by solving $a' = a + bx_1$ and $b' = \frac{b}{a}(a + bx_1)$ simultaneously for a and b. The expressions are:

$$b = \frac{a'b'}{a' + b'x_1}$$

$$a = \frac{(a')^2}{a' + b'x_1}$$

C can be evaluated by substituting a and b in the equation:

$$y_1 = \frac{x_1}{a + bx_1} + C$$

$$C = y_1 - \frac{x_1}{a + bx_1}$$

The equation apparently does not predict exact values for strain when EI/GJ equals 2.065 but the trend of the curve is established. The eight relationships between strain and EI/GJ in this experiment were developed in this way.

Coefficients A, B, and C, for the equation $e = \frac{EI/GJ}{A + B(EI/GJ)} + C$, describing the relationship between strain and EI/GJ for all eight loading conditions are given in Table XXI.

TABLE XXI

COEFFICIENTS FOR EQUATIONS RELATING e TO EI/GJ

$$e = \frac{EI/GJ}{A + B(EI/GJ)} + C$$

Strain Location (Slat No.)	Load Location (Slat No.)	A	B	C
1	1	.007	-.014	250.14
2	1	.058	-.088	123.95
3	1	-.149	.180	80.78
4	1	-.112	.126	67.52
1	2	.028	-.047	137.78
2	2	.015	-.027	189.39
3	2	.220	-.309	102.58
4	2	-.269	.345	86.12

Strain Versus EI/PL^2

The relationship between strain and the pi term, EI/PL^2, may be evaluated in a model test by considering EI/L^2 as a constant and varying P. A small value for P will result in a large value for the pi term, EI/PL^2. As P is increased, the value of the pi term will decrease. If the modeling material, plaster, demonstrates a linear stress-strain relationship, the variation of strain and P should be linear in the model tests. As EI/PL^2 increases, strain should decrease.

Experimental data showing the relationship between strain on slat one and EI/PL^2 with the load on slat one are plotted on Figure 23. The plot indicates that the data fit the log-log equation of the type $\log y = \log A + B(\log x)$. The logarithms of the data were fitted to a straight line by linear regression. Correlation coefficients indicated that the data fit well. Coefficients A and B for the equation $e = A(EI/PL^2)^{-B}$, describing the relationship between strain and EI/PL^2 for all eight loading conditions are given in Table XXII.

TABLE XXII

COEFFICIENTS OF EQUATIONS RELATING e TO EI/PL^2

$e = A(EI/PL^2)^{-B}$

Strain Location (Slat No.)	Load Location (Slat No.)	A	B	Correlation Coefficients
1	1	1577.52	1.029	0.996
2	1	1091.12	0.999	0.999
3	1	1021.72	1.014	0.998
4	1	1009.80	1.038	0.991
1	2	1156.82	1.039	0.995
2	2	1686.80	1.114	0.991
3	2	1111.30	1.039	0.996
4	2	1075.67	1.041	0.992

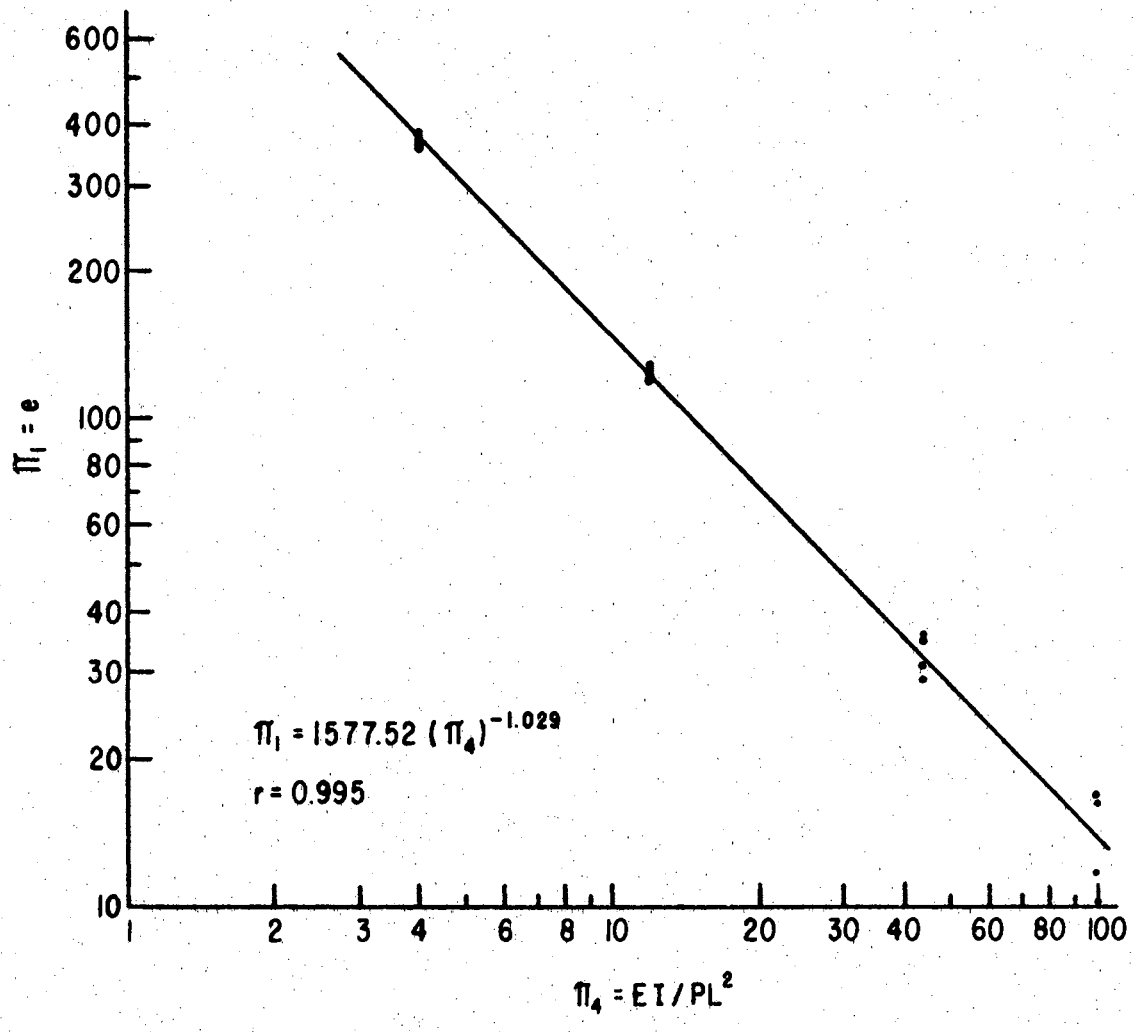

Figure 23. Relationship Between Strain on Slat One and the Pi Term, EI/PL^2, With Other Pi Terms Held Constant; Load on Slat One

B in the equation $e = A(EI/PL^2)^{-B}$ has a value of approximately one for each of the eight equations. This verifies that plaster demonstrates a linear stress-strain relationship. For any given grid EI/L^2 will be constant. Since B is negative, the equation can be written $e = A(L^2/EI)\ (P)$. This linear form of the equation was used in the prediction equation.

Strain Versus L/B

Cross tie length is a function of the slat spacing, B. The bending and deflection that is transmitted from the loaded slat to the unloaded slat is influenced by the deflection in the cross ties. This deflection in the cross tie may be expressed as a function of PL^3/EI, where L would be a function of B. This is the general expression for deflection in a beam. If L is short, differential deflection between the loaded and unloaded slats would be small and the cross tie would effectively transmit deflection away from the loaded slat. Moments would be influenced in a similar manner. If L is long, differential deflection between the loaded and unloaded slats would be large and the loaded slat would deflect more than the unloaded slats. The loaded slat would carry greater moment than the unloaded slat.

L was held constant in the model tests. The pi term, L/B, was varied by varying the slat spacing, B. As B increased, the pi term, L/B, decreased.

Experimental data showing the relationship between strain on slat one and L/B with the load on slat one are plotted on Figure 24. These data were handled in a manner similar to the data for strain versus EI/PL^2 since the plot indicates that it fits a log-log curve.

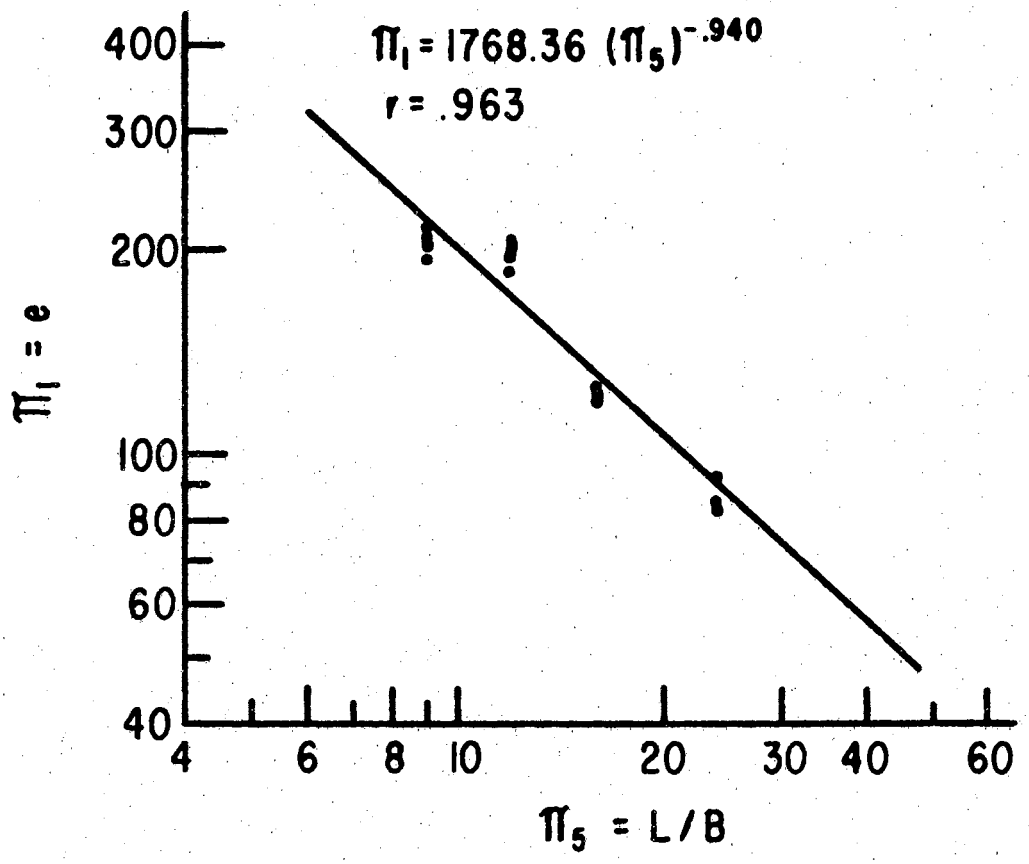

Figure 24. Relationship Between Strain on Slat One and the Pi Term, L/B, With Other Pi Terms Held Constant; Load on Slat One

The correlation coefficient of the regression analysis indicates that the data fit the log-log curve. Coefficients A and BB for the equation $e = A(L/B)^{-BB}$, describing the relationship between strain and L/B for all eight loading conditions, are given in Table XXIII.

TABLE XXIII

COEFFICIENTS OF EQUATIONS RELATING e TO L/B
$e = A(L/B)^{-BB}$

Strain Location (Slat No.)	Load Location (Slat No.)	A	BB	Correlation Coefficients
1	1	1768.36	.941	0.964
2	1	1223.27	.933	0.946
3	1	653.45	.752	0.912
4	1	366.87	.569	0.771
1	2	1207.31	.933	0.929
2	2	1119.09	.814	0.951
3	2	945.99	.864	0.939
4	2	642.12	.748	0.898

Strain Versus X/L

As X/L becomes larger, X must increase if L is held constant. As X increases, the loads are moved nearer to the center of the grid and strain at the center should increase.

A simple beam may be used to estimate the possible values of strain that may be expected to develop as slat one is loaded. The beams designed for the grid used to test for the effect of variation of X had a depth of 1.25 inches, and an I value of 0.2. If E is assumed at 1×10^6 psi, two loads of 15 pounds each would be required to keep EI/PL^2 constant at 12. An expression for estimating strain at

the center of slat one when slat one is loaded may be developed from flexure formula if a simple beam is assumed.

$$S = \frac{Mc}{I}$$

$$Ee = \frac{Mc}{I}$$

$$e = \frac{Mc}{EI}$$

If equal loads are placed each an equal distance, X, from each end of the beam, moment may be expressed as PX where P is the value for each of the two loads.

$$M = PX$$

$$e = \frac{PXc}{EI}$$

$$e = \frac{15(1.25/2)}{10^6(0.20)} X = 46(10)^{-6} X \text{ (inches/inch)}$$

or

$$46X \text{ (microinches/inch)}$$

Evaluating 46X and dividing by four may give an estimate of the strain at the center of one of the four slats in the grid.

$$X = 11, \quad X/L = 0.46, \quad 1/4\ e = 126$$

$$X = 9, \quad X/L = 0.38, \quad 1/4\ e = 104$$

$$X = 7, \quad X/L = 0.29, \quad 1/4\ e = 80$$

$$X = 4, \quad X/L = 0.17, \quad 1/4\ e = 46$$

Experimental data showing the relationship between strain on slat one and X/L with the load on slat one are plotted on Figure 25. The estimated values were larger than test data but a simply supported beam was assumed for the estimate and the actual grid had partially fixed ends on the slats. The correlation coefficient of the regression analysis indicates that the data fit the log-log curve better than a

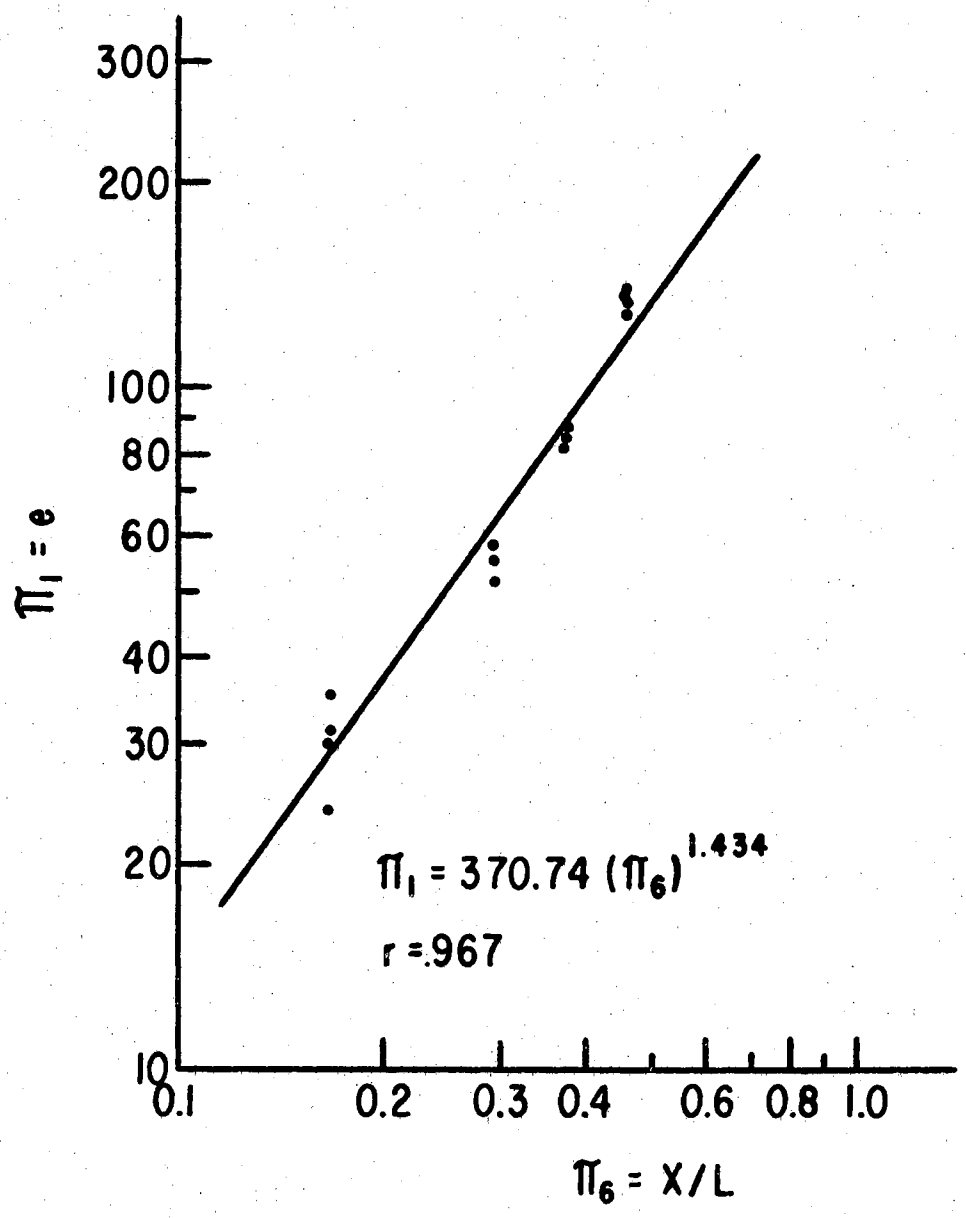

Figure 25. Relationship Between Strain on Slat One and the Pi Term, X/L, With Other Pi Terms Held Constant; Load on Slat One

linear curve. Coefficients A and B for the equation $e = A(X/L)^B$, describing the relationship between strain and X/L for all eight loading conditions, are given in Table XXIV. The values of the exponents of the pi term, X/L, indicate that strain is greatest in the loaded slat. The amount of strain transmitted away from the loaded slat decreases as the distance away from the loaded slat increases.

TABLE XXIV

COEFFICIENTS OF EQUATIONS RELATING e TO X/L

$e = A(X/L)^B$

Strain Location (Slat No.)	Load Location (Slat No.)	A	B	Correlation Coefficients
1	1	370.74	1.434	0.979
2	1	201.79	1.003	0.986
3	1	166.17	0.888	0.990
4	1	143.93	0.787	0.977
1	2	194.72	0.993	0.983
2	2	305.79	1.325	0.987
3	2	188.73	1.000	0.993
4	2	175.88	0.960	0.986

Strain Versus T

Increasing the number of cross ties in a grid may be expected to increase the stiffness of the grid and in turn reduce the strain at the center of the loaded slat. More strain should be transmitted to unloaded slats as the number of ties is increased. The Guyon-Massonnet (3, 8, 10, 14) procedure for analyzing grids indicated that these effects might not be great.

Figure 26 illustrates the relationship between number of ties and grid strain at the center of slat one when loads are applied to slat one in the position where X/L = 0.46. Strains are measured for loads having the magnitude necessary to maintain EI/PL^2 constant at 12.

The data were fitted to a straight line by means of a linear regression analysis. The data were fitted to a log-log curve and a semi-log curve, but correlation coefficients indicated that the linear relationship provided the best fit. The general form of the regression equation can be written:

$$e = A - B(T)$$

The linear regression of the data resulted in small values for slope, suggesting that the number of cross ties may not influence grid strain. Table XXV is a split-split plot analysis of variance designed to test if differences exist between strains for grids having 1, 2, 3, or 4 cross ties. Table XXVI lists the values of strain used in the analysis of variance.

The calculated F value is 15.13 for the differences between grids having 1, 2, 3, or 4 cross ties. The tabulated value is 4.02 at the 99 per cent level. This indicates that there probably is a difference in the strain pi term at the center of each slat that is due to differences in the number of cross ties. It should therefore be included in a combined prediction equation.

Coefficients A and B for the equation e = A - B(T), describing the relationship between strain and T for all eight loading conditions are given in Table XXVII.

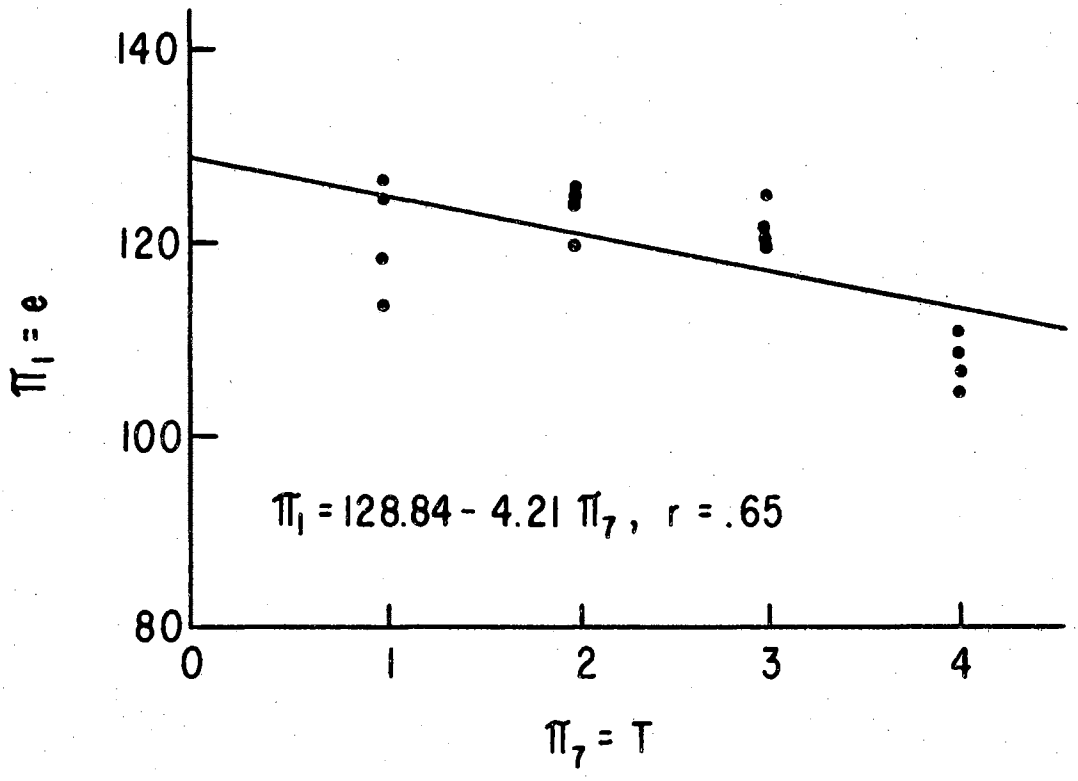

Figure 26. Relationship Between Strain on Slat One and the Pi Term, T, With Other Pi Terms Held Constant; Load on Slat One

TABLE XXV

ANALYSIS OF VARIANCE FOR GRID STRAIN VERSUS NUMBER OF TIES

Source	Degrees of Freedom	Sum of Squares	Mean Square	F
Load Location (Slat No.)	1	3.00	3.00	0.20
Strain Location (Slat No.)	3	13,901.70	4,633.90	316.64
Number of Ties	3	664.10	221.36	15.13
(Load Location) X (Strain Location) Interaction	3	5,190.00	1,730.00	118.21
(Load Location) X (No. of Ties) Interaction	3	60.90	20.30	1.39
(Strain Location) X (No. of Ties) Interaction	9	511.00	56.77	3.88
(Load Location) X (Strain Location) X (No. of Ties) Interaction	9	946.80	105.20	7.19
Error	96	1,404.90	14.63	
Total	127	22,682.40		

TABLE XXVI

GRID STRAIN AOV DATA

Number of Ties on Grid	Replication Number	Load on Slat 1				Load on Slat 2			
		Strain on Slat 1	Strain on Slat 2	Strain on Slat 3	Strain on Slat 4	Strain on Slat 1	Strain on Slat 2	Strain on Slat 3	Strain on Slat 4
		- microinches per inch -				- microinches per inch -			
1	1	124.56	97.00	91.13	78.89	104.23	99.38	90.85	81.49
1	2	118.37	104.02	91.69	75.83	98.75	98.37	87.40	85.01
1	3	126.21	99.17	91.46	78.30	106.50	106.02	92.40	86.82
1	4	113.40	102.07	89.82	77.46	99.36	103.57	100.96	94.61
2	1	119.58	88.98	86.39	82.68	86.65	110.43	87.37	87.41
2	2	125.81	91.69	82.57	77.00	94.70	114.46	84.46	78.38
2	3	125.66	89.95	81.14	79.96	85.13	109.91	81.76	81.41
2	4	123.95	93.84	80.89	71.77	89.19	109.79	88.41	82.43
3	1	124.48	99.59	84.22	69.79	97.71	108.20	87.90	79.73
3	2	121.61	112.58	85.90	71.56	93.24	101.19	87.94	84.08
3	3	120.29	98.75	86.69	76.54	106.46	115.29	95.16	91.80
3	4	119.86	96.58	82.13	77.79	100.65	109.88	94.52	91.81
4	1	110.40	96.23	83.11	80.06	96.93	101.76	87.78	84.38
4	2	108.17	91.45	84.35	83.33	95.13	96.85	90.22	85.16
4	3	104.00	91.36	81.00	72.70	90.74	99.04	87.10	82.64
4	4	106.78	93.98	84.72	78.12	93.23	101.73	90.25	84.02

TABLE XXVII

COEFFICIENTS A AND B AND CORRELATION COEFFICIENTS FOR THE LINEAR REGRESSION EQUATION e = A - B(T) FOR ALL CONDITIONS OF GRID LOADING

Strain Location (Slat No.)	Load Location (Slat No.)	A	B	Correlation Coefficients
1	1	128.84	4.21	0.65
2	1	99.50	1.12	0.21
3	1	90.75	2.12	0.64
4	1	77.27	0.11	0.03
1	2	99.66	1.40	0.25
2	2	107.49	0.85	0.17
3	2	91.23	0.63	0.16
4	2	86.16	0.44	0.11

The form of the equation used for combining the five functions of the strain pi term by multiplication is given in Table XXVIII along with the calculated values of $F(\overline{\pi}_3, \overline{\pi}_4, \overline{\pi}_5, \overline{\pi}_6, \overline{\pi}_7)$ for the eight conditions of grid loading. $F(\overline{\pi}_3, \overline{\pi}_4, \overline{\pi}_5, \overline{\pi}_6, \overline{\pi}_7)$ was taken as an average of five strain values computed from the five functions of strain that were developed from test data. Each of the five strain functions were calculated using the value of each independent pi term at which the pi terms were held constant for four of the test series.

The final form of the prediction equation and the coefficients for each of the eight grid loading conditions are given in Table XXIX. Regression line intercepts from the log-log plots were multiplied together and then divided by $F(\overline{\pi}_3, \overline{\pi}_4, \overline{\pi}_5, \overline{\pi}_6, \overline{\pi}_7)$ to evaluate the coefficient, K_1.

Eight prediction equations were written for strain. Four were written for loads on slat one, and four were written for loads on slat

two. Each set of four equations was written to predict strain at each of the four slats as a result of the load applied to slats one or two.

TABLE XXVIII

FORM OF THE EQUATION COMBINING THE FUNCTIONS OF STRAIN AND THE VALUES OF $F(\overline{\pi}_3, \overline{\pi}_4, \overline{\pi}_5, \overline{\pi}_6, \overline{\pi}_7)$ FOR EACH OF THE EIGHT CONDITIONS OF LOADING USED IN THE TEST SERIES

$$\pi_1 = \frac{F(\overline{\pi}_3, \pi_4, \pi_5, \pi_6, \pi_7)\ F(\pi_3, \overline{\pi}_4, \pi_5, \pi_6, \pi_7)\ F(\pi_3, \pi_4, \overline{\pi}_5, \pi_6, \pi_7)\ F(\pi_3, \pi_4, \pi_5, \overline{\pi}_6, \pi_7)\ F(\pi_3, \pi_4, \pi_5, \pi_6, \overline{\pi}_7)}{F(\overline{\pi}_3, \overline{\pi}_4, \overline{\pi}_5, \overline{\pi}_6, \overline{\pi}_7)^4}$$

Strain Location (Slat No.)	Load Location (Slat No.)	$F(\overline{\pi}_3, \overline{\pi}_4, \overline{\pi}_5, \overline{\pi}_6, \overline{\pi}_7)$
1	1	127.71
2	1	94.62
3	1	86.49
4	1	81.72
1	2	94.34
2	2	119.03
3	2	90.13
4	2	86.48

TABLE XXIX

FINAL PREDICTION EQUATION FOR GRID STRAIN AND THE VALUES OF COEFFICIENTS TO USE FOR EACH OF THE EIGHT CONDITIONS OF LOADING USED IN THE TEST SERIES

$$e = (K_1)\left(\frac{EI/GJ}{K_2 + K_3(EI/GJ)} + K_4\right)(PL^2/EI)(L/B)^{-K_5}(X/L)^{K_6}(K_7 - K_8(T))$$

Strain Location (Slat No.)	Load Location (Slat No.)	K_1	K_2	K_3	K_4	K_5	K_6	K_7	K_8
1	1	3.89	.007	-.014	250.14	.941	1.434	128.84	4.21
2	1	3.36	.058	-.088	123.95	.933	1.003	99.50	1.12
3	1	1.98	-.149	.180	80.78	.752	0.888	90.75	2.12
4	1	1.20	-.112	.126	67.52	.569	0.787	77.27	0.11
1	2	3.43	.028	-.047	137.78	.933	0.993	99.66	1.40
2	2	2.88	.015	-.027	189.39	.814	1.325	107.49	0.85
3	2	3.01	.220	-.309	102.58	.864	1.000	91.23	0.63
4	2	2.17	-.269	.345	86.12	.748	0.960	86.16	0.44

CHAPTER VIII

ANALYSIS OF DATA FOR GRID DEFLECTION TESTS

Deflection measurements using the five test series in Table XVII are tabulated in Appendix B. Appendix B, Table I lists deflection measurements taken for test series A, Table XVII in which the independent pi term EI/GJ was varied while other independent pi terms were held constant. Appendix B, Table II lists strain measurements taken for test series B, Table XVII in which the independent pi term EI/PL^2 was varied while other independent pi terms were held constant. Appendix B, Table III lists deflection measurements taken for test series C, Table XVII in which the independent pi term L/B was varied while other independent pi terms were held constant. Appendix B, Table IV lists deflection measurements taken for test series D, Table XVII in which the independent pi term X/L was varied while other independent pi terms were held constant. Appendix B, Table V lists deflection measurements taken for test series E, Table XVII in which the independent pi term T was varied while other independent pi terms were held constant.

Five curves were plotted using data taken from Appendix B, Tables I-V. The data plotted represent the deflection measurements taken on slat one when slat one was loaded. The function used to describe the relationships between deflection and each of the five independent pi terms were also plotted. The relationships of deflection

to the independent pi terms were similar for the other seven conditions of loading for each case so only one illustration is shown.

L/d Versus EI/GJ

It was shown for the relationship of strain to EI/GJ that strain on slat one may be expected to increase as EI/GJ increases. The same effect may be expected for the relationship between deflection and EI/GJ. This would cause an inverse relationship between L/d and EI/GJ. An analysis of the test grids using the Guyon-Massonnet procedure of analysis gave results in which a plot of calculated values would yield a curve having a negative slope between EI/GJ = 0.74 and EI/GJ = 3.87.

Experimental data showing the relationship between L/d on slat one and EI/GJ with the load on slat one are plotted on Figure 27. The logarithms of the data were fitted to a straight line by linear regression. Correlation coefficients indicated that the data did not fit a log-log curve as well as most other relationships in the test series, but correlation coefficients for the log-log curve were better than for linear or semi-log plots. Deflections for other loading conditions were analyzed in the same way.

Coefficients A and B for the equation $L/d = A(EI/GJ)^B$, describing the relationship between L/d and EI/GJ for all eight loading conditions are given in Table XXX.

The sign of the exponent, B, is negative on the loaded side of the grid and positive on the unloaded side. The magnitude increases from the unloaded to the loaded side. This has the effect of causing the pi term L/d to be smaller on the loaded side of the grid than on the unloaded side.

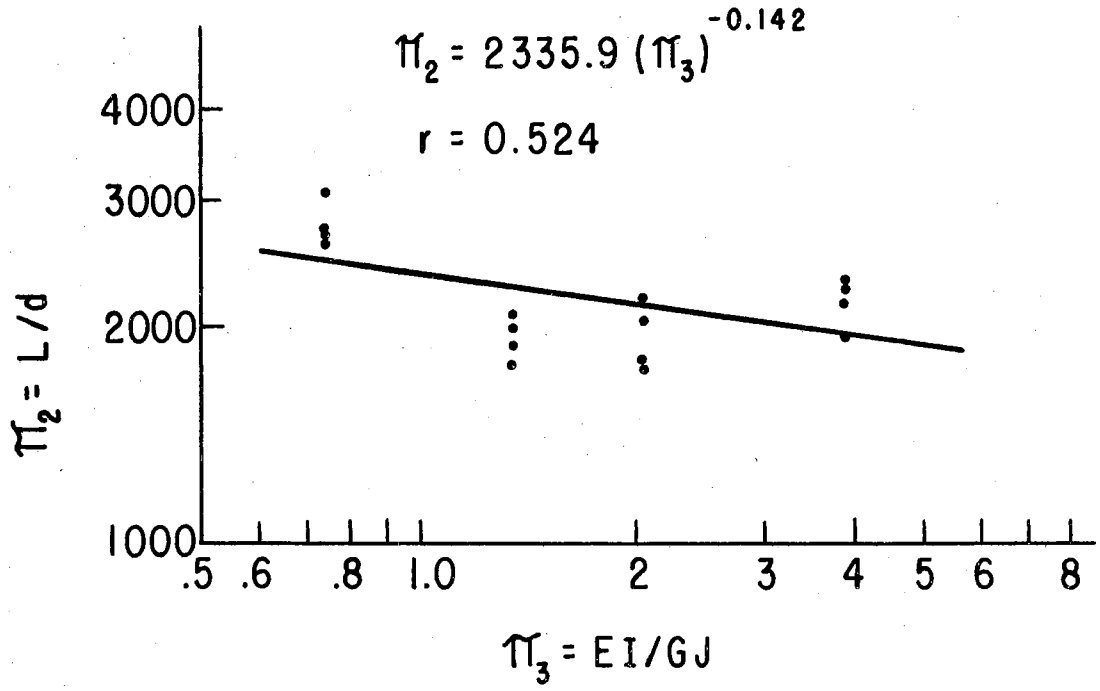

Figure 27. Relationship Between L/d on Slat One and the Pi Term, EI/GJ, With Other Pi Terms Held Constant; Load on Slat One

TABLE XXX

COEFFICIENTS FOR EQUATIONS RELATING L/d TO EI/GJ,
OTHER INDEPENDENT PI TERMS HELD CONSTANT

$$L/d = A(EI/GJ)^B$$

Deflection Location (Slat No.)	Load Location (Slat No.)	A	B	Correlation Coefficients
1	1	2335.9	-0.142	.524
2	1	2644.8	-0.073	.511
3	1	3042.1	+0.061	.471
4	1	3446.1	+0.200	.715
1	2	2617.9	-0.033	.194
2	2	2545.0	-0.049	.304
3	2	2798.2	-0.013	.090
4	2	2933.6	+0.027	.171

L/d Versus EI/PL^2

To evaluate the effect of EI/PL^2 on the pi term L/d, EI/L^2 and L were considered as being constant. EI/PL^2 is then increased as P decreases. An increasing EI/PL^2 should decrease the deflection. Therefore as EI/PL^2 increases, L/d may be expected to increase.

Experimental data showing the relationship between L/d on slat one and EI/PL^2 with the load on slat one are plotted on Figure 28. The plot indicates that the data fit the log-log equation of the type $\log y = \log A + B \log x$. The logarithms of the data were fitted to a straight line by linear regression. Correlation coefficients indicated that the data fit well. Coefficients A and B for the equation $L/d = A(EI/PL^2)^B$, describing the relationship between L/d and EI/PL^2 for all eight loading conditions are given in Table XXXI.

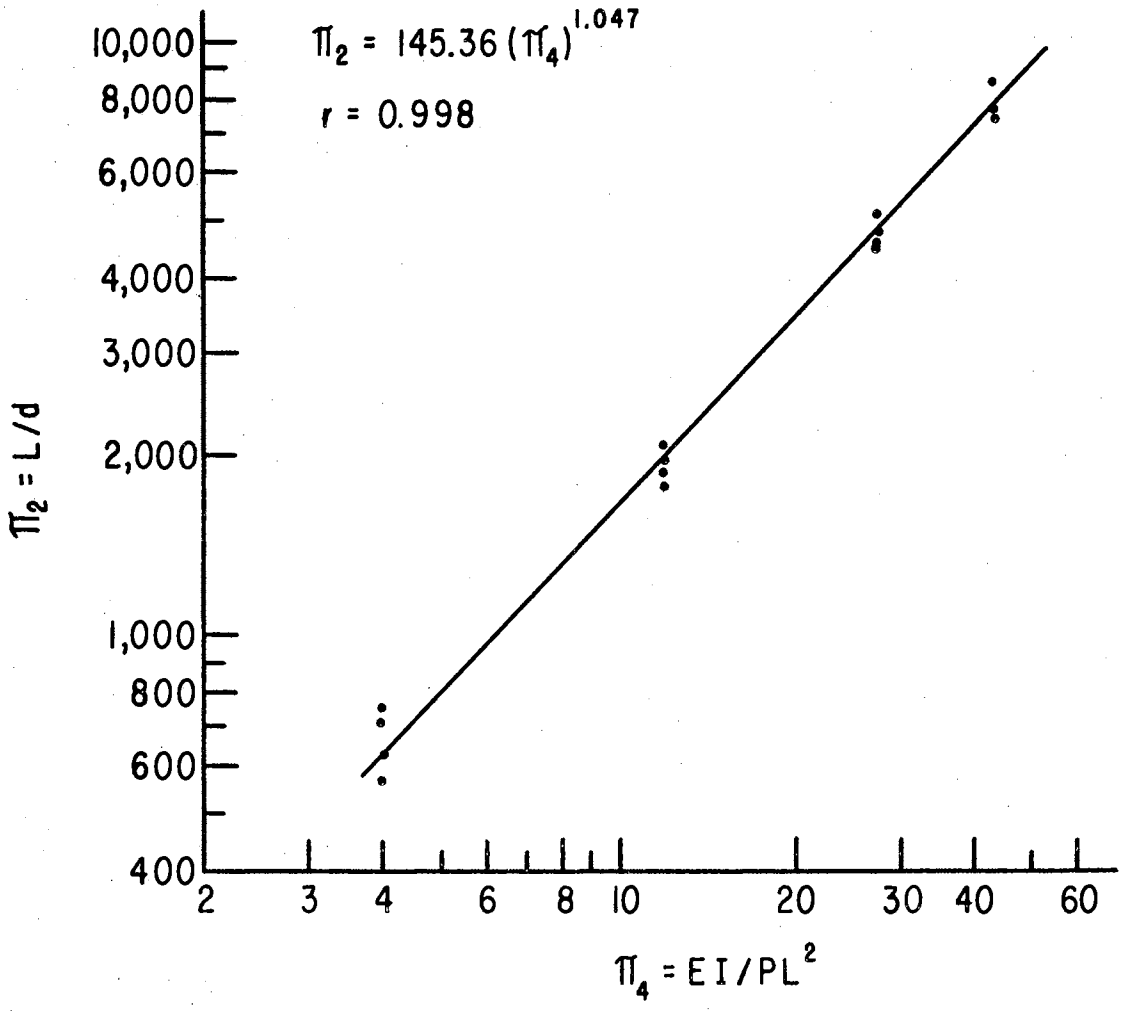

Figure 28. Relationship Between L/d on Slat One and the Pi Term, EI/PL^2, With Other Pi Terms Held Constant; Load on Slat One

TABLE XXXI

COEFFICIENTS FOR EQUATIONS RELATING L/d TO EI/PL^2, OTHER INDEPENDENT PI TERMS HELD CONSTANT

$L/d = A(EI/PL^2)^B$

Deflection Location (Slat No.)	Load Location (Slat No.)	A	B	Correlation Coefficients
1	1	145.4	1.048	.998
2	1	174.7	1.057	.999
3	1	212.8	1.058	.997
4	1	267.0	1.066	.986
1	2	169.9	1.069	.997
2	2	174.3	1.066	.998
3	2	186.9	1.067	.998
4	2	198.8	1.067	.997

B in the equation $L/d = A(EI/PL^2)^B$ has a value of approximately one for each of the eight equations. This verifies that plaster demonstrates a linear stress-strain relationship. For any given grid, EI/L^2 will be constant. The equation can be written:

$$L/d = (A)(EI/L^2)(P)^{-1}$$

This linear form of the equation was used in the prediction equation.

L/d Versus L/B

Cross tie length is a function of the slat spacing, B. The equation for the deflection of a simple beam is given as a function of PL^3/EI. If a function of this type is applied to cross ties of a grid, L is a function of B. If L is small, differential deflection will be small and unloaded slats will deflect nearly as much as the loaded slat. If L is large, differential deflection will be large so

the loaded slat will deflect to a greater degree than the unloaded slat. If L becomes very large, differential deflection will be very large and deflection of the loaded slat should approach that of a simple beam. The adjoining unloaded slat should deflect very little.

As B becomes large, L/B will become small and the deflection on the loaded slat should approach the deflection expected in a simple beam. Under the same conditions, deflection in the unloaded beams should become small which would make L/d large.

Figure 29 illustrates the relationships between L/d and L/B for each of the four slats in a grid when slat one is loaded. The curves represent the results of a linear regression of test data for each of the four cases. Test data are plotted for L/d on slat one when slat one is loaded to show the general relationship between the regression line and the data.

When L/B approaches zero for the case where L/d was recorded on slat one under a load on slat one, L/d should not approach zero. It should approach a value similar to that expected for a simple beam. A linear relationship gave these results where a log-log plot did not. Correlation coefficients were better for the linear relationship than for either log-log plots or semi-log plots. For these reasons, the linear relationship was selected.

If the unloaded slats are considered when L/B approaches zero, d on these slats should become very small and the pi term, L/d, should become large. This is partially demonstrated by a linear curve, but the effect probably should be greater. The linear regression fits the data better than a log-log curve for the reasons given for L/d on slat one under a load on slat one. The linear relationships were

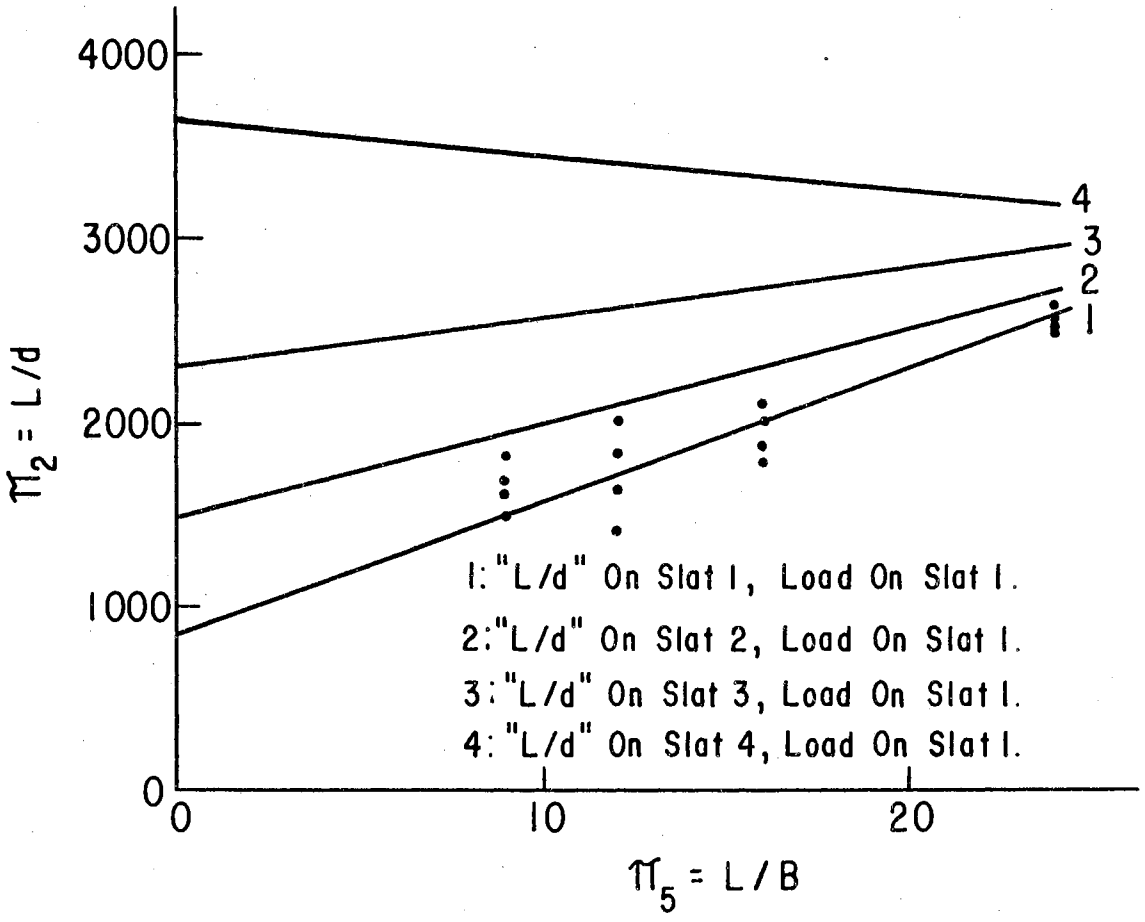

Figure 29. Relationship Between L/d on Each of the Four Slats and the Pi Term, L/B, With Other Pi Terms Held Constant; Load on Slat One

considered adequate for the range of values of L/B from nine to 24.

Coefficients A and C for the equation, $L/d = A + C(L/B)$, describing the relationship between L/d and L/B for all eight loading conditions are given in Table XXXII.

TABLE XXXII

COEFFICIENTS FOR EQUATIONS RELATING L/d TO L/B, OTHER INDEPENDENT PI TERMS HELD CONSTANT

$L/d = A + C(L/B)$

Deflection Location (Slat No.)	Load Location (Slat No.)	A	C	Correlation Coefficients
1	1	932.5	67.9	.924
2	1	1479.6	52.9	.915
3	1	2327.8	26.4	.571
4	1	3666.1	-19.9	.199
1	2	1291.6	65.5	.878
2	2	1436.2	57.8	.897
3	2	1729.8	49.4	.819
4	2	1991.5	41.6	.702

L/d Versus X/L

X in the pi term X/L represents the distance from the end of the grid to the load position. As load placement approaches the center of the grid, X/L increases and d should be expected to increase. As X/L increases, the pi term L/d should decrease.

An estimate of the values of L/d for different values of X/L may be made by assuming that a slat acts as a simply supported beam. Deflection can be computed on this basis and the deflection of a slat may be considered as being one-fourth of the sum of the deflections of all slats in the grid. For example, the deflection on slat one may

be estimated when slat one is loaded for the grid used in this test series.

$$d = \frac{Pa}{24EI}(3L^2 - 4a^2)$$

$$P = 15$$

$$E = 1 \times 10^6$$

$$I = 0.2$$

$$L = 24$$

$$d = \frac{15a}{24 \times 10^6 \times 0.2}(3 \times 24^2 - 4a^2)$$

$$= 3.12 \times 10^{-6}\, a(1728 - 4a^2)$$

$$a = 11"$$

$$d = 3.12 \times 10^{-6} \times 11(1728 - 484)$$

$$= 4.26 \times 10^{-2}$$

$$\frac{d}{4} = \frac{1}{4} \times 4.26 \times 10^{-2} = .0126"$$

$$a = 9"$$

$$d = 3.12 \times 10^{-6} \times 9(1728 - 324)$$

$$= 3.94 \times 10^{-2}$$

$$\frac{d}{4} = \frac{1}{4} \times 3.94 \times 10^{-2} = .0098"$$

$$a = 7"$$

$$d = 3.12 \times 10^{-6} \times 7(1728 - 196)$$

$$= 3.35 \times 10^{-2}$$

$$\frac{d}{4} = \frac{1}{4} \times 3.35 \times 10^{-2} = .0084"$$

$$a = 4"$$

$$d = 3.12 \times 10^{-6} \times 4(1728 - 64)$$

$$= 2.08 \times 10^{-2}$$

$$\frac{d}{4} = \frac{1}{4} \times 2.08 \times 10^{-2} = .0052"$$

Experimental data showing the relationship between L/d on slat one and X/L with the load on slat one are plotted in Figure 30. Where X/L equals 0.46, L/d was 1940 and 1900 from test data and estimates respectively. Where X/L equals 0.38, L/d was 2155 and 2450 from test data and estimates respectively. Where X/L equals 0.29, L/d was 2655 and 2860 from test data and estimates respectively. Where X/L equals 0.21, L/d was 3805 and 4600 from test data and estimates respectively. The estimated values followed the trend of the test data. Differences between computed values and values from test data may be explained by the fact that a simple beam was assumed for the calculations while the test slats had end restraints. These data were handled in a manner similar to the data for L/d versus EI/PL^2 since the plot indicates that it fits a log-log curve. The correlation coefficient of the regression analysis indicates that the data fitted the log-log curve. Coefficients A and B for the equation $L/d = A(X/L)^2$, describing the relationship between L/d and X/L for all eight loading conditions, are given in Table XXXIII.

L/d Versus T

Figure 31 illustrates the relationship between the number of cross ties in a grid and the deflection pi term at the center of slat one when loads are applied at slat one in the position where X/L = 0.46.

As the number of ties in a grid is increased, the stiffness of the grid should be expected to increase. When the stiffness of the grid increases, the deflection on the loaded slat should be expected to decrease and the ratio of L/d should be expected to increase. Increasing the number of ties should transmit stress away from the

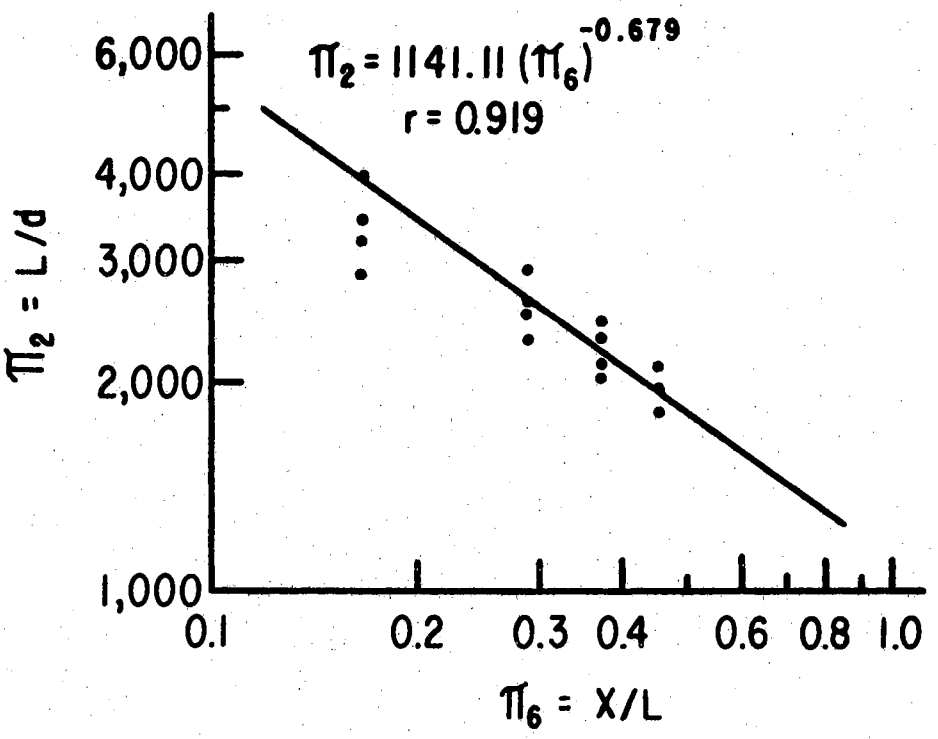

Figure 30. Relationship Between L/d on Slat One and the Pi Term, X/L, With Other Pi Terms Held Constant; Load on Slat One

TABLE XXXIII

COEFFICIENTS FOR EQUATIONS RELATING L/d TO X/L, OTHER INDEPENDENT PI TERMS HELD CONSTANT

$$L/d = A(X/L)^{-B}$$

Deflection Location (Slat No.)	Load Location (Slat No.)	A	B	Correlation Coefficients
1	1	1141.1	.679	.920
2	1	1335.1	.738	.986
3	1	1552.3	.802	.897
4	1	1481.2	1.148	.704
1	2	1448.4	.635	.970
2	2	1469.1	.649	.974
3	2	1621.0	.614	.974
4	2	1751.3	.588	.976

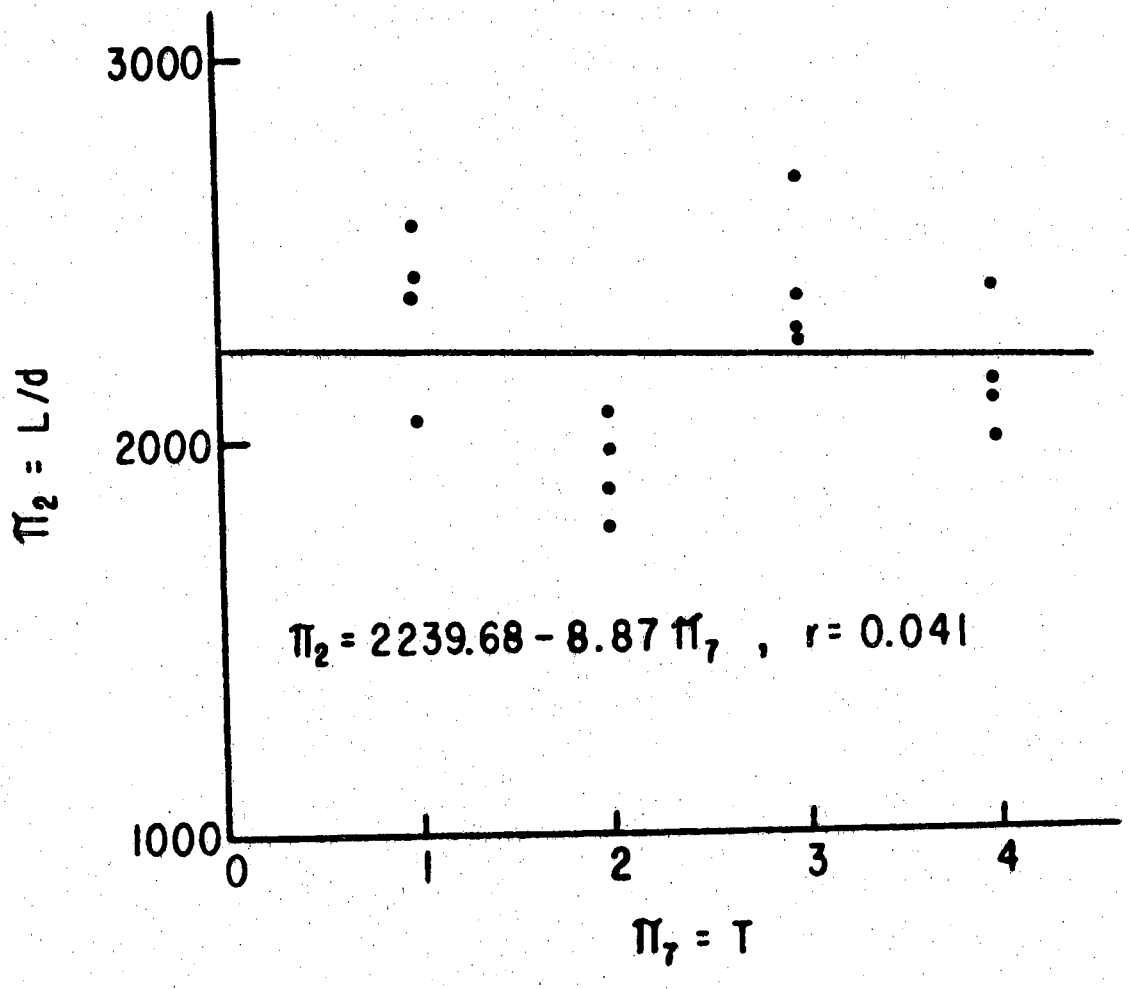

Figure 31. Relationship Between L/d on Slat One and the Pi Term, T, With Other Pi Terms Held Constant; Load on Slat One

loaded slat and cause a greater proportion of the deflection to be shared by the unloaded slats.

When T is equal to one or three in Figure 31, a cross tie is located at the center of the grid. This coincides with the point at which the deflection readings were made in each test. When T equals two or four, the deflection readings were made at the center of the grid which is half way between two cross ties located nearest the center of the grid. In these tests, load placements occurred between the cross ties where deflection is measured. Greater deflection apparently occurs at the center of the grid if there is no cross tie located at that position. The plot of the data indicates that values for the ratio of L/d oscillate from high to low values between situations where there were cross ties at the center of the grid and where there were no cross ties at the center of the grid. When no cross tie is located at the center of the grid, the slats probably are free to bend to a greater degree than if a cross tie does exist at the center of the slat.

Rather than attempt to predict the effects of the oscillation in a final prediction equation, the trend that was indicated by the data was used. Fitting the data to a straight line by using linear regression analysis would provide a line that would be very close to the line around which the data oscillates.

Coefficients A and B for the equation $L/d = A - B(T)$, describing the relationship between L/d and T for all eight loading conditions, are given in Table XXXIV. The deflection on slat one apparently increases slightly under a load on slat one as the number of ties was increased. This does not agree with the anticipated performance of

this slat under load. The confidence intervals for the slopes of the regression line are given in Table XXXIV. For the curve in Figure 40 the confidence interval ranges from 91.7 to -109.4. This would indicate that the negative slope for the line may have resulted from experimental error and that additional testing could show a positive slope which would agree with the expected performance of the system.

The data in Table XXXIV also indicates that increasing the number of ties caused unloaded slats to deflect at a greater rate. This was an expected response for grids as grid stiffness was increased.

TABLE XXXIV

COEFFICIENTS FOR EQUATIONS RELATING L/d TO T, OTHER INDEPENDENT PI TERMS HELD CONSTANT

$L/d = A - B(T)$

Deflection Location (Slat No.)	Load Location (Slat No.)	Intercept A	Slope B	Correlation Coefficient	Slope Confidence Interval	
1	1	2239.7	8.88	.042	91.7	-109.4
2	1	2601.0	32.11	.163	59.6	-123.9
3	1	3161.1	62.79	.347	17.0	-142.6
4	1	3723.0	116.62	.318	47.0	-280.2
1	2	2638.6	28.21	.175	47.0	-103.1
2	2	2775.0	39.80	.214	45.8	-125.4
3	2	2982.1	64.04	.352	16.1	-144.1
4	2	3032.1	53.79	.334	17.7	-125.3

The five functions of the deflection pi term were combined by multiplication. Combinations by addition and by methods involving addition of some terms and multiplication of others were evaluated. The combination by multiplication produced an equation that best described the deflection of the prototype used as part of the test.

The form of the equation used for combining the pi terms by multiplication is given in Table XXXV along with the calculated values of $F(\bar{\pi}_3, \bar{\pi}_4, \bar{\pi}_5, \bar{\pi}_6, \bar{\pi}_7)$ for the eight conditions of grid loading. $F(\bar{\pi}_3, \bar{\pi}_4, \bar{\pi}_5, \bar{\pi}_6, \bar{\pi}_7)$ was taken as an average of five deflection values computed from the five functions of deflection that were developed from test data. Each of the five deflection functions were calculated using the value of each independent pi term at which the pi terms were held constant for four of the test series.

The final form of the prediction equation and the coefficients for each of the eight grid loading conditions are given in Table XXXVI. Regression line intercepts from the log-log plots were multiplied together and then divided by $F(\bar{\pi}_3, \bar{\pi}_4, \bar{\pi}_5, \bar{\pi}_6, \bar{\pi}_7)$ to evaluate the coefficient, K_1,.

Eight prediction equations were written for the deflection parameter for the same loading conditions used for strain. The equations can be adapted to design problems in the same manner as the strain equations are adapted.

TABLE XXXV

FORM OF THE EQUATION COMBINING THE FUNCTIONS OF DEFLECTION AND THE VALUES OF $F(\bar{\pi}_3, \bar{\pi}_4, \bar{\pi}_5, \bar{\pi}_6, \bar{\pi}_7)$ FOR EACH OF THE EIGHT CONDITIONS OF LOADING USED IN THE TEST SERIES

$$\pi_2 = \frac{F(\bar{\pi}_3, \pi_4, \pi_5, \pi_6, \pi_7)\ F(\pi_3, \bar{\pi}_4, \pi_5, \pi_6, \pi_7)\ F(\pi_3, \pi_4, \bar{\pi}_5, \pi_6, \pi_7)\ F(\pi_3, \pi_4, \pi_5, \bar{\pi}_6, \pi_7)\ F(\pi_3, \pi_4, \pi_5, \pi_6, \bar{\pi}_7)}{F(\bar{\pi}_3, \bar{\pi}_4, \bar{\pi}_5, \bar{\pi}_6, \bar{\pi}_7)}$$

Deflection Location (Slat No.)	Load Location (Slat No.)	$F(\bar{\pi}_3, \bar{\pi}_4, \bar{\pi}_5, \bar{\pi}_6, \bar{\pi}_7)$
1	1	2036.89
2	1	2386.60
3	1	2865.80
4	1	3457.24
1	2	2387.09
2	2	2420.20
3	2	2604.49
4	2	2737.85

TABLE XXXVI

FINAL PREDICTION EQUATION FOR GRID DEFLECTION AND THE VALUES OF COEFFICIENTS TO USE FOR EACH OF THE EIGHT CONDITIONS OF LOADING USED IN THE TEST SERIES

$$L/d = (K_1)(EI/GJ)^{K_2}(EI/PL^2)(K_3 + K_4(L/B)(X/L)^{-K_5}(K_6 - K_7(T))$$

Deflection Location (Slat No.)	Load Location (Slat No.)	K_1	K_2	K_3	K_4	K_5	K_6	K_7
1	1	$2.25X10^{-5}$	-0.142	932.5	67.9	.679	2239.7	8.875
2	1	$1.90X10^{-5}$	-0.073	1479.6	52.9	.738	2601.0	23.109
3	1	$1.49X10^{-5}$	+0.061	2327.8	26.4	.802	3161.1	62.792
4	1	$0.95X10^{-5}$	+0.200	3666.1	-19.9	1.148	3723.0	116.621
1	2	$1.98X10^{-5}$	-0.033	1291.6	65.5	.635	2638.6	28.205
2	2	$1.90X10^{-5}$	-0.049	1436.2	57.8	.649	2775.0	39.800
3	2	$1.84X10^{-5}$	-0.013	1729.8	49.4	.614	2982.1	64.038
4	2	$1.82X10^{-5}$	+0.027	1991.5	41.6	.588	3032.1	53.788

CHAPTER IX

DISCUSSION OF RESULTS

Comparison of Predicted π_1 With Observed π_1

Figure 32 is a plot of observed values of π_1 compared to values computed from the prediction equations in Table XXIX. The curve was plotted to evaluate the precision with which the experimental data taken from the models were described by values computed from the prediction equations. Thirty observed values for strain were selected at random from all of the observations made in the tests. The intercept of the regression curve was -1.08 and the slope of the line was 1.005. The confidence interval on the slope ranged from 0.99 to 1.02. The correlation coefficient was 0.99.

Figure 33 is a plot of observed values of π_1 compared to values computed from the prediction equations for the prototype grid having a length of 47 inches. The data plotted are for strain on slat one under loads on slat one. Data for the prototype are tabulated in Appendix C. The curve was plotted to evaluate the precision with which the experimental data taken from the prototype were described by values computed from the prediction equation. The intercept of the regression curve was 1.93 and the slope of the line was 1.081. The confidence interval on the slope ranged from 1.08 to 1.09. The correlation coefficient was 0.99.

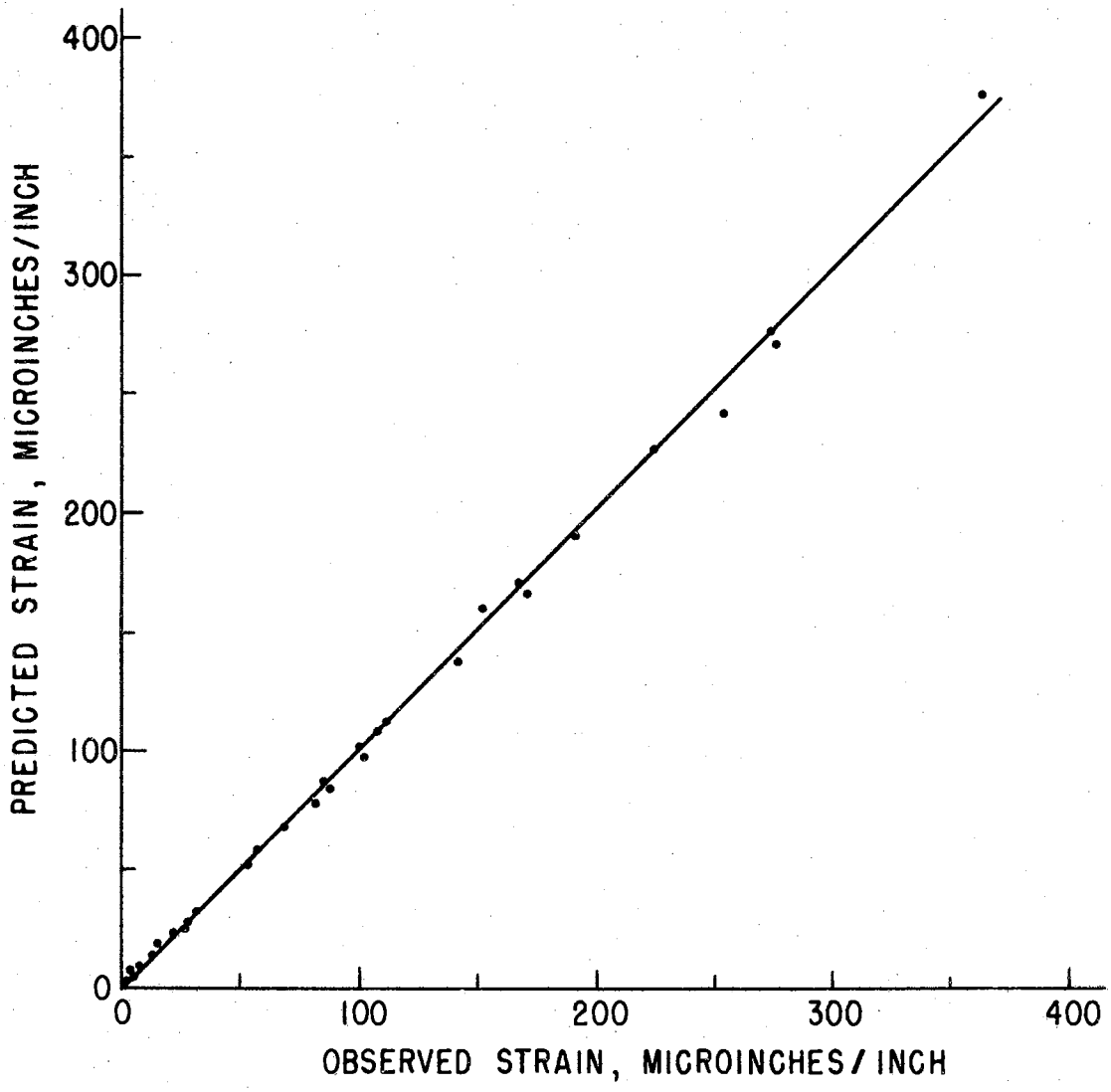

Figure 32. Observed Values of π_1 Compared to Values Computed from Prediction Equations for Strain Derived from Experimental Data Taken from the Model Tests

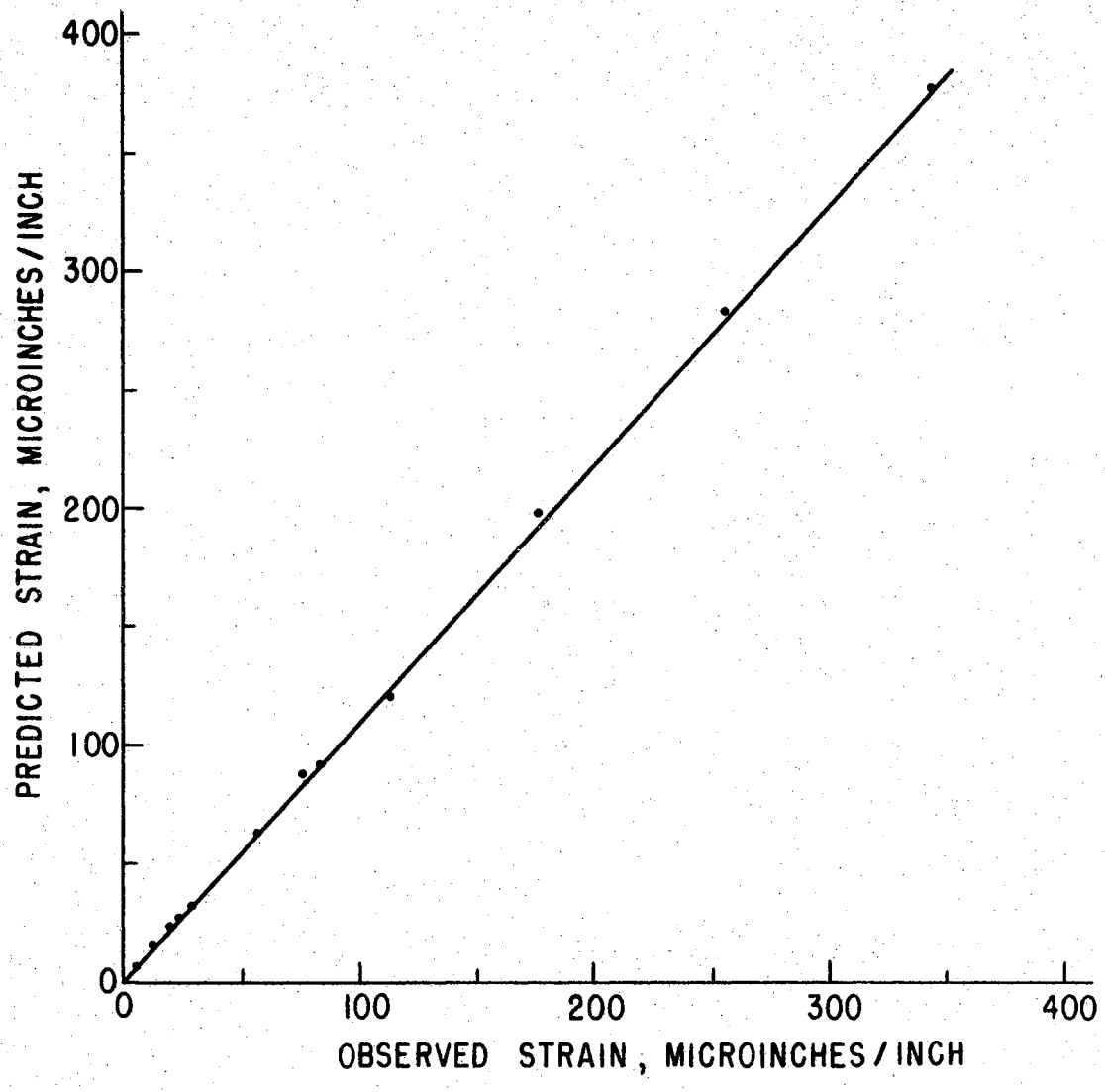

Figure 33. Observed Values of π_1 Compared to Values Computed from Prediction Equations for Strain on Slat One Under Loads on Slat One from Prototype Data in Appendix C

In both cases, the intercept of the regression line is near zero and the slope of the line is approximately one. This indicates that values computed from the prediction equation closely approximated the observed values. The confidence interval for the slope of the line plotted for data from the models ranged above and below one. The high and low values of the confidence interval for the slope of the line for data from the prototype having a length of 47 inches were both greater than one. This indicates that the prediction equation did not estimate the performance of the prototype with as much precision as it did for the model.

Comparison of Predicted π_2 With Observed π_2

Figure 34 is a plot of observed values of π_2 compared to values computed from the prediction equation in Table XXXVI. The curve was plotted to evaluate the precision with which the experimental data taken from the models were described by values computed from the prediction equation. Thirty observed values for L/d were selected at random from all of the observations made in the tests. The intercept of the regression line was 55.4 and the slope of the line was 0.98. The confidence interval on the slope of the line ranged from 0.97 to 0.99. The correlation coefficient was 0.99.

Figure 35 is a plot of observed values of π_2 compared to values computed from the prediction equations for the prototype grid having a length of 47 inches. The data plotted are for L/d values on slat one under loads on slat one. Data for the prototype are tabulated in Appendix D. The curve was plotted to evaluate the precision with which the experimental data taken from the prototype were described by values

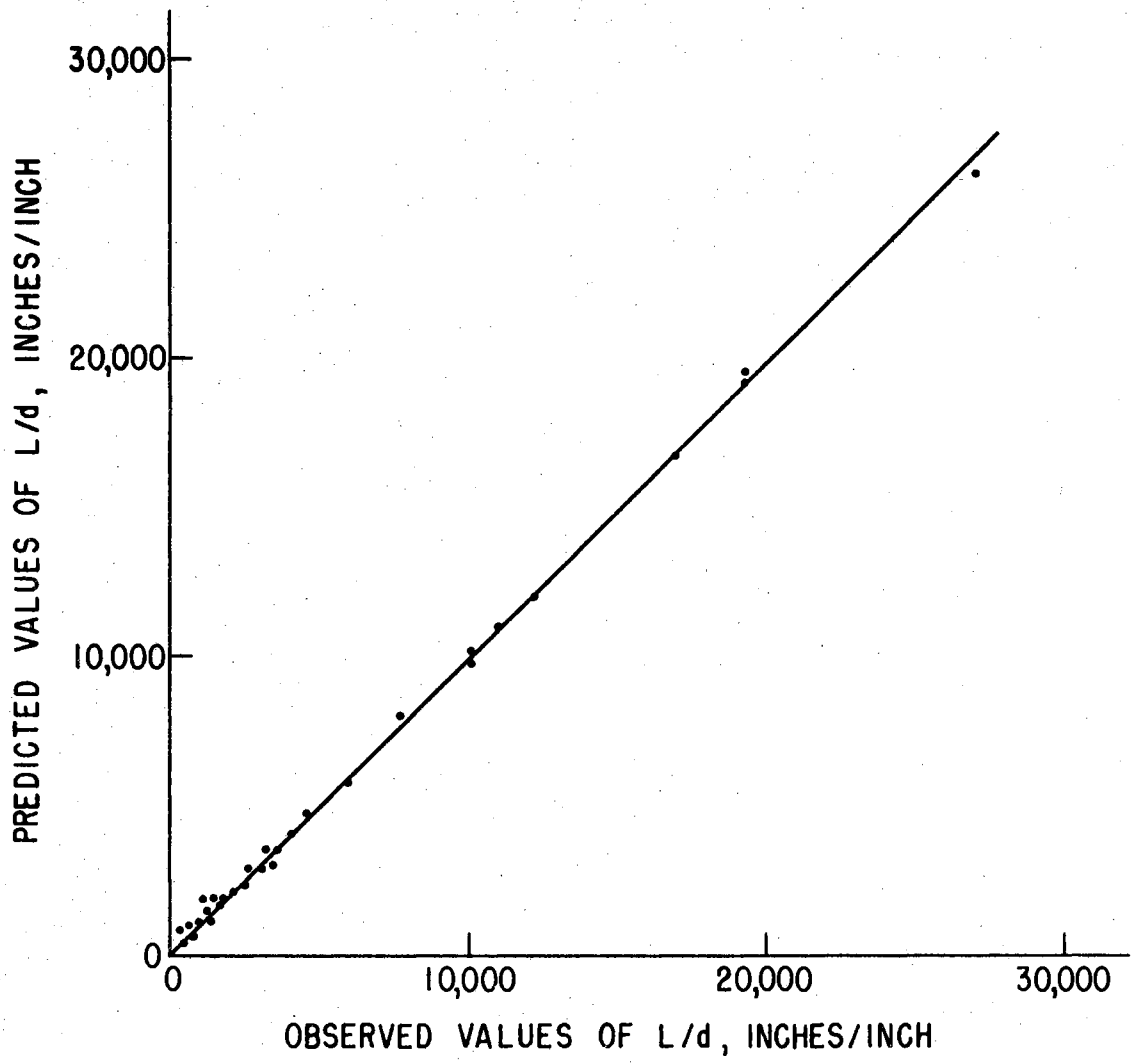

Figure 34. Observed Values of π_2 Compared to Values Computed from Prediction Equations for L/d Derived from Experimental Data Taken from Model Tests

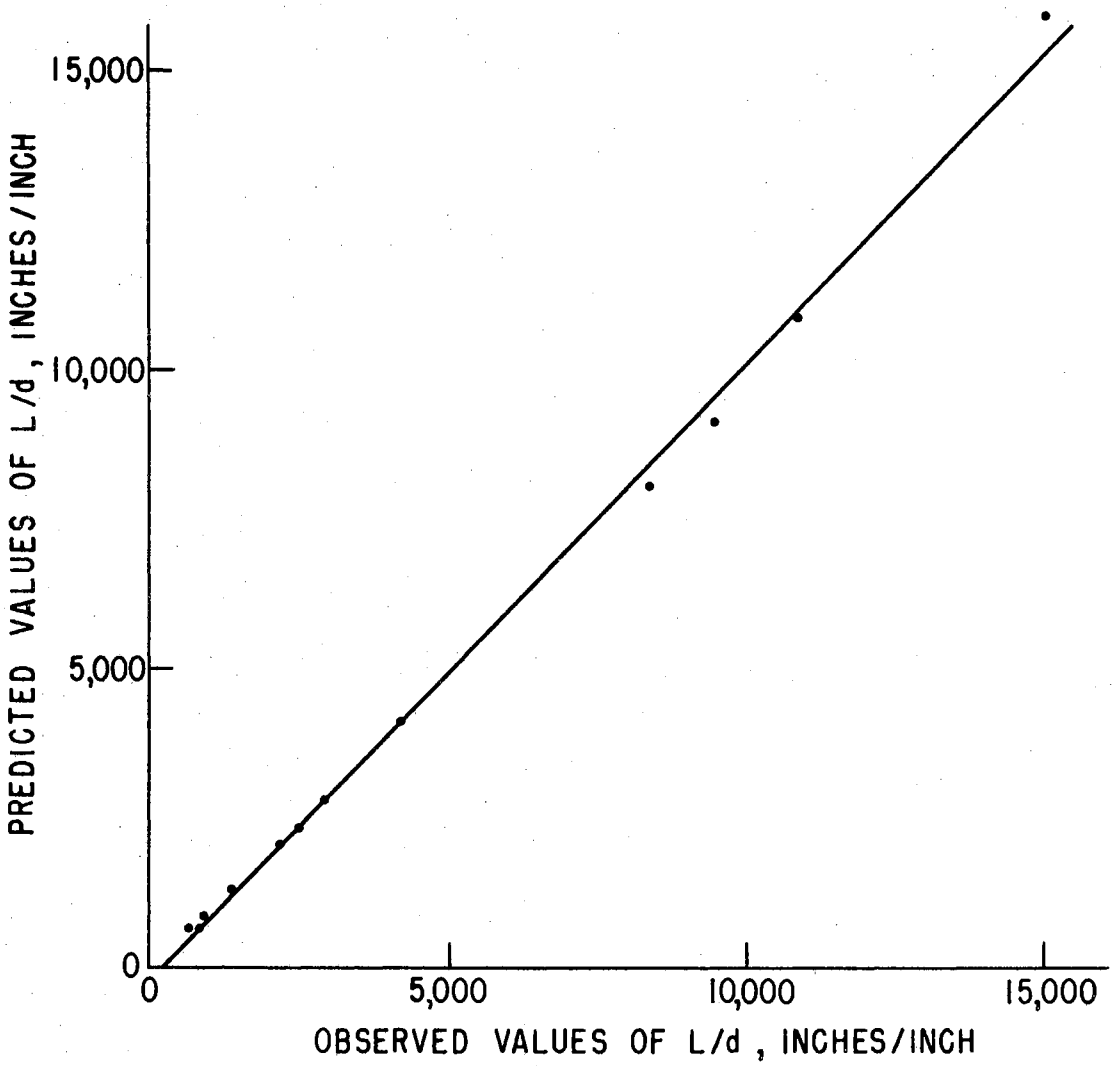

Figure 35. Observed Values of π_2 Compared to Values Computed from Prediction Equations for L/d on Slat One Under Loads on Slat One from Prototype Data in Appendix D

computed from the prediction equation. The intercept of the regression curve was 0.01 and the slope of the line was 1.11. The confidence interval on the slope of the line ranged from 1.10 to 1.12. The correlation coefficient was 0.99.

The intercept of one curve was 55.4 and for the other curve it was 0.00. The maximum values of L/d plotted in Figure 34 were almost 27,000, and in Figure 35 the maximum plotted value of L/d was about 15,000. When the maximum values are considered, the deviations of the intercepts from zero are small. The slopes of both lines are approximately one indicating that values computed from the prediction equations closely approximated the observed values. Since both confidence intervals are in the neighborhood of one, it further indicates that the prediction equations give good estimates of the deflection of grids.

Test Strain Data and Test Deflection Data Compared with Results of Guyon-Massonnet Design Procedures

The Guyon-Massonnet procedure (4, 9, 11, 15) for analyzing grids is a system of distributing moments and deflections. Moments and deflections are computed for the loaded slat in a grid as if the slat were a simple beam. These values are divided by the number of slats. Distribution factors are computed for each beam by the Guyon-Massonnet method and are multiplied by the mean deflection and moments.

Using the Guyon-Massonnet procedure, distribution factors for bending moment were computed for the prototype grid having a length of 47 inches. The loading arrangement selected for the calculations was for two loads of 24.66 pounds each placed 21.5 inches from the ends of slat one on the grid.

For this analysis, strain values were converted to bending moments using the assumption that plaster has a linear stress-strain relationship, and that shear strain may be neglected. For beams having rectangular cross sections, the flexure formula is written:

$$\frac{\text{Moment}}{\text{Stress}} = \frac{I}{C} = \frac{1}{6} bh^2$$

b represents the width of the beam and h the depth.

Stress is computed by multiplying the strain by the modulus of elasticity which for the prototype plaster was 669,760 pounds per square inch. I/C was computed using b = h = 2.2 inches

$$\frac{1}{6} bh^2 = \frac{1}{6}(2.2)(2.2)^2 = 1.77$$

Table XXXVII lists bending moments computed from the strain prediction equation for the prototype having a load on slat one.

TABLE XXXVII

BENDING MOMENT ON PROTOTYPE SLATS WITH LOAD ON SLAT ONE

P = 49.32 pounds

Strained Slat	Strain (Inches/Inch)	Stress	Bending Moment (Inch-Pounds)
1	$124X10^{-6}$	83	147
2	$94X10^{-6}$	63	111
3	$88X10^{-6}$	59	105
4	$84X10^{-6}$	56	99

Table XXXVIII lists the Grid Distribution Factors for bending moment as calculated by the Guyon-Massonnet method and as calculated from the values from Table XXXVII for the prototype grid. The sum of

the bending moments for the four slats when slat one is loaded is 147 inch-pounds + 111 inch-pounds + 105 inch-pounds + 99 inch-pounds = 462 inch-pounds. The average of the four slats is 116 inch-pounds. The distribution factors are computed by dividing. They are 1.27, .96, .91, and .85.

TABLE XXXVIII

GRID DISTRIBUTION FACTORS FOR BENDING MOMENT FOR LOAD ON SLAT ONE OF PROTOTYPE

	Slat 1 Stressed	Slat 2 Stressed	Slat 3 Stressed	Slat 4 Stressed
Distribution Factors for Mean Value of Bending Moment from Guyon-Massonnet Analysis	1.17	1.03	0.94	0.85
Distribution Factors for Mean Value of Bending Moment Computed from Prototype Test Data	1.27	0.96	0.91	0.85

In this example, the heavily stressed slats would tend to be under-designed if the Guyon-Massonnet procedure were used. If the moment to be distributed were calculated on the basis of a simple beam, its value would be 21.54 inches X 24.66 pounds or 531 inch-pounds. Compared to the sum of 462 inch-pounds taken from the test data, the simple beam assumption is conservative. This conservative assumed moment for the Guyon-Massonnet analysis compensates for the unconservative distribution factors to some degree. A less conservative moment assumption could be made by using a fixity factor for

the cross ties at the ends of the grid. A fully fixed end beam assumption would be inappropriate, but the amount of fixity required cannot be assessed readily.

The distribution factors used for deflection determinations by the Guyon-Massonnet procedure have the same magnitude as the factors for moments. Table XXXIX lists the grid distribution factors for

TABLE XXXIX

GRID DISTRIBUTION FACTORS FOR DEFLECTION
FOR LOAD ON SLAT ONE OF PROTOTYPE

	Slat 1 Deflected	Slat 2 Deflected	Slat 3 Deflected	Slat 4 Deflected
Distribution Factors for Mean Value of Deflection from Guyon-Massonnet Analysis	1.17	1.03	0.94	0.85
Distribution Factors for Mean Value of Deflection Computed from Prototype Test Data	1.26	1.05	0.89	0.74

deflection as calculated by the Guyon-Massonnet method and as computed from the test data. Deflection values on slats 1, 2, 3, and 4 of the prototype with a load on slat one were used to compute distribution factors for Table XXXIX. Data are from Appendix E. The sum of the deflections for the four slats when slat one is loaded is 0.024 inches + 0.020 inches + 0.017 inches + 0.014 inches = 0.075 inches. The average of the four slats is 0.019 inches. The distribution factors are computed by dividing. They are 1.26, 1.05, 0.89, and 0.74.

As with the distribution factors for bending moment, the heavily loaded slat would be under-designed by the Guyon-Massonnet procedure as compared to the test data. If the deflection to be distributed were calculated on the basis of a simple beam, its value would be

$$d = \frac{Pa}{24EI}(3L^2 - 4a^2)$$

$$= \frac{50.70 \times 21.54}{48 \times 669,760 \times 1.81}(3(47)^2 - 4(21.54)^2)$$

$$= .0894 \text{ inches}$$

The test data value was .071. The simple beam assumption is conservative for the Guyon-Massonnet design which compensates to some extent for the unconservative distribution factor. Full fixed end beams used in the assumption would result in an under-design.

Application of Test Results to Grid Design

The prediction equations for strain may be used to design four slat gridwork systems that will be safe in flexure. A grid configuration may be assumed and the prediction equation can be used to determine the bending moment that the grid can resist. This determination can be based on the prediction equations for strain induced at the surface of slats in the grid at the center of the span.

The strain at this point can be converted to stress at the point by using the modulus of elasticity. Since plaster of Paris has approximately a linear stress-strain relationship, a linear decrease in stress in plaster models will exist from the extreme fiber of the beam to the neutral axis.

For reinforced concrete, the stress variation from the extreme fiber of the concrete to the neutral axis is normally not linear.

In Figure 36, A illustrates the general shape of the stress distribution curve that normally exists in concrete of a reinforced concrete beam. It is maximum at the extreme fiber but decreases in a non-linear manner to the neutral axis. In reinforced concrete design, the tensile stress that concrete carries is disregarded. Tensile stress is concentrated in the reinforcing steel.

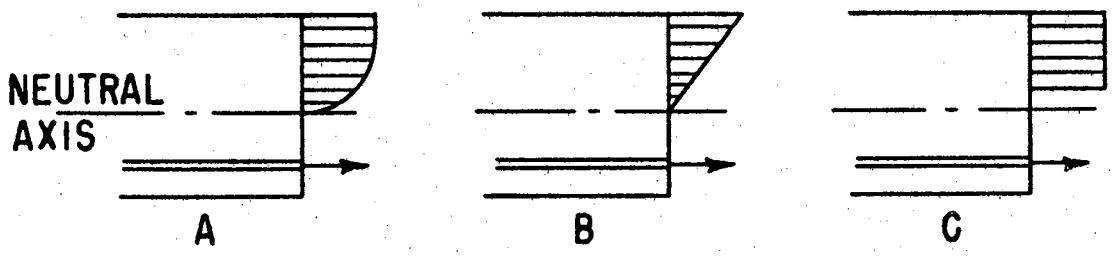

Figure 36. Compressive Stress Distribution in Reinforced Concrete Beams

In the elastic design procedure used for reinforced concrete, a linear stress distribution is assumed as illustrated by B in Figure 36. This design procedure has been used for concrete but tends to yield conservative designs.

In the ultimate strength procedure of design of reinforced concrete beams, an equivalent stress block is assumed to describe stress distribution in the concrete acting in compression. This is illustrated by C in Figure 36. This design procedure describes the actual stress distribution in concrete better than the method used in elastic design.

Values for variables must be assumed to adapt prediction equations to the design of grids for safety in bending. These variables

include: the number of ties, grid length, slat and tie dimensions, slat spacing, load placement, load magnitude, and concrete and steel strength characteristics.

Morice and Little (12) indicate that sufficient accuracy can be obtained for reinforced concrete beams by computing their torsional and flexural stiffnesses on the basis of the cross sectional shape of the concrete alone. E and G for concrete can be used to complete the stiffness calculations.

Loading placements that will give maximum strain can be used for determining design moments. For example, if all loads are placed on slat one as shown in Figure 1, maximum strain will occur on slat one. The prediction equation for the load on slat one - strain on slat one can be used to calculate maximum strain. Slat one can be designed from these results. Load placement on slat one may be taken from Burgener (2) and Hoibo (6). Two of the equal loads placed a distance X from each end of the grid can be substituted into the prediction equation. Strain at the center will be computed. A second pair of equal loads placed at another distance X from each end of the grid can be substituted into the prediction equation. Strain at the center will be computed. A third pair of equal loads placed at another distance X from each end of the grid can then be used to compute strain at the center of the slat. Other pairs of loads can be substituted to determine their contribution to the strain at the center of the slat. Total strain at M_1 can be determined by summing component strains. This strain information can be used with an appropriate reinforced concrete design procedure to design prototype grids.

Other loading assumptions may be made that could produce maximum strain values that exceed those that develop when all loads are placed on slat one. Another loading arrangement that may be examined is the situation where loads are placed on slat one and slat four. Under this assumption, it may be reasonable to assume less load on each of the two slats than was assumed when all loads were placed on slat one.

Another loading assumption that could be made would be load placement on all slats in the grid. If slat loadings were the same, the design could be done assuming each slat to be a simple beam. Under this loading arrangement, the load per slat may be taken as being less than the load per slat if only two slats are loaded, since cattle population could not be maximum on all slats at one time.

Example Problem

To illustrate the use of the strain prediction equation for the design of a four-slat grid, consider a grid having slat cross section configurations as shown in Figure 37. Assume that the grid has two cross ties and is loaded on slat one with loads as shown in Figure 2. Let P equal 500 pounds, grid length equal 96 inches, and slat spacing equal 1.5 inches.

The problem is to find the stress in the concrete at the top of the slat and the stress in the steel reinforcing rod for the slat in Figure 37 in the given gridwork system. Include both live load and dead load in the design.

The design of the grid will be done using procedures based on elastic theory.

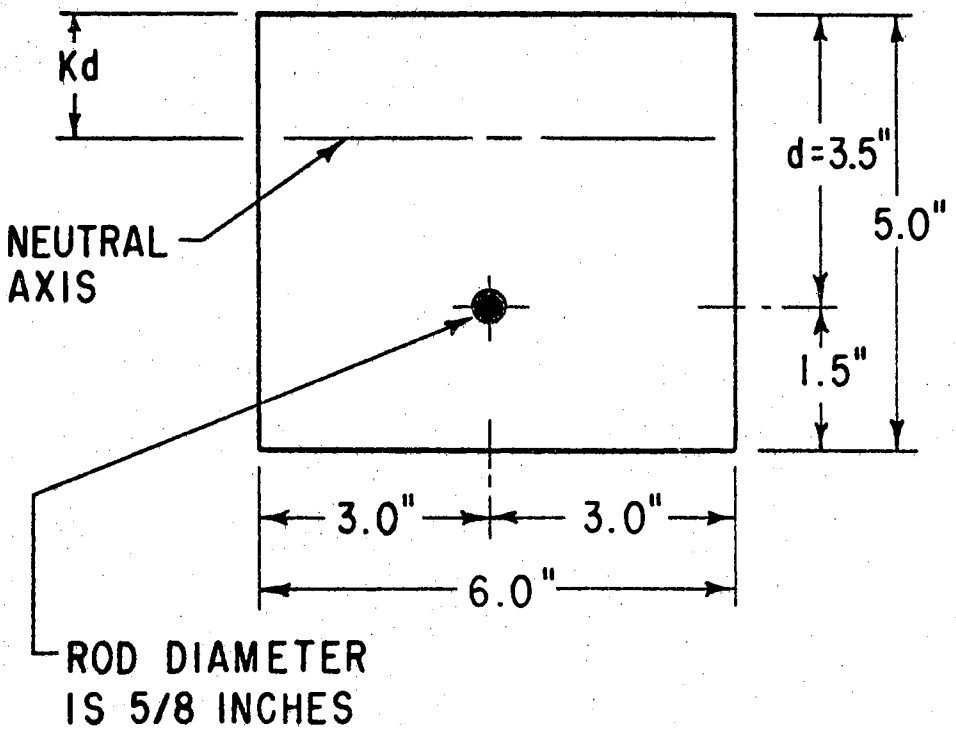

Figure 37. Cross Section of Slat Used in the Example Problem

E for concrete = 4×10^6

G for concrete = 0.4E

n for concrete = 10 for concrete having f'_c = 3,000 psi

Use the prediction equation for strain at the center of slat one when slat one is loaded

$$\text{Strain} = (3.89)\left(\frac{EI/GJ}{.007 - .014(EI/GJ)} + 250.14\right)(PL^2/EI)(L/B)^{-.941}$$

$$(X/L)^{1.434}(128.84 - 4.21T)$$

$\pi_3 = EI/GJ$ Assume that this ratio will be equal to the ratio for a solid concrete cross section. I and J may change as the tension concrete fails under loading, but the assumption here is that the ratio will not change. Calculations were based on an h that included the cover concrete over the bottom of the rod and d.

$$I = \frac{1}{12} bh^3 = 62.5 \text{ inches}^4$$

$$J = \frac{1}{16} bh^3\left(\frac{16}{3} - 3.36 \frac{h}{b}\left(1 - \frac{1}{12}\left(\frac{h}{b}\right)^4\right)\right) = 124.0$$

$$\frac{EI}{GJ} = \frac{62.5}{.4 \times 124.0} = 1.26$$

$\pi_4 = \frac{EI}{PL^2}$ For this ratio, the moment of inertia computed by the transformed section for reinforced concrete was used.

Transform the area of steel

$$A_t = nA_s = 10 \times 0.31 = 3.10 \text{ square inches}$$

$$p = \frac{A_s}{bd} \frac{0.31}{6 \times 3.5} = 0.015$$

$$K = ((np)^2 + 2np)^{1/2} - np = 0.43$$

$$\text{Transformed } I = \frac{1}{3} bd^3 + A_t (d - (Kd))^2 = 17.1$$

$$= \frac{EI}{PL^2} = \frac{4 \times (10)^6 \times 17.1}{500 \times (96)^2} = 14.8$$

$$\pi_5 = \frac{L}{B} = \frac{96}{7.5} = 12.80$$

$\pi_6 = \frac{X}{L}$ This is computed in three pairs of points: 6 inches, 18 inches, and 42 inches from the ends of the grid.

$$\frac{6}{96} = 0.06$$

$$\frac{18}{96} = 0.19$$

$$\frac{42}{96} = 0.44$$

$$\pi_7 = T = 2$$

Strain (1) is the strain at the center of slat one caused by loads placed on slat one at points X = 6 inches from the ends of the grid.

$$\text{Strain (1)} = (3.89)\left(\frac{1.26}{.007 - .014(1.26)} + 250.14\right)(14.8)^{-1.0}(12.80)^{-.941}(.06)^{1.434}(128.84 - 4.21(2))$$

Strain (1) = 6.6 microinches/inch

Strain (2) is the strain at the center of slat one caused by loads placed on slat one at points X = 18 inches from the ends of the grid.

Strain (2) = 32.1 microinches/inch

Strain (3) is the strain at the center of slat one caused by loads placed on slat one at points X = 42 inches from the ends of the grid.

Strain (3) = 108.1 microinches/inch

Total strain = strain (1) + strain (2) + strain (3) + strain (3)

Total strain = 255.0 microinches/inch

Concrete stress due to live load = (Modulus of Elasticity)(Strain)$(10)^{-6}$

$= (4 \times 10^6)(255)(10)^{-6} = 1020$ psi

The resisting moment in the beam due to live load = $\frac{(\text{stress})(I)}{Kd}$

Resisting moment due to live load = 12,050 inch-pounds

The moment due to dead load = 1/8 wL^2. This moment was computed by considering the beam as a solid concrete beam.

Moment due to dead load = 3,000 inch-pounds

The total moment in the beam equals the moment due to live load plus the moment due to dead load

Total moment = 12,050 + 3,000 = 15,050 inch-pounds

The stress in concrete due to total moment = Mc/I

Stress in concrete = 1,274 psi

The stress in the steel due to total moment = $n(\frac{M}{I})(d - Kd)$

Stress in steel = 18,041 psi

The beam used in this example will safely resist a total moment of 15,050 inch-pounds.

The grid used in the example was analyzed using the Guyon-Massonnet procedure. The analysis indicated that the effect of the torsion was significant. The total live load moment in beam one when that beam was loaded as illustrated in Figure 2 was 2,250 foot-pounds. The mean moment per slat for a four slat system was 562 foot-pounds. Factors for distributing the mean moments were computed as 1.2, 1.05, 0.95, and 0.80. The large factor was for the loaded slat and the values decreased for slats farther from the loaded slat. The live load moment for the loaded slat was adjusted by the distribution factor to a value of 674 foot-pounds. Live load plus dead load makes a total design moment of 924 foot-pounds or about 11,100 inch-pounds.

The moment computed from the prediction equation was 15,050 inch-pounds.

Burgener (2) records the design for bending of slats designed as simple beams. If the loading shown in Figure 2 is applied to a simple beam eight feet long, the dead load moment and live load moment generated total 29,880 inch-pounds. This moment is about two times as large as the moment of 15,050 inch-pounds that was computed from the prediction equation for strain recorded in Table XXIX.

Molding Plaster as a Structural Modeling Material

Stress-strain relationships for molding plaster were approximately linear for the Barga Lucca from the National Gypsum Company that was used in the testing program. Other forms of molding plaster have higher values of strength characteristics, but the Barga Lucca had good characteristics of workability and the strength was adequate.

The grid models were fabricated by casting molding plaster blocks with overall dimensions equal to those of the grid models. Slots were cut in the blocks with a sabre saw to create the desired grid configuration. The molding plaster prototype was made twice as large as the average model. Slots were formed in the grid by using styrofoam plastic as form material. The plastic was removed from the cast plaster prototype leaving the proper slot configuration. This work indicated that models four feet long and two inches thick could be formed of molding plaster with no complications. Larger models probably reduce the effects of imperfections in the molding plaster on the overall performance of the system. A minimum of mechanical shaping was needed on the prototype in contrast to the models that were shaped with a sabre saw. Shaping plaster models by sawing introduced a potential for generating imperfections in the models.

The linear stress-strain relationship of the molding plaster provides results that should be valid for other materials in ranges of their stress-strain curve that are approximately linear. Validation of the tests results indicated that the molding plaster gave reliable results.

CHAPTER X

SUMMARY AND CONCLUSIONS

The problem considered in the investigation was the evaluation of design procedures to be used for gridwork systems suitable for perforated floors for livestock. The objectives of the work were to determine if a prediction equation could be developed from data collected in a series of tests using grid models; and to validate existing design procedures by using the prediction equations that might be developed.

Quantities describing grid configurations, the strength characteristics of the materials used for grids, the positions in which loads are placed, and the magnitude of the loads were considered as being pertinent to the design of the grids. These quantities were combined into dimensionless pi terms. Models were constructed in such a way that each pi term could be varied while other terms were held constant.

Molding plaster was used to fabricate the grid models. The relationships between the deformations and the pi terms in which loads were included plotted on log-log paper as straight lines with slopes very near to unity. This indicates that the plaster demonstrates a linear stress-strain relationship. This was further indicated by the tests for the simple beams used to determine modulus of elasticity and shear modulus values. Plaster that is used for modeling structural systems should have good strength characteristics. It should also cure

at a rate that makes it possible to cast the models with ease. The molding plaster used in the tests had good curing characteristics that made it possible to cast models of good quality. Trials with plaster of Paris indicated that its curing characteristics were erratic. It tended to flash set before molding was completed. The strength characteristics for the plaster of Paris were better than for the molding plaster. Proper design of the tests for the models compensated for this characteristic of the molding plaster.

Two loads of equal magnitude were placed each an equal distance from each end of a slat being loaded. This created maximum deformations at the center of the slats so measurements of strain and deflection were taken at these points. This loading arrangement could be adapted to a suitable loading assumption for cattle. The strain values that were measured in the tests were used to calculate the stresses that were being developed.

The prediction equation developed for determining strain at the center of the slats in a grid took the following form:

$$e = K_1\left(\frac{EI/GJ}{K_2 + K_3(EI/GJ)} + K_4\right)(PL^2/EI)(L/B)^{-K_5}(X/L)^{K_6}(K_7 - K_8(T))$$

Eight equations were written for predicting strain. Four equations were written for strain at the center of slats 1, 2, 3, and 4 when slat one was loaded. Four other equations were written for strain on slat 1, 2, 3, and 4 when slat two was loaded. Coefficients for the eight equations are given in Table XXIX. These equations can be used to predict strain at the center of the slats.

The prediction equation developed for determining deflection at the center of the slats in a grid took the following form:

$$L/d = K_1(EI/GJ)^{K_2}(EI/PL^2)(K_3 + K_4(L/B))(X/L)^{-K_5}(K_6 - K_7(T))$$

Eight equations were written for predicting deflection for the same loading deformation relationships used for the strain equations. Equations were written for deflection on each of the four slats when loads were placed on slats one and two. Coefficients for the eight equations are given in Table XXXVI. These equations can be used to predict deflection at the center of the slats.

Figures 41-44 indicate that the prediction equations for strain and deflection yield calculated values that closely approximate observed values for the models and the plaster prototype. Results from tests on plaster models are apparently valid for designing prototypes if the prototypes are stressed in the elastic range of the materials used for their fabrication. For this to be true, it is also necessary that the prototype material demonstrate a nearly linear stress-strain relationship in its elastic range.

Distribution factors for moment and deflection were calculated by the theory presented by Guyon and Massonnet (3, 9) for the prototype grid having a length of 47 inches. For purposes of comparison, distribution factors were computed from data from tests on the prototype. They were developed using both the strain and deflection data and were designed to be used in the same way as the factors developed by Guyon and Massonnet. When slat one was loaded, the Guyon-Massonnet procedure produced estimated deformations on the loaded slat that were smaller than those calculated from experimental data. This indicates that the theoretical results lead to slat designs that are over-stressed. Designs based on the prediction equations would therefore be conservative.

Designs were developed for a four slat reinforced concrete gridwork having a length of 96 inches. The design was based on flexure. A slat having a depth of five inches, a width of six inches, and a five-eights inch diameter reinforcing rod placed one and one-half inches from the slat bottom was designed to resist moment of 15,050 inch-pounds. This moment was calculated from the prediction equation developed for strain on slat one when the load was on slat one. The loading arrangement used was similar to that suggested by Burgener (2) for a single beam type slat. All load was concentrated on slat one with no loading considered on the other slats in the grid. Under similar loading conditions, a moment of 11,100 inch-pounds was calculated using the Guyon-Massonnet procedure. Here again, the design that would result from the theoretical procedure would be less conservative than that from the design based on the prediction equation developed to estimate the strain at the center of the slat.

The comparison of the observed values of the deformations with the values calculated by the prediction equations indicates that the prediction equations give good estimates of the deformations that can be expected in loaded gridwork systems. This was shown to be true for both the models used to develop the equations and the plaster prototype having a length of 47 inches. Determining design moments by the Guyon-Massonnet method results in values that are not conservative. These results indicate that grids designed with bending moments calculated from the prediction equation for strain will be suitable for livestock floors.

Suggestions for Further Study

1. Reinforced concrete grids should be load tested to determine how precise the prediction equations describe their performance. Test results from the prototype that was fabricated from molding plaster indicated that the prediction equation was reliable in that application. Reinforced concrete is not homogeneous. The decrease in stress from the top of the beam to the neutral axis is not linear. These variables along with others found in reinforced concrete suggest the need for validating the prediction equation for concrete.

2. Prediction equations should be developed for grids having three, five, and six main slats. The four slat grid systems evaluated here have characteristics that adapt well to cattle floors, however, alternate designs should be evaluated. If the number of main slats is included as a variable in a prediction equation, it is difficult to identify the loaded slat in a way that adapts to all grid designs. Holding the number of main slats constant in each test series is one way to overcome this difficulty.

3. Some reinforced concrete slat systems are being cast in place forming gridwork systems that are interconnected over the entire floor. Design procedures for this type of system should be evaluated. Availability of reuseable forms could make this system economically feasible.

4. Grids cast in sections having four main slats might be made more economical by interconnecting the sections. Mechanical devices should be developed to connect adjoining grid sections when they are put in place in the floor system. The economy of using such devices should be analyzed.

5. The amount of torsion that is generated in the slats and ties of grids should be analyzed. Plaster models with strain gauges could be used to measure the torsion induced by loads. Under normal design conditions, torsion in reinforced concrete sections is kept to a minimum if possible. If the torque that is developed in the slats or cross ties is large, the design of the reinforced concrete grids should be adjusted.

6. Grid designs are based on assumed load locations and load magnitudes. These assumptions are intended to provide the most severe conditions that might be encountered. The reliability of the design loadings could be evaluated by installing a set of strain gauges on a grid system being used under field conditions. Automatic recording equipment in connection with the strain gauges could be used to record the maximum strains actually induced in grids.

BIBLIOGRAPHY

BIBLIOGRAPHY

(1) Berhe, B. "An Experimental Analysis of Bending Stresses Induced in Floor Grids Subjected to Loads from Beef Cattle." (unpub. M. S. thesis, Oklahoma State University, 1967).

(2) Burgener, Maurice L. "Designs for Concrete Slatted Floors for Livestock." Paper Number 61-407. St. Joseph, Michigan: American Society of Agricultural Engineers, 1961.

(3) Ferguson, P. M. "Analysis of Three-Dimensional Beam and Girder Framing." Journal of the American Concrete Institute, Vol. 22, September, 1950, 61-72.

(4) Guyon, Y. "Calcul des Ponts Larges a Poutres Multiples Solidarises Par des Entretoises." Annales des Ponts et Chausees. Paris. September-October, 1946, 553-612.

(5) Hetenyi, M. Handbook of Experimental Stress Analysis. New York: John Wiley and Sons, Inc., 1950.

(6) Hoibo, H. "Concrete Slats for Cattle Pens." Proceedings No. 40 Institute of Building Construction, Vollebekk: The Agricultural University of Norway, 1960.

(7) Johnson, L. H. Nomography and Emperical Equations. New York: John Wiley and Sons, Inc., 1952.

(8) Lightfoot, E. and F. Sawko. "Structural Frame Analysis by Electronic Computer. Grid Frameworks Resolved by Generalized Slope Deflection." Engineering. London. Vol. 187, January 2, 1959, 18-20.

(9) Martin, I. and J. Hernandes. "Orthogonel Gridworks Loaded Normally to Their Planes." Journal of the Structural Division. Proceedings of the American Society of Civil Engineers. Vol. 86, January, 1960, 1-12.

(10) Massonnet, C. "Methode de Calcul des Points a Poutres Multiples Tenant Compt de Leur Resistance a la Torsion." Publications, International Association for Bridge and Structural Engineering. Zurich. Vol. 10, 1950, 147-182.

(11) Mattock, A. H. "Structural Model Testing - Theory and Applications." Journal of Portland Cement Association - Research and Development Laboratories. Vol. 4, No. 3, September, 1962, 12-23.

(12) Morice, P. B. and G. Little. "Load Distribution in Prestressed Concrete Bridge Systems." The Structural Engineer. Vol. 32, No. 3, March, 1954, 83-111.

(13) Murphy, G. Similitude in Engineering. New York: The Ronald Press Co., 1950.

(14) Preece, B. W. and J. A. Sandover. "Plaster Models and Reinforced Concrete Design." Structural Concrete. Vol. 1, No. 3, May-June, 1962, 148-154.

(15) Roark, R. J. and R. S. Hartenberg. "Predicting the Strength of Structures from Tests of Plaster Models." Engineering Experiment Station Bulletin No. 81. Madison: University of Wisconsin, 1935.

(16) Rowe, R. E. Concrete Bridge Design. New York: John Wiley and Sons, Inc., 1962.

(17) Seely, F. S. Resistance of Materials, 2nd ed. New York: John Wiley and Sons, Inc., 1935.

(18) "Slatted Floors for Efficient Livestock Production." Concrete for Agriculture. Number F170. Chicago: Portland Cement Association, 1964.

(19) Timoshenko, S. and D. H. Young. Elements of Strength of Materials, 4th ed. Princeton: D. Van Nostrand Co., Inc., January, 1962.

(20) Timoshenko, S. and S. Weinowsky - Krieger. Theory of Plates and Shells, 2nd ed. New York: McGraw-Hill, 1959.

(21) Tolaba, J. H. "Analysis of Rectangular Grids by Stiffness Method." (unpub. M. S. thesis, Oklahoma State University, 1962).

(22) Tuma, J. J. and J. H. Tolaba. "Analysis of Rectangular Grids by Stiffness Methods." School of Civil Engineering Research Publication No. 20. Stillwater: Oklahoma State University, 1963.

(23) Wianecki, J. "Mechanical Properties of Plaster of Paris with a View to Its Use for Scale Models." RILEM Bulletin. Paris. No. 20, September, 1963, 103-112.

APPENDIXES

APPENDIX A

GRID STRAIN TEST DATA

APPENDIX A, TABLE I

STRAIN VALUES FROM TESTS WHERE EI/GJ WAS VARIED, OTHER PI TERMS WERE HELD CONSTANT

$EI/PL^2 = 12$ X/L=.458 L/B=16 T=2

TEST SERIES	SLAT UNDER LOAD	EI/GJ	STRAIN ON SLAT ONE (MICRO-IN/IN)	STRAIN ON SLAT TWO (MICRO-IN/IN)	STRAIN ON SLAT THREE (MICRO-IN/IN)	STRAIN ON SLAT FOUR (MICRO-IN/IN)
A1	1	.744	38.99	27.56	24.98	25.00
A1	1	.744	37.25	29.44	29.20	25.24
A1	1	.744	32.19	29.21	29.84	25.59
A1	1	.744	29.14	32.60	29.85	30.64
A2	1	1.220	119.58	93.84	86.39	82.68
A2	1	1.220	125.81	89.95	82.57	77.00
A2	1	1.220	125.66	91.69	81.14	79.96
A2	1	1.220	123.95	88.98	80.89	71.77
A3	1	2.065	160.03	109.65	97.54	95.84
A3	1	2.065	171.56	112.14	93.72	89.56
A3	1	2.065	161.72	113.26	100.38	87.77
A3	1	2.065	172.73	122.50	106.70	94.33
A4	1	3.870	165.66	105.67	85.49	74.83
A4	1	3.870	176.18	115.83	92.08	77.97
A4	1	3.870	163.95	103.30	77.48	74.49
A4	1	3.870	171.20	114.15	95.63	80.65
A1	2	.744	28.16	34.42	29.54	29.14
A1	2	.744	30.10	34.77	26.39	29.69
A1	2	.744	24.59	33.94	27.48	26.58
A1	2	.744	27.23	34.99	28.19	27.32
A2	2	1.220	86.65	110.43	87.37	87.41
A2	2	1.220	94.70	114.46	84.46	78.38
A2	2	1.220	85.13	109.91	81.76	81.41
A2	2	1.220	89.19	109.79	88.41	82.43
A3	2	2.065	112.82	149.99	107.26	104.20
A3	2	2.065	115.43	149.89	101.04	95.06
A3	2	2.065	110.18	141.97	104.40	100.85
A3	2	2.065	119.48	145.94	105.93	95.19
A4	2	3.870	111.35	146.98	100.68	91.59
A4	2	3.870	110.30	144.83	97.77	84.33
A4	2	3.870	109.76	145.02	99.05	93.21
A4	2	3.870	116.10	142.15	93.87	87.13

APPENDIX A, TABLE II

STRAIN VALUES FROM TESTS WHERE EI/PL^2 WAS VARIED, OTHER PI TERMS WERE HELD CONSTANT

EI/GJ=1.220 X/L=.458 L/B=16 T=2

TEST SERIES	SLAT UNDER LOAD	EI/PL^2	STRAIN ON SLAT ONE (MICRO-IN/IN)	STRAIN ON SLAT TWO (MICRO-IN/IN)	STRAIN ON SLAT THREE (MICRO-IN/IN)	STRAIN ON SLAT FOUR (MICRO-IN/IN)
B1	1	4	367.83	278.21	256.68	251.58
B1	1	4	385.20	273.36	249.79	232.17
B1	1	4	373.31	274.50	243.02	234.17
B1	1	4	368.14	266.52	246.64	223.09
B2	1	12	125.66	91.69	81.14	79.96
B2	1	12	123.95	88.98	80.89	71.77
B2	1	12	125.81	89.95	82.57	77.00
B2	1	12	119.58	93.84	86.39	82.68
B3	1	44	29.31	26.79	24.46	21.26
B3	1	44	31.48	23.25	21.77	20.58
B3	1	44	35.60	25.22	22.28	23.88
B3	1	44	35.15	24.42	20.61	16.75
B4	1	100	10.35	12.71	11.46	8.36
B4	1	100	11.67	9.25	9.00	8.73
B4	1	100	16.69	11.26	9.91	12.11
B4	1	100	16.50	10.87	7.95	5.19
B1	2	4	269.17	338.25	268.66	266.43
B1	2	4	284.26	345.73	258.46	243.36
B1	2	4	255.53	336.03	247.77	247.45
B1	2	4	267.54	347.07	260.15	239.60
B2	2	12	86.65	110.43	87.37	87.41
B2	2	12	94.70	114.46	84.46	78.38
B2	2	12	85.13	109.91	81.76	81.41
B2	2	12	89.19	109.79	88.41	82.43
B3	2	44	20.28	27.59	21.44	22.32
B3	2	44	25.77	30.37	21.18	18.39
B3	2	44	23.16	27.68	21.40	21.04
B3	2	44	24.34	23.51	25.96	25.28
B4	2	100	6.34	10.19	7.60	8.65
B4	2	100	11.30	12.71	7.90	5.79
B4	2	100	10.15	10.41	8.72	8.36
B4	2	100	10.72	5.39	12.84	13.27

APPENDIX A, TABLE III

STRAIN VALUES FROM TESTS WHERE L/B WAS VARIED,
OTHER PI TERMS WERE HELD CONSTANT

EI/GJ=1.276 EI/PL^2=12 X/L=.458 T=2

TEST SERIES	SLAT UNDER LOAD	L/B	STRAIN ON SLAT ONE (MICRO-IN/IN)	STRAIN ON SLAT TWO (MICRO-IN/IN)	STRAIN ON SLAT THREE (MICRO-IN/IN)	STRAIN ON SLAT FOUR (MICRO-IN/IN)
C1	1	9	194.62	134.37	106.52	82.70
C1	1	9	209.94	139.41	108.88	84.23
C1	1	9	204.47	141.43	108.80	93.76
C1	1	9	218.58	141.96	114.30	88.19
C2	1	12	186.92	141.20	110.09	106.61
C2	1	12	200.89	140.25	127.38	114.41
C2	1	12	195.41	148.02	120.33	121.95
C2	1	12	206.40	146.76	126.12	115.87
C3	1	16	119.58	93.84	86.39	82.68
C3	1	16	125.81	89.95	82.57	77.00
C3	1	16	125.66	91.69	81.14	79.96
C3	1	16	123.95	88.98	80.89	71.77
C4	1	24	85.53	56.86	57.97	59.06
C4	1	24	93.82	64.61	56.21	54.63
C4	1	24	82.96	58.43	57.39	55.15
C4	1	24	90.10	61.02	53.72	51.58
C1	2	9	130.71	171.46	119.95	108.60
C1	2	9	138.22	168.39	128.03	106.65
C1	2	9	130.16	173.59	127.99	112.66
C1	2	9	147.28	178.12	128.60	103.07
C2	2	12	143.68	171.88	121.69	116.93
C2	2	12	138.95	161.93	133.76	120.77
C2	2	12	153.67	185.40	140.12	130.42
C2	2	12	144.98	167.03	131.39	115.57
C3	2	16	86.65	110.43	87.37	87.41
C3	2	16	94.70	114.46	84.46	78.38
C3	2	16	85.13	109.91	81.76	81.41
C3	2	16	89.19	109.79	88.41	82.43
C4	2	24	63.32	83.82	63.01	62.35
C4	2	24	63.09	88.30	57.48	56.39
C4	2	24	51.35	75.87	56.86	53.43
C4	2	24	61.48	86.20	55.58	51.19

APPENDIX A, TABLE IV

STRAIN VALUES FROM TESTS WHERE X/L WAS VARIED,
OTHER PI TERMS WERE HELD CONSTANT

$EI/GJ=1.220$ $EI/PL^2=12$ $L/B=16$ $T=2$

TEST SERIES	SLAT UNDER LOAD	X/L	STRAIN ON SLAT ONE (MICRO-IN/IN)	STRAIN ON SLAT TWO (MICRO-IN/IN)	STRAIN ON SLAT THREE (MICRO-IN/IN)	STRAIN ON SLAT FOUR (MICRO-IN/IN)
D1	1	.458	128.79	91.39	84.15	80.42
D1	1	.458	136.24	83.48	78.65	72.18
D1	1	.458	136.49	88.63	78.09	76.52
D1	1	.458	135.62	86.00	79.90	69.41
D2	1	.375	85.91	81.75	74.47	73.38
D2	1	.375	86.83	83.77	74.34	72.48
D2	1	.375	83.65	78.29	69.69	70.82
D2	1	.375	83.42	74.07	69.14	62.62
D3	1	.292	52.65	58.13	57.53	58.08
D3	1	.292	64.71	59.55	57.16	52.67
D3	1	.292	56.68	57.72	56.21	55.83
D3	1	.292	58.09	65.72	55.83	54.91
D4	1	.167	30.94	34.98	33.79	38.44
D4	1	.167	35.15	34.11	34.54	34.22
D4	1	.167	24.22	29.63	29.93	32.67
D4	1	.167	30.47	32.50	35.49	33.44
D1	2	.458	81.72	116.56	83.22	83.70
D1	2	.458	91.82	124.72	81.63	76.52
D1	2	.458	81.79	119.75	79.79	80.07
D1	2	.458	88.27	118.75	85.54	79.89
D2	2	.375	77.15	81.01	77.65	76.69
D2	2	.375	83.13	76.90	72.63	65.21
D2	2	.375	72.32	75.55	69.85	69.83
D2	2	.375	75.35	75.18	74.86	69.50
D3	2	.292	58.37	54.08	56.49	55.28
D3	2	.292	60.42	57.57	56.42	56.95
D3	2	.292	57.45	56.45	55.60	56.36
D3	2	.292	57.06	56.41	57.39	55.53
D4	2	.167	30.77	28.59	31.53	29.96
D4	2	.167	36.55	29.24	30.83	30.23
D4	2	.167	28.25	32.31	32.09	35.20
D4	2	.167	34.43	28.99	28.97	28.41

APPENDIX A, TABLE V

STRAIN VALUES FROM TESTS WHERE T WAS VARIED,
OTHER PI TERMS WERE HELD CONSTANT

EI/GJ=1.276 EI/PL^2=12 X/L=.458 L/B=16

TEST SERIES	SLAT UNDER LOAD	T	STRAIN ON SLAT ONE (MICRO-IN/IN)	STRAIN ON SLAT TWO (MICRO-IN/IN)	STRAIN ON SLAT THREE (MICRO-IN/IN)	STRAIN ON SLAT FOUR (MICRO-IN/IN)
E1	1	1	124.56	97.00	91.13	78.89
E1	1	1	118.37	104.02	91.69	75.83
E1	1	1	126.21	99.17	91.46	78.30
E1	1	1	113.40	102.07	89.82	77.46
E2	1	2	119.58	88.98	86.39	82.68
E2	1	2	125.81	91.69	82.57	77.00
E2	1	2	125.66	89.95	81.14	79.96
E2	1	2	123.95	93.84	80.89	71.77
E3	1	3	124.48	99.59	84.22	69.79
E3	1	3	121.61	112.58	85.90	71.56
E3	1	3	120.29	98.75	86.69	76.54
E3	1	3	119.86	96.58	82.13	77.79
E4	1	4	110.40	96.23	83.11	80.06
E4	1	4	108.17	91.45	84.35	83.33
E4	1	4	104.00	91.36	81.00	72.70
E4	1	4	106.78	93.98	84.72	78.12
E1	2	1	104.23	99.38	90.85	81.49
E1	2	1	98.75	98.37	87.40	85.01
E1	2	1	106.50	106.02	92.40	86.82
E1	2	1	99.36	103.57	100.96	94.61
E2	2	2	86.65	110.43	87.37	87.41
E2	2	2	94.70	114.46	84.46	78.38
E2	2	2	85.13	109.91	81.76	81.41
E2	2	2	89.19	109.79	88.41	82.43
E3	2	3	97.71	108.20	87.90	79.73
E3	2	3	93.24	101.19	87.94	84.08
E3	2	3	106.46	115.29	95.16	91.80
E3	2	3	100.65	109.88	94.52	91.81
E4	2	4	96.93	101.76	87.78	84.38
E4	2	4	95.13	96.85	90.22	85.16
E4	2	4	90.74	99.04	87.10	82.64
E4	2	4	93.23	101.73	90.25	84.02

APPENDIX B

GRID DEFLECTION TEST DATA

APPENDIX B, TABLE I

DEFLECTION VALUES FROM TESTS WHERE EI/GJ WAS VARIED, OTHER PI TERMS WERE HELD CONSTANT

$EI/PL^2=12$ X/L=.458 L/B=16 T=2

TEST SERIES	SLAT UNDER LOAD	EI/GJ	DEFLECTION ON SLAT ONE (IN.)	DEFLECTION ON SLAT TWO (IN.)	DEFLECTION ON SLAT THREE (IN.)	DEFLECTION ON SLAT FOUR (IN.)
A1	1	.744	.0104	.0098	.0089	.0088
A1	1	.744	.0105	.0097	.0089	.0084
A1	1	.744	.0092	.0095	.0084	.0083
A1	1	.744	.0103	.0097	.0094	.0092
A2	1	1.344	.0134	.0098	.0079	.0057
A2	1	1.344	.0128	.0104	.0079	.0054
A2	1	1.344	.0121	.0105	.0085	.0077
A2	1	1.344	.0115	.0099	.0090	.0076
A3	1	2.065	.0137	.0108	.0080	.0061
A3	1	2.065	.0117	.0092	.0076	.0056
A3	1	2.065	.0110	.0097	.0082	.0068
A3	1	2.065	.0135	.0098	.0068	.0057
A4	1	3.870	.0111	.0094	.0073	.0061
A4	1	3.870	.0107	.0093	.0067	.0056
A4	1	3.870	.0126	.0101	.0073	.0041
A4	1	3.870	.0104	.0094	.0069	.0057
A1	2	.744	.0107	.0110	.0094	.0092
A1	2	.744	.0099	.0097	.0095	.0091
A1	2	.744	.0096	.0096	.0088	.0090
A1	2	.744	.0089	.0088	.0090	.0084
A2	2	1.344	.0105	.0100	.0094	.0090
A2	2	1.344	.0108	.0106	.0094	.0086
A2	2	1.344	.0093	.0091	.0089	.0084
A2	2	1.344	.0101	.0099	.0094	.0090
A3	2	2.065	.0110	.0111	.0093	.0088
A3	2	2.065	.0103	.0102	.0099	.0096
A3	2	2.065	.0093	.0095	.0096	.0080
A3	2	2.065	.0097	.0099	.0090	.0083
A4	2	3.870	.0093	.0094	.0080	.0072
A4	2	3.870	.0086	.0086	.0080	.0076
A4	2	3.870	.0095	.0092	.0080	.0066
A4	2	3.870	.0083	.0091	.0082	.0079

APPENDIX B, TABLE II

DEFLECTION VALUES FROM TESTS WHERE EI/PL^2 WAS VARIED, OTHER PI TERMS WERE HELD CONSTANT

EI/GJ=1.344 X/L=.458 L/B=16 T=2

TEST SERIES	SLAT UNDER LOAD	EI/PL^2	DEFLECTION ON SLAT ONE (IN.)	DEFLECTION ON SLAT TWO (IN.)	DEFLECTION ON SLAT THREE (IN.)	DEFLECTION ON SLAT FOUR (IN.)
B1	1	4	.0416	.0305	.0249	.0179
B1	1	4	.0392	.0318	.0238	.0165
B1	1	4	.0368	.0323	.0263	.0242
B1	1	4	.0354	.0306	.0280	.0232
B2	1	12	.0134	.0098	.0079	.0057
B2	1	12	.0128	.0104	.0079	.0054
B2	1	12	.0121	.0105	.0085	.0077
B2	1	12	.0115	.0099	.0090	.0076
B3	1	28	.0054	.0039	.0030	.0022
B3	1	28	.0053	.0042	.0034	.0022
B3	1	28	.0051	.0043	.0034	.0030
B3	1	28	.0047	.0040	.0035	.0031
B4	1	44	.0032	.0023	.0018	.0013
B4	1	44	.0032	.0026	.0023	.0014
B4	1	44	.0031	.0026	.0020	.0017
B4	1	44	.0028	.0024	.0021	.0019
B1	2	4	.0325	.0310	.0291	.0273
B1	2	4	.0331	.0327	.0286	.0267
B1	2	4	.0294	.0297	.0283	.0267
B1	2	4	.0313	.0306	.0291	.0276
B2	2	12	.0105	.0100	.0094	.0090
B2	2	12	.0108	.0106	.0094	.0086
B2	2	12	.0093	.0091	.0089	.0084
B2	2	12	.0101	.0099	.0094	.0090
B3	2	28	.0042	.0041	.0038	.0038
B3	2	28	.0044	.0043	.0039	.0034
B3	2	28	.0036	.0037	.0034	.0032
B3	2	28	.0041	.0040	.0038	.0036
B4	2	44	.0025	.0024	.0023	.0024
B4	2	44	.0026	.0025	.0024	.0020
B4	2	44	.0021	.0021	.0019	.0018
B4	2	44	.0025	.0024	.0023	.0022

APPENDIX B, TABLE III

DEFLECTION VALUES FROM TESTS WHERE L/B WAS VARIED, OTHER PI TERMS WERE HELD CONSTANT

EI/GJ=1.276 EI/PL^2=12 X/L=.458 T=2

TEST SERIES	SLAT UNDER LOAD	L/B	DEFLECTION ON SLAT ONE (IN.)	DEFLECTION ON SLAT TWO (IN.)	DEFLECTION ON SLAT THREE (IN.)	DEFLECTION ON SLAT FOUR (IN.)
C1	1	9	.0108	.0088	.0065	.0050
C1	1	9	.0114	.0088	.0071	.0056
C1	1	9	.0121	.0085	.0065	.0039
C1	1	9	.0100	.0087	.0069	.0055
C2	1	12	.0128	.0100	.0087	.0065
C2	1	12	.0116	.0099	.0078	.0068
C2	1	12	.0098	.0086	.0070	.0058
C2	1	12	.0091	.0086	.0067	.0057
C3	1	16	.0134	.0098	.0079	.0057
C3	1	16	.0128	.0104	.0079	.0054
C3	1	16	.0121	.0105	.0085	.0077
C3	1	16	.0115	.0099	.0090	.0076
C4	1	24	.0135	.0128	.0120	.0113
C4	1	24	.0139	.0133	.0124	.0115
C4	1	24	.0135	.0129	.0121	.0118
C4	1	24	.0143	.0132	.0125	.0117
C1	2	9	.0104	.0105	.0083	.0071
C1	2	9	.0087	.0083	.0078	.0070
C1	2	9	.0101	.0090	.0088	.0073
C1	2	9	.0092	.0092	.0075	.0077
C2	2	12	.0105	.0090	.0088	.0085
C2	2	12	.0103	.0102	.0101	.0103
C2	2	12	.0079	.0077	.0073	.0067
C2	2	12	.0072	.0081	.0071	.0069
C3	2	16	.0105	.0100	.0094	.0090
C3	2	16	.0108	.0106	.0094	.0086
C3	2	16	.0093	.0091	.0089	.0084
C3	2	16	.0101	.0099	.0094	.0090
C4	2	24	.0132	.0135	.0130	.0124
C4	2	24	.0125	.0129	.0126	.0122
C4	2	24	.0119	.0124	.0117	.0118
C4	2	24	.0129	.0126	.0123	.0118

APPENDIX B, TABLE IV

DEFLECTION VALUES FROM TESTS WHERE X/L WAS VARIED,
OTHER PI TERMS WERE HELD CONSTANT

EI/GJ=1.344 $EI/PL^2=12$ L/B=16 T=2

TEST SERIES	SLAT UNDER LOAD	X/L	DEFLECTION ON SLAT ONE (IN.)	DEFLECTION ON SLAT TWO (IN.)	DEFLECTION ON SLAT THREE (IN.)	DEFLECTION ON SLAT FOUR (IN.)
D1	1	.458	.0133	.0095	.0077	.0053
D1	1	.458	.0126	.0102	.0074	.0046
D1	1	.458	.0121	.0104	.0080	.0075
D1	1	.458	.0114	.0097	.0089	.0075
D2	1	.375	.0118	.0086	.0066	.0046
D2	1	.375	.0113	.0090	.0073	.0047
D2	1	.375	.0103	.0087	.0075	.0065
D2	1	.375	.0098	.0087	.0077	.0066
D3	1	.292	.0104	.0073	.0049	.0031
D3	1	.292	.0096	.0077	.0059	.0036
D3	1	.292	.0091	.0076	.0069	.0059
D3	1	.292	.0081	.0072	.0063	.0055
D4	1	.208	.0083	.0054	.0032	.0012
D4	1	.208	.0075	.0059	.0045	.0018
D4	1	.208	.0070	.0055	.0049	.0042
D4	1	.208	.0061	.0054	.0048	.0042
D1	2	.458	.0103	.0097	.0091	.0087
D1	2	.458	.0105	.0104	.0090	.0082
D1	2	.458	.0088	.0087	.0081	.0081
D1	2	.458	.0101	.0099	.0092	.0087
D2	2	.375	.0093	.0090	.0084	.0080
D2	2	.375	.0094	.0092	.0085	.0078
D2	2	.375	.0087	.0085	.0084	.0078
D2	2	.375	.0087	.0084	.0082	.0080
D3	2	.292	.0079	.0077	.0073	.0071
D3	2	.292	.0079	.0076	.0071	.0066
D3	2	.292	.0076	.0073	.0070	.0066
D3	2	.292	.0076	.0073	.0073	.0070
D4	2	.208	.0062	.0058	.0055	.0054
D4	2	.208	.0060	.0058	.0056	.0051
D4	2	.208	.0060	.0061	.0056	.0055
D4	2	.208	.0059	.0056	.0054	.0055

APPENDIX B, TABLE V

DEFLECTION VALUES FOR TESTS WHERE T WAS VARIED,
OTHER PI TERMS WERE HELD CONSTANT

$EI/GJ=1.276$ $EI/PL^2=12$ $X/L=.458$ $L/B=16$

TEST SERIES	SLAT UNDER LOAD	T	DEFLECTION ON SLAT ONE (IN.)	DEFLECTION ON SLAT TWO (IN.)	DEFLECTION ON SLAT THREE (IN.)	DEFLECTION ON SLAT FOUR (IN.)
E1	1	1	.0099	.0088	.0072	.0066
E1	1	1	.0093	.0083	.0072	.0069
E1	1	1	.0116	.0109	.0086	.0079
E1	1	1	.0101	.0089	.0075	.0065
E2	1	2	.0134	.0098	.0079	.0057
E2	1	2	.0128	.0104	.0079	.0054
E2	1	2	.0121	.0105	.0085	.0077
E2	1	2	.0115	.0099	.0090	.0076
E3	1	3	.0106	.0096	.0084	.0075
E3	1	3	.0105	.0095	.0080	.0077
E3	1	3	.0101	.0091	.0075	.0073
E3	1	3	.0090	.0080	.0074	.0066
E4	1	4	.0112	.0107	.0087	.0082
E4	1	4	.0114	.0098	.0085	.0079
E4	1	4	.0100	.0091	.0082	.0070
E4	1	4	.0117	.0101	.0079	.0070
E1	2	1	.0087	.0081	.0072	.0074
E1	2	1	.0087	.0078	.0078	.0077
E1	2	1	.0089	.0085	.0081	.0085
E1	2	1	.0090	.0088	.0080	.0076
E2	2	2	.0105	.0100	.0094	.0090
E2	2	2	.0108	.0106	.0094	.0086
E2	2	2	.0093	.0091	.0089	.0084
E2	2	2	.0101	.0099	.0094	.0090
E3	2	3	.0096	.0092	.0088	.0086
E3	2	3	.0097	.0093	.0088	.0087
E3	2	3	.0085	.0087	.0082	.0083
E3	2	3	.0086	.0082	.0080	.0076
E4	2	4	.0088	.0089	.0087	.0089
E4	2	4	.0098	.0087	.0084	.0080
E4	2	4	.0094	.0089	.0088	.0083
E4	2	4	.0099	.0096	.0087	.0086

APPENDIX C

STRAIN ON PROTOTYPE GRID MODELS

APPENDIX C, TABLE I

STRAIN VALUES FOR PLASTER PROTOTYPE GRID
HAVING A LENGTH OF 47 INCHES

EI/GJ=1.208 L/B=15.7 T=2

SLAT UNDER LOAD	EI/PL^2	X/L	STRAIN ON SLAT ONE (MICRO-IN/IN)	STRAIN ON SLAT TWO (MICRO-IN/IN)	STRAIN ON SLAT THREE (MICRO-IN/IN)	STRAIN ON SLAT FOUR (MICRO-IN/IN)
1	4	.458	345.02	238.84	214.82	206.37
1	12	.458	114.11	78.77	70.60	67.91
1	44	.458	30.09	20.54	18.14	17.57
1	4	.375	256.48	198.88	181.84	177.42
1	12	.375	84.68	65.62	59.99	58.50
1	44	.375	22.06	17.06	15.56	15.17
1	4	.292	176.92	158.13	147.59	146.82
1	12	.292	58.29	52.19	48.93	48.54
1	44	.292	14.95	13.52	12.84	12.62
1	4	.167	77.38	94.91	92.73	96.33
1	12	.167	25.37	31.35	31.08	32.03
1	44	.167	6.29	8.06	8.37	8.38
2	4	.458	234.61	297.27	220.16	216.56
2	12	.458	77.96	98.86	72.65	71.55
2	44	.458	21.04	26.80	19.04	18.80
2	4	.375	196.79	226.46	185.13	184.75
2	12	.375	65.30	75.55	61.41	61.26
2	44	.375	17.43	20.58	16.35	16.29
2	4	.292	157.92	161.07	149.02	151.42
2	12	.292	52.30	53.94	49.75	50.43
2	44	.292	13.77	14.78	13.51	13.61
2	4	.167	96.73	75.42	91.91	97.23
2	12	.167	31.90	25.48	31.13	32.70
2	44	.167	8.15	7.08	8.83	9.12

APPENDIX D

DEFLECTION ON PROTOTYPE GRID MODELS

APPENDIX D, TABLE I

DEFLECTION VALUES FOR PLASTER PROTOTYPE GRID HAVING A LENGTH OF 47 INCHES

EI/GJ=1.208 L/B=15.7 T=2

SLAT UNDER LOAD	EI/PL	X/L	DEFLECTION ON SLAT ONE (IN.)	DEFLECTION ON SLAT TWO (IN.)	DEFLECTION ON SLAT THREE (IN.)	DEFLECTION ON SLAT FOUR (IN.)
1	4	.458	.0638	.0543	.0463	.0404
1	12	.458	.0211	.0178	.0152	.0132
1	44	.458	.0055	.0046	.0038	.0033
1	4	.375	.0559	.0477	.0406	.0351
1	12	.375	.0185	.0157	.0133	.0114
1	44	.375	.0049	.0040	.0034	.0028
1	4	.292	.0474	.0405	.0344	.0294
1	12	.292	.0158	.0134	.0113	.0095
1	44	.292	.0043	.0035	.0029	.0022
1	4	.167	.0328	.0282	.0238	.0199
1	12	.167	.0110	.0093	.0079	.0063
1	44	.167	.0031	.0025	.0021	.0014
2	4	.458	.0547	.0530	.0497	.0485
2	12	.458	.0180	.0175	.0162	.0158
2	44	.458	.0047	.0045	.0040	.0039
2	4	.375	.0483	.0465	.0440	.0430
2	12	.375	.0160	.0153	.0144	.0140
2	44	.375	.0042	.0040	.0036	.0034
2	4	.292	.0413	.0396	.0378	.0370
2	12	.292	.0137	.0131	.0124	.0120
2	44	.292	.0037	.0034	.0031	.0029
2	4	.167	.0291	.0275	.0269	.0265
2	12	.167	.0098	.0091	.0089	.0086
2	44	.167	.0028	.0024	.0023	.0020

VITA

George Lewis Pratt

Candidate for the Degree of

Doctor of Philosophy

Thesis: AN EXPERIMENTAL ANALYSIS OF STRAIN AND DEFLECTION IN GRIDWORK PANELS FOR FLOOR SYSTEMS FOR LIVESTOCK

Major Field: Agricultural Engineering

Biographical:

Personal Data: Born in Fargo, North Dakota, January 31, 1926, the son of Robert W. and Anne M. Pratt.

Education: Attended grade school in Gardner and Grandin, North Dakota; graduated from Grandin High School in 1943; received the Bachelor of Science degree from the North Dakota State University in June, 1950; received the Master of Science degree from the Kansas State University, with a major in Agricultural Engineering, in August, 1951; completed requirements for the Doctor of Philosophy degree in July, 1967.

Professional Experience: Served as an enlisted man in the United States Marine Corps from April, 1943 to May, 1945; accepted an appointment as Acting Instructor in the Agricultural Engineering Department at the North Dakota State University in July, 1951 and served until July, 1952; sales representative from July, 1952 to July, 1953 for the Clay Equipment Corporation of Cedar Falls, Iowa, a supplier of steel farm building equipment; accepted an appointment to the staff of the Agricultural Engineering Department at the North Dakota State University in July, 1953 and now hold a rank of Associate Professor in that department; granted a Sabbatical leave from June, 1963 to June, 1964 to take graduate work at the Oklahoma State University. Professional Society memberships include The American Society of Agricultural Engineers, The American Society of Engineering Education, and The North Dakota Academy of Science. Registered Professional Engineer in North Dakota.